Generation and Characterization of Induced Neural Cells from Fibroblasts by Defined Factors

TSE, Chi Lok

A Thesis Submitted in Partial Fulfillment
of the Requirement for the Degree of
Master of Philosophy
in
Molecular Biotechnology

The Chinese University of Hong Kong

September 2011


23 JAN 2013

Thesis/Assessment Committee

Professor LAU Kwok Fai (Chair)

Professor KWAN Kin Ming (Thesis Supervisor)

Professor TSANG Suk Ying, Faye (Committee Member)

Professor YAO Kwok Ming (External Examiner)

Abstract of the thesis entitled

Generation and Characterization of Induced Neural Cells from Fibroblasts by Defined Factors

Submitted by

TSE Chi Lok

for the degree of Master of Philosophy
in Molecular Biotechnology
at the Chinese University of Hong Kong
in September 2011

Regenerative medicine is an important area of research in modern biological science. The nervous system, which lacks regenerative capacity, has drawn much attention of study. Today, one of the common approaches to regenerative medicine is using embryonic stem (ES) cells. However, the use of ES cells poses threats of carcinogenesis and is highly controversial. Therefore, new methods for achieving regeneration are actively sought.

The work presented in this thesis is aimed at using the transdifferentiation approach to generate cerebellar Purkinje cells and granule cells. The target cell fates were induced in mouse embryonic fibroblasts (MEF) by transfecting them with core transcription factors specific to Purkinje cells and granule cells respectively. After characterizing the molecular properties of the induced cells, two factors, *Ptf1a* and *Rora*, were identified to be essential to the induction of Purkinje cell characteristics, and *Lhx5* could enhance the effect of the two factors, though the majority of induced cells displayed immature properties. The possible events at molecular level underlying transdifferentiation were also proposed. We suggest that recapitulation of development is a key principle to the success of transdifferentiaiton. Particularly, expression of *Ptf1a* and *Rora* simulates gene expression programme of the early

development of Purkinje cells, leading to the induction of molecular and morphological properties of young Purkinje cells in MEF, while the failure of granule cell fate induction was resulted from the failure of recapitulating granule cell development.

The present work showed that neurons of specific subtypes could be transdifferentiated from other differentiated somatic cells and provided evidence for the feasibility of direct transdifferentiation approach in regeneration. It also gave insight into the mechanism of cell fate switching events and reiterated the importance of knowledge of developmental biology in regenerative medicine.

摘要

再生醫學是現代生物科學的一個重要課題，以神經系統爲對象的研究尤其受重視。再生醫學普遍應用胚胎幹細胞爲再生組織的來源，但是胚胎幹細胞可分化成癌細胞，加上這種技術在道德上極具爭議，因此，科學界仍努力研究新的再生醫學技術。

本論文旨在利用轉分化技術去產生小腦的蒲金耶氏細胞和顆粒細胞。我們分別利用蒲金耶氏細胞和顆粒細胞特有的轉錄因子去誘導胚胎纖維母細胞分化成兩種目標的細胞。我們分析了受誘導細胞的分子特徵，發現 Ptf1a 及 Rora 是誘導產生蒲金耶氏細胞特徵的兩個必要因子，而 Lhx5 能促進上述兩個因子的誘導功能。然而，大部分受誘導的細胞都呈現不成熟的特性。

我們也對轉分化過程於分子層面的變化提出建議。我們相信，重演發育程序是轉分化作用的成功關鍵。Ptf1a 及 Rora 的表達有效模擬蒲金耶氏細胞的早期發育的基因程序，促使胚始纖維母細胞被誘導成產生年幼蒲金耶氏細胞的分子及外觀特徵。而我們不能產生誘導顆粒細胞則是由於導入的因子不能重演顆粒細胞的發育程序。

本項研究展示了已分化的體細胞轉化成特定神經細胞的可能，以及證明了直接轉化應用於再生醫學的可行性。此外，本項研究啓示了轉分化作用的機理，及重申了發育生物在再生醫學的重要地位。

ACKNOWLEDGEMENTS

Praise to the Lord Jesus Christ for His grace and guidance

I am thankful to my supervisor, Dr Kin Ming Kwan, for his guidance, patience and support from the beginning to the end of my study. This thesis would not have been possible without his help and encouragement.

I would like to thank my thesis committee members Dr Kwok Fai Lau and Dr Suk Ying Tsang for their support in ideas and materials.

I offer my regards and blessings to my colleagues who give me technical and moral support.

Last but not least, I owe my deepest gratitude to my family for their love and support.

TABLE OF CONTENTS

CHAPTER 1
General Introduction

CHAPTER 2
Materials and General Methods

CHAPTER 3
Generation and Characterization of Induced Neurons

CHAPTER 4

Future Directions

List of Figures

List of Tables

List of Abbreviations

ATP	adenosine 5'-triphosphate
BSA	bovine serum albumin
$CaCl_2$	calcium chloride
CTP	cytosine 5'-triphosphate
dATP	deoxyadenosine 5'-triphosphate
dCTP	deoxycytosine 5'-triphosphate
dGTP	deoxyguanidine 5'-triphosphate
dTTP	deoxythymidine 5'-triphosphate
DEPC	diethylpyrocarbonate
DMEM	Dulbecco's modified Eagle Medium
DMSO	dimethylsulphoxide
DNA	deoxyribonucleic acid
EtBr	ethidium bromide
GTP	guanidine 5'-triphosphate
HCl	hydrochloric acid
KAc	potassium acetate
KCl	potassium chloride
$MgCl_2$	magnesium chloride
$MgSO_4$	magnesium sulphate
NaCl	sodium chloride
NaOH	sodium hydroxide
PBS	phosphate buffered saline
RNA	ribonucleic acid
RNase	ribonuclease
SDS	sodium dodecyl sulphate
Tris	tris(hydromethyl)aminomethane
UTP	uridine 5'-triphosphate
bp	base pair
℃	degree Celcius
g	gram
g	gravitational force constant
h	hour
kb	kilobase
L	litre
M	molar
mg	milligram

ml	millilitre
mM	millimolar
min	minute
N	normal
nm	nanometre
OD	optical density
s	second
µg	microgram
µl	microlitre
µM	micromolar
µm	micrometre
v/v	volume per volume
w/v	weight per volume

CHAPTER 1

GENERAL INTRODUCTION

1.1 Regenerative Medicine

Mammals and other vertebrates are multicellular organisms composed of various types of specialized cells performing specific functions but yet organized into tissues, organs and systems to carry out complex life processes in a coordinated and orchestrated manner. The complexity and diversity of cells and their organization, however, originate from a single-celled zygote formed by the fusion of a sperm and an egg during fertilization. During development, a zygote undergoes many rounds of cell division to increase the number of cells and develops into an embryo. Cells of the embryo become more specialized and are restricted to take up identities of a certain lineage only. At early stages, all cells in an embryo are identical and have the potential to develop into any kind of cells. They are described as totipotent. Soon after that, the embryo enters the blastocyst stage, where it is composed of an outer layer of trophoblasts which later contributes to the formation of extra-embryonic tissues such as placenta, and an inner cell mass which develops into the embryo. At this stage, the cells in the inner cell mass, or epiblasts, are pluripotent, that is, they are able to give rise to all kinds of cells of the body except the extra-embryonic tissues. As development continues, the embryo undergoes gastrulation, where it reorganizes to form three germ layers: ectoderm, mesoderm and endoderm. The three germ layers contribute to the formation of different tissues and organs and are not inter-convertible. These cells go to more specific lineages upon further development.

The human body is made up of around 10^{13} to 10^{14} cells of several hundred types. Some types such as keratinocytes and epithelial cells in the gut face strong

mechanical stress and are worn out continuously. Their number, and thus the functions of the organs, is maintained by the constant replacement of the wounded tissues. This is achieved by cell division of the adult stem cells of the respective cell types. Adult stem cells are a population of multipotent cells that give rise to cells of a limited lineage. Some cell types such as hepatocytes are capable of cell division for recovery when the liver is damaged. In some lower vertebrates, regenerative capacity is not only limited to continual worn out tissues, but also in heart like zebrafish and limbs in salamanders. However, regenerative capacity in human is limited. For example, mature cardiomyocytes and neurons are incapable of undergoing cell division and, once lost, cannot be replaced. Therefore, people who suffer from heart attack, stroke or neurodegenerative diseases often enter irrecoverable and deteriorating conditions. Since surgical and pharmacological treatments cannot provide effective and long term cure to these diseases, the need in regenerative medicine, where damaged tissues are replaced by healthy and functional ones, and which allow more complete recovery, is keen.

Nowadays, two approaches are being investigated for regenerative medicine. The first approach involves the direct injection of stem cells to stimulate and/or participate in the recovery of the injured tissues (cell therapy). The second approach involves the production of new cells, tissues and organs *in vitro* for replacement (tissue engineering). However, the feasibility of these two methods for treatment of a particular tissue injury is greatly limited by the availability and easiness of isolation of adult stem cells. Moreover, these approaches seem not to be applicable to cardiomyocytes and neurons because adult stem cells for these two types of cells have not been identified.

In cases where adult stem cells are absent, the mature cells may undergo dedifferentiation, a process of regression to a less mature state. This often allows the

dedifferentiated cells to proliferate again and produce new cells for replacement. Naturally occurring dedifferentiation includes regeneration of zebrafish heart and urodele amphibian limbs. However, human and other mammals do not have this capacity (Jopling et al., 2011).

1.2 Embryonic Stem Cells and Reprogramming

Given the limitation of adult stem cells, embryonic stem (ES) cells, which can become virtually all cell types, have been a popular alternative in studies of regenerative medicine. Before the discovery of ES cells, embryonal carcinoma (EC) cells have been used in study of embryonic development. However, EC cells have abnormal karyotype. In 1981, the first pluripotent mouse cell line with normal karyotype was isolated from the inner cell mass of an embryo at blastocyte stage (Evans et al., 1981), and the cells were called embryonic stem (ES) cells (Martin, 1981). ES cells are derived from the inner cell mass of an embryo at blastocyst stage, and are characterized by two properties, self-renewal and pluripotency. Self-renewal is the ability to go through many cell cycles while maintaining undifferentiated. Pluripotency refers to the ability to differentiate into cells of derivatives of all three germ layers. By giving suitable cues, ES cells can differentiate into any desired cell types *in vitro*. Since their establishment in cell lines, ES cells have become an important tool in biological studies as well as in medicine. They can serve as a tool for study of development of zygote to adult, and a valuable source for cell therapy in regenerative medicine.

Today, besides direct isolation from embryos, ES cells are commonly produced by reprogramming – a process of reversing the state of differentiation and bringing cells back to a pluripotent state. It has been achieved by 3 methods (reviewed by Yamanaka and Blau, 2010). The first method is nuclear transfer. This is well

illustrated by Wilmut and colleagues (1997) by the production of the famous cloned sheep Dolly. In this approach, the nucleus from a somatic cell is isolated and injected into an enucleated oocyte. The resulting cell is able to develop into a viable and fertile animal, demonstrating that somatic nuclei contain all the information necessary for the development of a whole organism. ES cells can be derived from the "fertilized egg" when it is at the blastocyte stage and these ES cells are called ntES cells.

The second method is cell fusion. In this approach, a somatic cell is fused with an ES cell (Tada et al., 2001), resulting in a heterokaryon if the fused cell does not divide or two hybrid cells if cell division occurs. After fusion, the gene products of the ES cell can activate the previously silent pluripotency genes in the somatic cell, leading to the acquisition of pluripotency. The extent of reprogramming is dictated by the balance of transcriptional regulators that are present (Blau et al., 1983, 1985; Blau and Baltimore, 1991).

The third approach is invented by Yamanaka in 2006 (Takahashi and Yamanaka, 2006) which is termed induced pluripotent stem (iPS) cell. In this approach, pluripotency-related genes are ectopically expressed in somatic cells. These genes products bring about epigenetic changes to the genome and activate the endogenous transcriptional programme specific to ES cells, conferring the somatic cells with pluripotency. In their report in 2006, Takahashi and Yamanaka first selected 24 genes that are specific to or enriched in ES cells as candidates for induction of pluripotency. After series of experiments, they identified four transcription factors, *Oct4*, *Sox2*, *Klf4* and *c-Myc*, are essential for pluripotency induction. Further studies into iPS cells have shown that only *Oct4* is indispensible for reprogramming and the other three factors can be discarded depending on the original cell type and whether additional chemicals are used (Eminli et al., 2008; Huangfu et al., 2008; Nakagawa et

al., 2008; Zhu et al., 2010).

Although the ways to obtain ES cells or pluripotent cells are pretty well established, the tremendous potential of ES cells in regenerative medicine is limited first, by our knowledge of what cues are needed for ES cells to go into a specific lineage. Second, there is a risk that undifferentiated ES cells can develop into malignant tumors *in vivo*. Third, the isolation of ES cells requires destruction of human embryos which is a very controversial ethical issue. Fourth, ES cells, whose genetic make-up is different from the patients', will cause immune rejection from the host when transplanted. In addition, ntES cells cannot avoid the controversy over the use of human embryos and nuclear transfer is technically difficult. Cell fusion is technically simple but it generates tetraploid (4n) cells which has no value in clinical application.

The iPS cell seems to be a better choice as it provides a way to circumvent those drawbacks. First, it avoids the use of embryos and the accompanying ethical concerns. Second, because the source cells are obtained from patients' own tissues, immunological rejection will not occur. However, iPS cells have several weaknesses. First, the most common method of factor delivery in iPS cells generation involves the use of retrovirus or lentivirus, where the transgenes will be integrated into the cells' genome. This could cause insertional mutagenesis and pose risk of tumorigenesis. Second, the efficiency of reprogramming by iPS cell generation is relatively low compared with the other two approaches. Nevertheless, progress has been made to optimize the iPS cell technology. Non-integrative factor delivery methods have been attempted by using adenovirus (Stadtfeld et al., 2008), proteins (Kim et al., 2009; Zhou et al., 2009), excisable DNA vectors (Woltjen et al., 2009) and mRNA (Warren et al., 2010). Different chemicals (Shi et al., 2008; Zhao et al., 2008), culture conditions (Yoshida et al., 2009) and pathway manipulations (Hong et

al., 2009; Yang et al., 2010) have also been applied to improve the generation efficiency.

1.3 Transdifferentiation

The invention of iPS cells has opened up a new field of study in biology. Through the same technique, forced expression of defined factors, transdifferentiation has become direct and cells do not have to go through the pluripotent state. Actually, transdifferentiation has been demonstrated long before the invention of iPS cells. Davis et al. (1987) showed that ectopic expression of a single transcription factor *MyoD* could convert fibroblasts to myobalsts, and Xie et al. (2004) showed the conversion of B cells to macrophages by the expression of C/EBPα and C/EBPβ.

Transdifferentiation also occurs in nature. The regeneration of lens in newt is an excellent illustration. When the lens of a newt is removed, pigmented epithelial cells from dorsal iris first dedifferentiate and proliferate to generate a new lens vesicle, and then differentiate into the cells that make up the lens (Jopling et al., 2011).

In recent years, several cell types have been directly converted from other somatic cell types. For example, cardiomyocytes were generated from mouse mesoderm by expression of *Gata4*, *Tbx5* and *Baf60c* (Takeuchi and Bruneau, 2009), and from fibroblasts by *Gata4*, *Mef2c* and *Tbx5* (Ieda et al., 2010); multilineage blood progenitors from human fibroblasts by expression of OCT4 with addition of Flt3 ligand and SCF (Szabo et al., 2010); and neurons from fibroblasts by expression of *Ascl1*, *Brn2* and *Myt1l* (Vierbuchen et al., 2010).

If iPS cells generation is also considered a kind of transdifferentiation, then from the mechanism of induction of pluripotency, it is conceivable that transdifferentiation may also work in similar manner. During reprogramming, the cell

is first primed and become amendable, then epigenetic modification occurs such that the originally active genes are shut down and ES-specific gene expression is turned on and maintained (Jopling et al., 2011). If this mechanism is applicable to other transdifferentiation events, then the focus of transdifferentiation should reside in identifying factors that are able to first, priming the cells for modification; second, modify the epigenome and, third, induce the endogenous profile of target cell-specific gene expression.

1.4 The Cerebellum

The cerebellum is a part of the brain at the posterior region. Though it only accounts for 10% of volume of the brain, it contains about half of the total number of neurons in the brain. Primarily, the cerebellum is responsible for the control of motor function, and there is increasing evidence suggesting that it plays a role in the cognitive functions such as learning and language (Stoodley, 2011).

1.4.1 Functions of the cerebellum

Studies of cerebellar functions were initiated by observing symptoms of patients suffering from lesions of the cerebellum in the 19th century. Those patients showed symptoms including motor disturbance, uncoordinated movement, dysmetria and slower onset of motion, which could be collectively referred to as ataxia. These early discoveries suggested the cerebellum controlled the accuracy and coordination of movement. The motor learning ability was also implicated from experiments studying the recovery from cerebellar lesions (Ito, 2002). The motor control function of the cerebellum is supported by anatomical evidence that it receives from and projects to the regions of cerebral cortex which control motor activity (Middleton and Strick, 1998).

More and more evidence suggested that the cerebellum does not solely contribute to motor control, but also language, cognition and emotion (Baillieux et al., 2008; Leiner et al., 1986; Schahmann and Sherman, 1998). The first evidence revealed that the cerebellum has connected with the areas of cerebral cortex that concern with language and cognitive functions (Leiner et al., 1987, 1989, 1991, 1993). Lesions in cerebellum can also result in cerebellar cognitive affective syndrome, affecting executive, visual spatial and linguistic ability (Stoodley and Schmahmann, 2010). Furthermore, neuroimaging technology uncovers solid functional indication of the involvement of cerebellum in these processes. Using functional magnetic resonance imaging (fMRI), there is evidence suggesting that the cerebellum plays a part in the language network (Ghosh et al., 2010), working memory (Beneventi et al., 2010), spatial processing (Fink et al., 2000), executive function (Lie et al., 2006) and emotion (Lee et al., 2004). In fact, the language function of cerebellum is implicated in genetics. *Foxp2* is a gene which shows high expression in the cerebellum, and mutation in this gene results in speech and language disorder in human (Ackermann, 2008; Lai et al., 2003).

1.4.2 Structure and organization of the cerebellum

At gross anatomical level, the cerebellum can be divided into a central vermis situated in between two hemispheres (Fig. 1.1). When cut sagittally, it can be seen that the cerebellum is highly foliated, forming 10 lobules (Fig. 1.2).

Although the cerebellum contains half of the neurons of the brain, it has a relatively simple and regular cellular organization compared to the cerebrum. The cortex of the cerebellum is divided into 3 layers, the outer molecular layer which is composed of the dendrites of the Purkinje cells, axons of granule cells (parallel fibres), stellate cells and basket cells; the middle Purkinje cell layer where the cell

bodies of Purkinje cells dwell; and the inner granular layer which contains densely packed granule cells and a small amount of Golgi cells. Beneath the cortex lies the white matter which is composed of deep cerebellar nuclei (DCN) and myelinated nerve fibres.

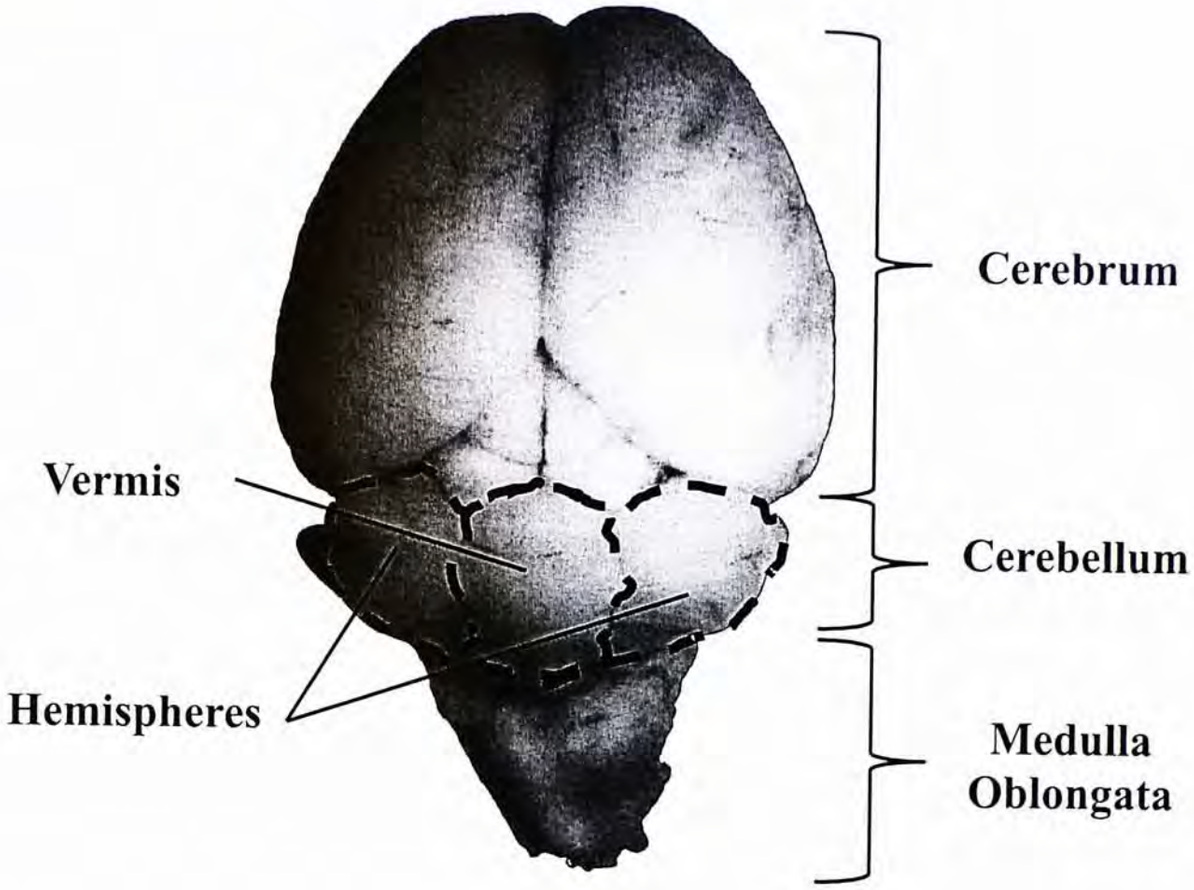

Fig. 1.1 The adult mouse brain. Cerebellum is situated between the cerebrum and medulla oblongata. It is divided into a central vermis and two hemispheres on two sides.

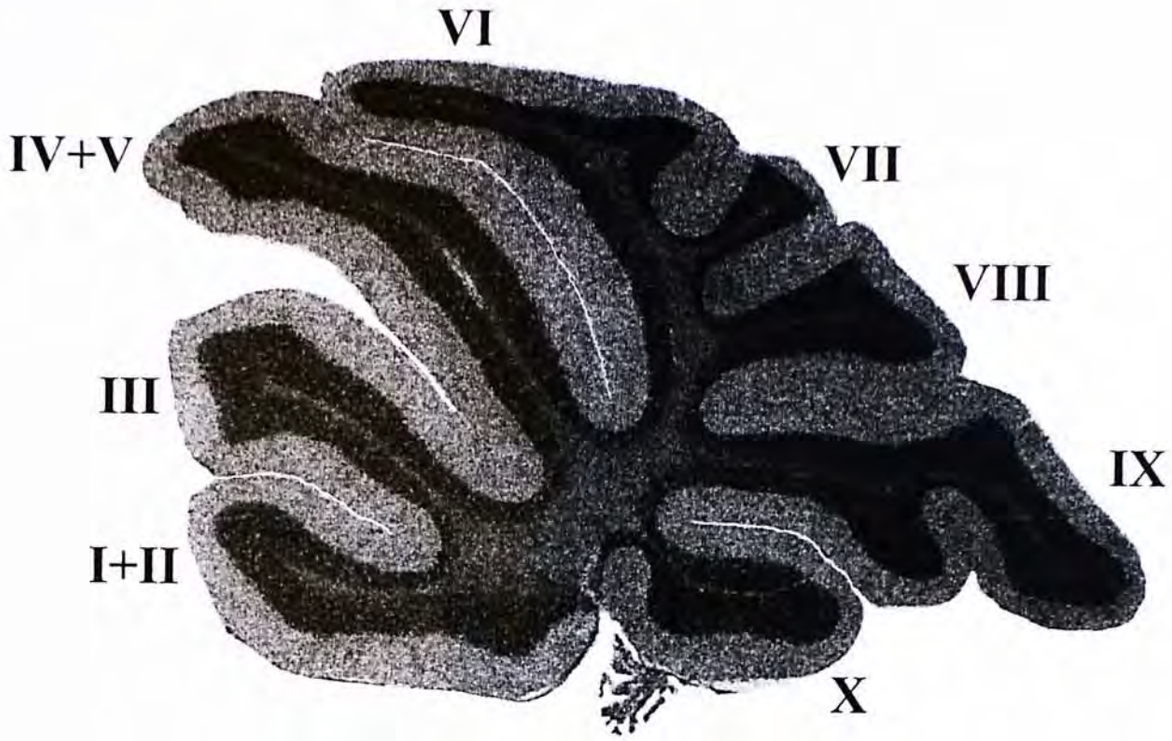

Fig. 1.2 The adult mouse cerebellum in sagittal view with the 10 lobules depicted.

1.4.3 Principle cellular components in the cerebellum

Two major types of cells and two major types of axons form the backbone of the neuronal circuit in the cortex of cerebellum. Other neurons and some glial cells are associated with the functions and the development of the cerebellar neurons.

1.4.3.1 Purkinje cells

Purkinje cells are characterized by their extensive dendritic tree. Serving as the major output of the cerebellar cortex, they are a class of GABAergic neurons and synapse with and receive signals from parallel fibres of granule cells and climbing fibres of the inferior olive. At the base of each Purkinje cell is an axon which sends inhibitory signals to one or more deep cerebellar nuclei.

Purkinje cells have their own characteristic electrical activity. They fired spontaneously at regular frequency (Raman and Bean, 1999). When injected with depolarizing current, voltage-gated sodium channel dependent action potentials are evoked which are tetrodotoxin (TTX)-sensitive. When the amplitude of the injected current increases, a second form of large and sustained action potentials appears. This form of spikes is blocked by cadmium ions and thus is mediated by voltage-gated calcium channels (Llinas and Sugimori, 1980; Raman and Bean, 1999).

Defects in Purkinje cells can lead to spinocerebellar ataxia where the patients display symptoms including tremor, poor coordination of movements and speech.

1.4.3.2 Granule cells

Granule cells are the smallest and the most abundant neurons in the cerebellar cortex. Their cell bodies are closely packed and dwell in the granular layer. Each granule cells has 3-5 dendrites and an axon. The granule cell's axon passes through

the granular and Purkinje cell layer particularly to the molecular layer where it bifurcates and extends horizontally, forming a characteristic T shape at the junction. The horizontal portion of the axon is called parallel fibres. The granule cells are a class of excitatory neurons which utilize the neurotransimitter glutamate. They receive input from pontine nuclei via mossy fibres and relay the signals to Purkinje cells through parallel fibres. The parallel fibres also synapse with basket cells, stellate cells and Golgi cells.

1.4.3.3 Mossy fibres

The mossy fibres are one of the two main inputs into the cerebellum. They are axons originating from a mixed population of neurons, with the majority from pontine nuclei (gray nucleus and reticulotegmental nucleus) located in the pons, and the remaining from different nuclei in the spinal cord (central cervical nucleus, Clarke's column) and brain stem (vestibular nuclei, external cuneate nucleus, trigeminal sensory nucleus and lateral reticular nucleus) (Altman and Bayer, 1997; Sotelo, 2004). They innervate the granule cells and relay excitatory signals.

1.4.3.4 Climbing fibres

The climbing fibres are the other main input into the cerebellum. They are axons of the inferior olive neurons located in the medulla oblongata. They synapse with Purkinje cells as well as deep cerebellar nuclei.

1.4.3.5 Deep cerebellar nuclei

The deep cerebellar nuclei (DCN), the output of cerebellum to various part of the brain, are located beneath the cerebellar cortex in the white matter of the cerebellum. These nuclei are divided into four types: dentate, emboliform, globose

and fastigial (Ramnani, 2006). They receive inhibitory signals from Purkinje cells and excitatory signals from collaterals of climbing and mossy fibres. It is interesting to note their connection with Purkinje cells and climbing and mossy fibres. Synapses from Purkinje cells are mostly located on or close to the cell bodies of the DCN. This arrangement enables Purkinje cells to regulate DCN efficiently at sites in close proximity to the action potential trigger zone (Altman and Bayer, 1997). As for the connection with climbing and mossy fibres, those fibres that preferentially connect to the vermis, paravermis, hemisphere or flocculonodular lobe project collaterals preferentially to the corresponding DCN or extracerebellar nuclei, i.e., fastigial, interpositus (a collective term referring to emboliform and globose), dentate and vestibular nuclei (in medulla oblongata) respectively. This arrangement allows the DCN that receive excitation from climbing or mossy fibres of a particular input also receive indirect inhibition from the same input (Altman and Bayer, 1997).

1.4.3.6 Other cerebellar neurons

Five more types of neurons can be found in the cerebellar cortex. The basket cells and stellate cells are located in the molecular layer while the Golgi cells dwell in the granular layer. Basket cells are an inhibitory interneuron that uses the neurotransmitter γ-aminobutyric acid (GABA). Their dendrites are in contact with parallel fibres and their axons synapse on the cell bodies of Purkinje cells. While each Purkinje cell makes contact with several basket cells, each basket cell only receives input from one Purkinje cell. They send inhibitory signals to Purkinje cells when excited by parallel fibres (Altman and Bayer, 1997; Ito, 2006).

Stellate cells are similar to basket cells in that they are also GABAergic inhibitory interneurons and receive input from parallel fibres. But unlike basket cells which occupy the lower one third of the molecular layer, stellate cells are located at

the upper two thirds of the layer. Besides, their axons remain within the molecular layer and form synapses with the smooth dendrites of Purkinje cells (Altman and Bayer, 1997).

Golgi cells are also GABAergic inhibitory interneurons. They are found in the granular layer and are distinguished from granule cells by their large size. They receive input from parallel fibres via AMPA and NMDA receptors and mGluR2 (Ito, 2006) and output inhibitory signals on mossy fibre-granule cell transmission. They form a negative feedback loop with the granule cells.

Lugaro cells are a recently characterized GABAergic inhibitory interneuron. Their cell bodies are located in or slightly below the Purkinje cell layer (Aoki et al., 1986). Cells in the IGL with similar properties are also included into the group (Laine and Axelrad, 2002). They synapse with Golgi cell in a way that axons from more than 10 Lugaro cells make synaptic contact with a single Golgi cell, while the axon of one Lugaro cell can branch onto 150 Golgi cells (Dieudonne and Dumoulin, 2000; Ito, 2006). The input to Lugaro cells is not well characterized. The only identified presynaptic component contacting somata and dendrites of Lugaro cells is the Purkinje cell collaterals (Geurts et al., 2003; Larramendi and Lemkey-Johnston, 1970). Unlike other neurons in the cerebellum, Lugaro cells are highly sensitive to excitation mediated by serotonin (Dieudonne and Dumoulin, 2000).

The last type of neurons is the unipolar brush cells (UBCs) which is a member of glutaminergic neurons. They are found in the IGL and have size intermediate between granule cells and Golgi cells. Each UBC possesses a single dendrite which branches into a paint brush-like structure of dendrioles (Mugnaini et al., 1997), and receives signals from and form synapses with a single mossy fibre in the glomeruli. They also make dendro-dendritic synapses with granule cells. Their axons form synapses with granule cells. They contribute to a feed forward excitation and may

counteract the inhibition from Golgi cells (Dino et al., 2000).

1.4.3.7 Neuroglia of the cerebellum

Three types of neuroglia are found in the cerebellum. The first type, the astroglia, is located in the IGL and is responsible for migration and compartmentalization of neurons.

The second type is oligodendroglia which lie in the medulla and myelinate axons of Purkinje cells, mossy and climbing fibres in the cerebellum. In addition, these cells are an absolute requirement for Purkinje cell maturation and granule cell proliferation and differentiation. Ablation of oligodendroglia causes impaired growth of Purkinje and granule cells, resulting in reduced size of the cerebellum and failure of formation of normal lamination (Collin et al., 2007).

The third and the most distinctive type of neuroglia is the Bergmann glia. Their cell bodies dwell within or underneath the Purkinje cell layer, and they possess several ascending processes (radial fibres) that extend through molecular layer to the pial surface (Bellamy, 2006). They play a very important role in the guidance of granule cell migration. They are characterized by the expression of molecular markers such as nestin and brain lipid binding protein (BLBP), but the expression is transient and lost after the completion of granule cell migration. After that they lose their radial glial properties and become the radially oriented processes of mature astrocytes (Sotelo, 2004).

These neuroglia are derived from progenitors in the ventricular zone after the end of neuronal production (Altman and Bayer, 1997). The switch of neurogenesis to gliogenesis is probably mediated by the transcription factor *Sox9* as in other parts of the CNS (Stolt et al., 2003).

1.4.4 Circuitry of the cerebellum

The circuitry of the cerebellum is the basis of cerebellar functions. The circuitry ultimately arises from the cerebral cortex and projects to the cerebellum through cortico-olivary-cerebellar and cortico-ponto-cerebellar pathway. Within the cerebellum, the centre of the circuitry is the Purkinje cells which integrate the two main afferents of extra-cerebellar origin and provide the sole output of the cerebellar cortex which is inhibitory in nature. As described above, climbing fibres, a component of the cortico-olivary-cerebellar pathway, convey excitatory signals exclusively from inferior olive to multiple Purkinje cells, while each Purkinje cell only receives input from one climbing fibre (Apps and Garwicz, 2005).

Mossy fibres, a component of the cortico-ponto-cerebellar projections, originate mainly from potine nuclei, and in a lesser extent, from nuclei of spinal cord and brain stem, form another input and interact with Purkinje cells in an indirect way. Upon reaching the white matter of the cerebellum, each mossy fibre may branch into several fibres and synapse with granule cells in the glomeruli, a place where dendrites of granule cells are in contact with the presynaptic swellings of mossy fibres called rosettes (Altman and Bayer, 1997). Receiving signals from mossy fibres, granule cells, one of the two cortical glutaminergic excitatory neurons in cerebellum, relay the signals to Purkinje cells, as well as stellate, basket and Golgi cells through parallel fibres. In contrast to the synapsing pattern of climbing fibres with Purkinje cells, each Purkinje cell can receive signals from up to ~200,000 parallel fibres (Tyrrell and Willshaw, 1992).

In addition to the two afferents above, Purkinje cells also receive signals from basket and stellate cells. Basket and stellate cells are excited by parallel fibres and regulate Purkinje cells activity by inducing inhibitory post-synpastic potential (IPSP).

Apart from direct interaction with Purkinje cells, the complete circuitry involves interneurons that exert their influences on neurons other than Purkinje cells. Golgi cells receive excitatory signals from parallel fibres and inhibitory signals from Lugaro cells. Each Golgi cell projects an extensively branched axon to and inhibits the glomerular synapses between granule cells and mossy fibres (Altman and Bayer, 1997; Palkovits et al., 1971). It is suggested that inhibition from Golgi cells help reduce noise in parallel fibre discharge in the face of noisy mossy fibres inputs (Philopona and Coenen, 2004). The Golgi cells also produce significant crosstalk with non-postsynapstic cells around the Golgi cell-granule cell junction by the spillover of neurotransmitter GABA (Ito, 2006). This crosstalk may serve to regulate the number of active granule cells in the cortex (Rossi and Hamann, 1998). Moreover, Golgi cells induce IPSP on UBCs by glycine (Dugue et al., 2005).

In addition, Golgi cells are innervated by Lugaro cells as described in Section 1.4.3.6. Activated mainly by serotonin, Lugaro cells inhibit a large number of Golgi cells and may serve to synchronize the activity of Golgi cells (Ito, 2006; Vos et al., 1999).

Besides these inhibitory interneurons, the excitatory UBCs also play a role in the circuitry. Induced by a long lasting excitatory postsynaptic potential (EPSP) caused by mossy fibres, UBCs produce a train of action potentials that lasts for tens of milliseconds (Kinney et al., 1997), enabling a powerful feed forward amplification of signals on granule cells (Geurts et al., 2003).

As for the output, Purkinje cells in the cortex convey inhibitory signals to DCN and a few structures outside the cerebellum (Altman and Bayer, 1997). The DCN then return projections to the cerebral cortex through the thalamus, completing the closed loop system composed of cerebral cortex and the cerebellum (Asanuma et al., 1983; Middleton and Strick, 1997; Thach, 1972; Thach and Jones, 1979). The

destinations of the cerebellar circuitry in the cerebral cortex are mostly regions involved in motor control (Middleton and Strick, 1998), such as the primary motor cortex (Asanuma et al., 1983; Evarts and Thach, 1969; Allen and Tsukahara, 1974) and the ventral premotor area (Schell and Strick, 1984). Moreover, it is suggested that some output are connected to the regions of cerebral cortex concerning cognitive and language functions (Leiner et al., 1987, 1989, 1991, 1993).

Although the cellular organization of the cerebellar cortex is very regular and uniform, the cortex can be divided into functionally distinct and independent regions and each region forms its own closed loop system with a specific area of the cerebral cortex. It is conceivable that different information from different functional aspects is processed using similar mechanism (Ramnani, 2006).

In summary, the main route of signal transmission begins from mossy fibres (via granule cells) and climbing fibres to Purkinje cells, and then to DCN to various parts of the brain (Fig. 1.3); while other interneurons directly or indirectly modulate the activity of Purkinje cells.

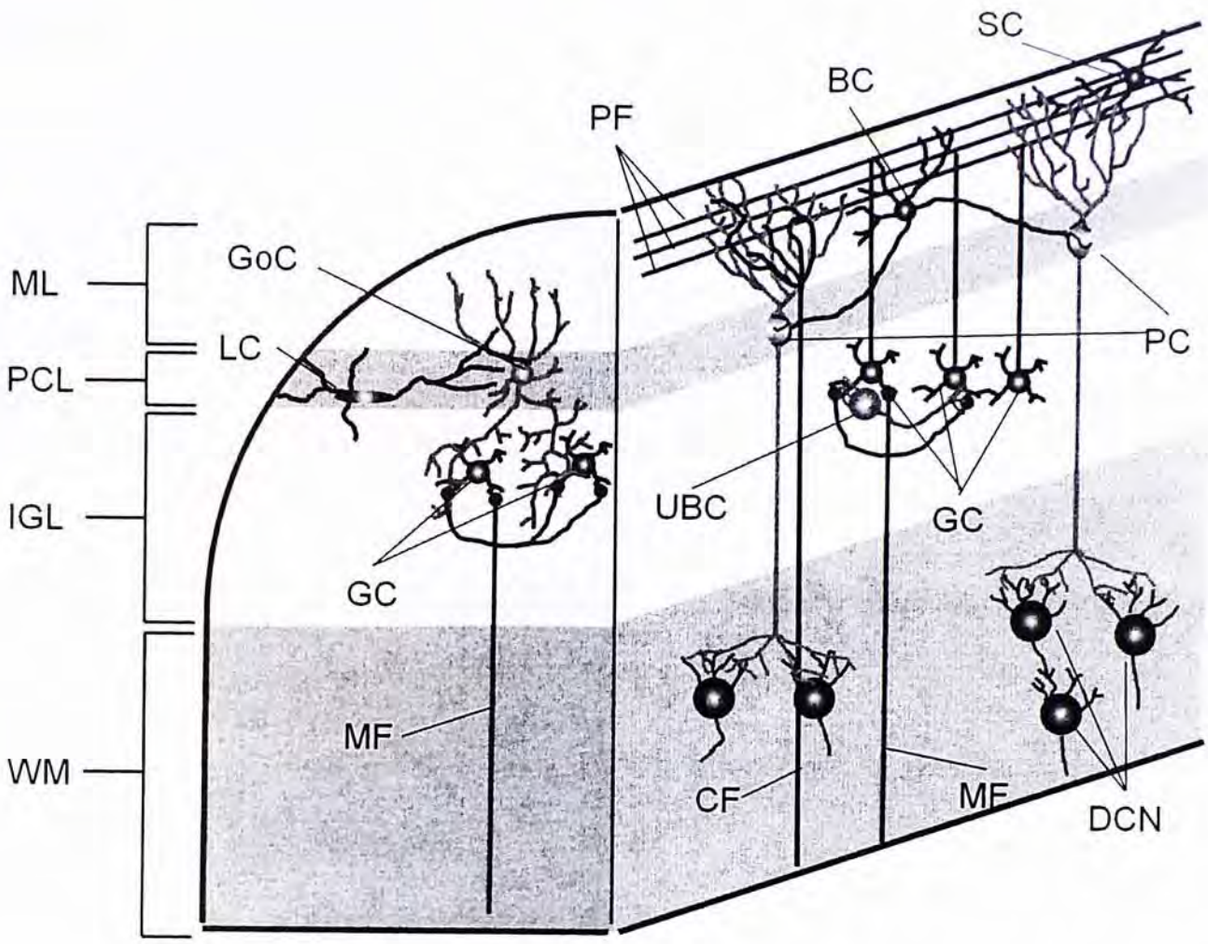

Fig. 1.3 Schematic diagram showing the circuitry of the cerebellum. The cerebellum is divided into molecular layer, Purkinje cell layer, internal granular layer and the white matter. The first three layers form the cortex. Climbing fibres, Purkinje cells and DCN form the cortico-olivary-cerebellar pathway while mossy fibres, granule cells, Purkinje cells and DCN form the cortico-ponto-cerebellar pathway. Interneuorns such as basket cells, stellate cells, Golgi cells and unipolar brush cells modulate the activity of Purkinje cells and granule cells. Lugaro cells modulate the activity of Golgi cells. BC, basket cell; CF, climbing fibre; DCN, deep cerebellar nuclei; GC, granule cell; GoC, Golgi cell; IGL, internal granular layer; LC, Lugaro cell; MF, mossy fibre; ML, molecular layer; PC, Purkinje cell; PCL, Purkinje cell layer; PF, parallel fibre; SC, stellate cell; UBC, unipolar brush cell; WM, white matter.

1.5 Development of the Cerebellum

1.5.1 Anatomical changes during cerebellar development

The cerebellum originates from the metencephalon of the rhombencephalon of the developing neural tube. It starts to appear at around E12 in rat (equivalent to mouse E10) when it is identified as a structure called cerebellar primordium (Fig. 1.4). From E13 to E16 (mouse E11 to E14), the medullary velum and tela choroidea which are situated between the cerebellar primordium and the precerebellar primordium invaginate into the cavity of the fourth ventricle of the neural tube. The tectal primordium, which is located anterior to the cerebellar primordium, increases in size and expands backward and downward, which results in the cerebellar primordium being pushed deeper into the fourth ventricle. These two changes together bring the anterior cerebellar primordium and the posterior precerebellar primordium into close proximity on E16 (Fig. 1.5). On E17 (mouse E15), a proliferative matrix called external granular layer (EGL) is formed at the posterior region of the cerebellar neuroepithelium that will gradually spread forward and then downward over the surface of the cerebellum until E20 (mouse E17). The Purkinje cell layer (PCL) is also formed beneath the EGL. A group of migrating cells identified as formative fastigial nuclei appears in the anterodorsal portion of the cerebellum which will later form the deep cerebellar nuclei. By E22 (mouse E18.5), the cerebellum has adopted its typical shape with some of the lobular structures and fissures being formed (Fig. 1.5). Some drastic changes occur in the first month of the postnatal life. Between postnatal day 0 (P0) when the animal is just born and P5, the appearance of the cerebellum is very similar to that in E22 except some fissures have deepened. However, from P5 to P10, the changes are more obvious. First, more secondary fissures and sublobules appear. Second, the EGL undergoes a massive

thickening attributable to the expansion of the inner, loosely packed cell zone of the migratory population of granule cells. Third, the Purkinje cell layer starts to orientate to become a thin monolayer. Fourth, a clearly identifiable granular layer emerges. In the next 10 days, further changes occur. First, the virtual disappearance of the EGL is accompanied by the expansion of granular layer and the emersion of a clear molecular layer. Outside the cortex, the medullary layer is considerably thickened and delineated from the granular layer by P20. By this time, the morphology of the cerebellum has completely developed and acquired the highly foliated conformation with 10 clearly defined lobules. The first phase of cellular development has also come to an end. Further development centres on the circuitry organization and is not reflected in morphological changes (Altman and Bayer, 1997).

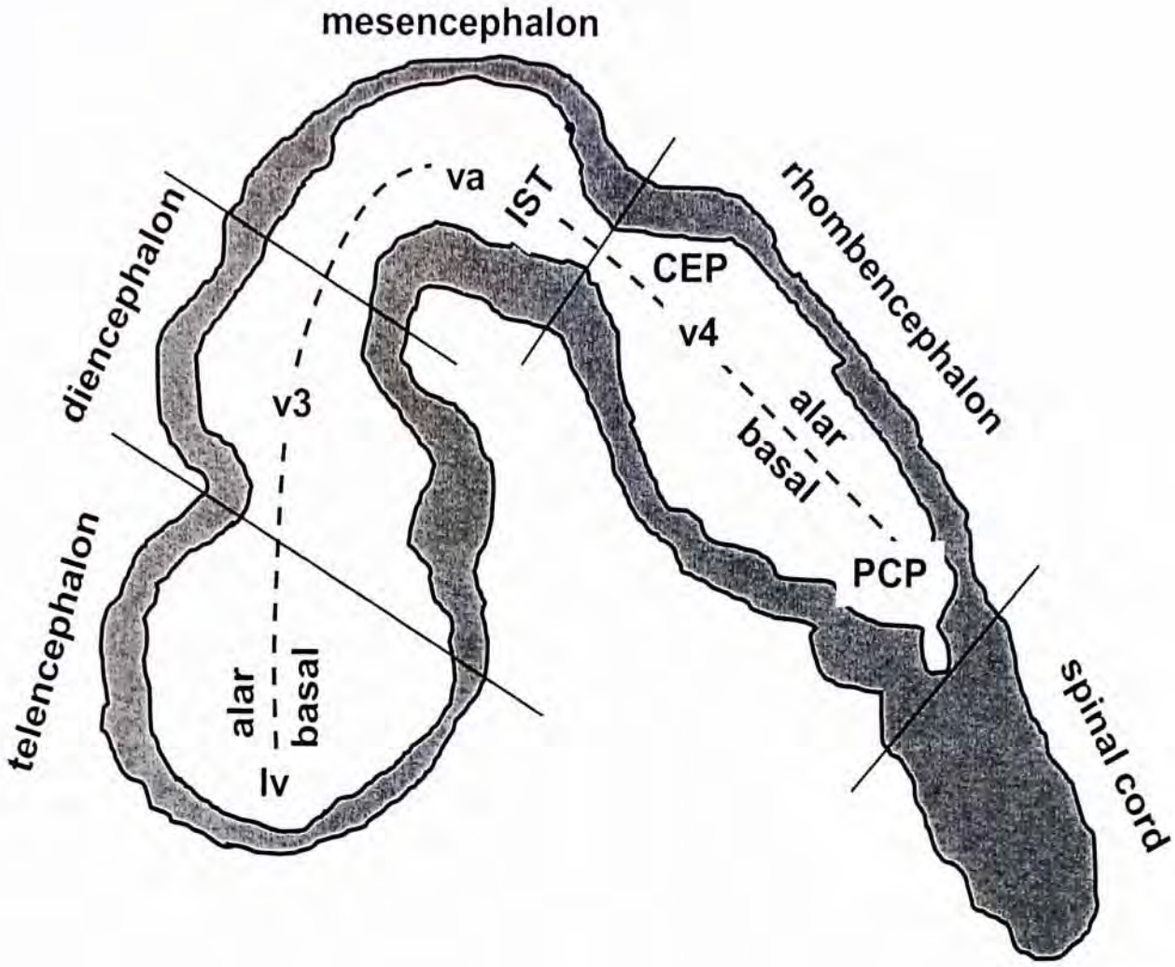

Fig. 1.4 Schematic diagram showing the sagittal section of the developing neural tube of an E12 rat, with a rough delineation of the alar and basal plate components of the four cephalic vesicles (Altman and Bayer, 1997). The cerebellum arises from the rhombencephalon and is known as cerebellar primordium at this stage. Abbreviation: CEP, cerebellar primordium; lv, lateral ventricle; PCP, precerebellar primordium; va, aqueduct; v3 third ventricle; v4, fourth ventricle.

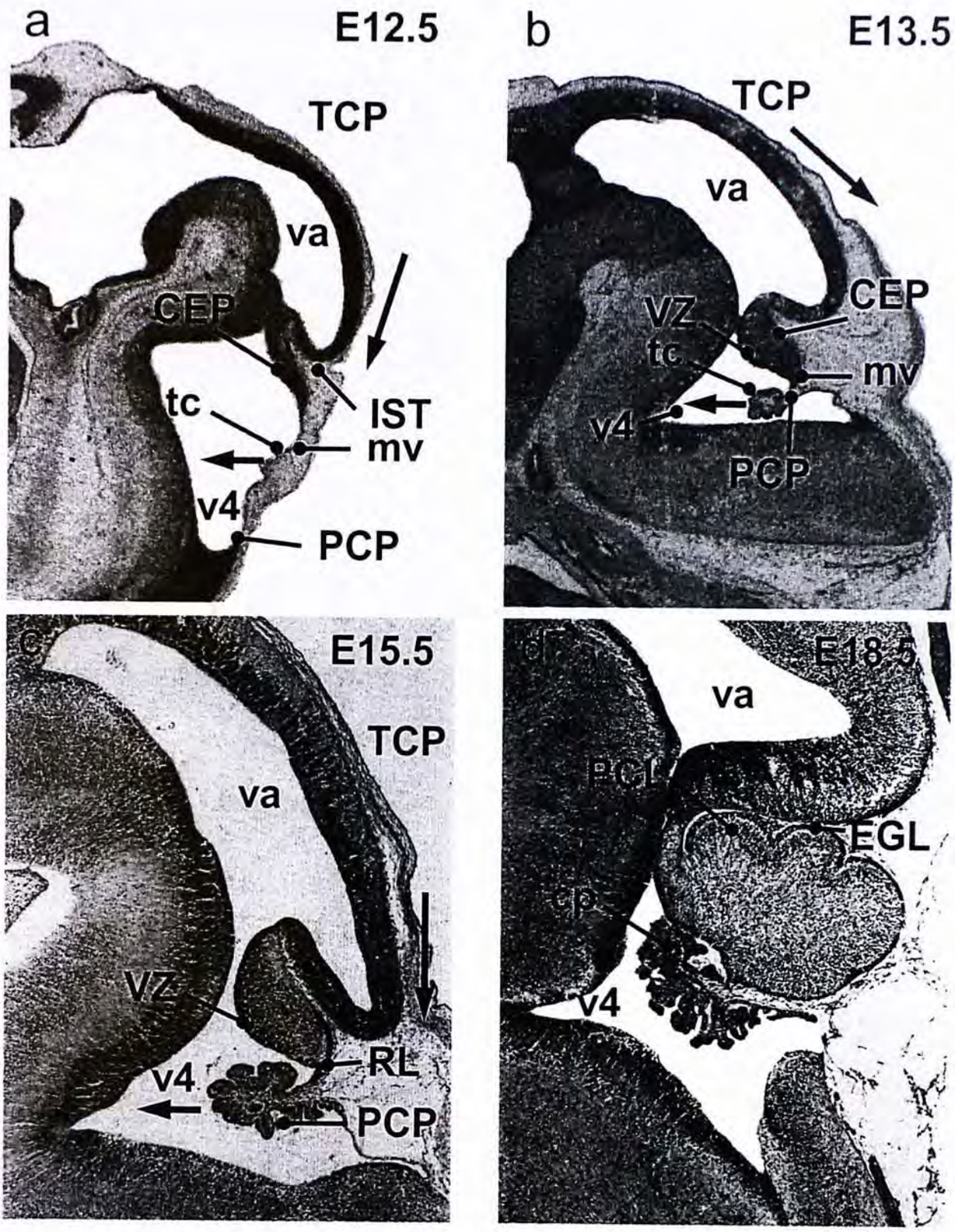

Fig. 1.5 Sagittal sections showing the hindbrain in E12.5, E13.5, E15.5 and E18.5 mice. (a-c) The expansion and downward growth of tectal primordium (downward arrow) and invagination of tectal choroidea and medullary velum (horizontal arrow) bring the cerebellar primordium and precerebellar primordium into close proximity. (d) Appearance of EGL, PCL and foliation of the cerebellum in E18.5 (Altman and Bayer, 1997). Abbreviations: cp, choroid plexus; CEP, cerebellar primordium; EGL, external granular layer; IST, isthmus; mv, medullary velum; PCP, precerebellar primordium; tc, tela choroidea; TCP, tectal primordium; va, aqueduct; v4, fourth ventricle.

1.5.2 Molecular control of cerebellar development

1.5.2.1 Specification of the cerebellar region

After gastrulation when the three germ layers are defined, neural development begins in the ectoderm. Appearance of the neural plate marks the start of neurulation, followed by the formation of the neural tube, which is a long hollow structure at the dorsal side of vertebrates. The dorsoventral axis of the neural tube is established by the dorsalizing factors bone morphogenesis proteins (BMPs) produced by the roof plate and ventralizing factor sonic hedgehog (Shh) produced from the floor plate and the notochord (Echelard et al., 1993; Lee and Jessell, 1999). Patterning also occurs along the length of the neural tube. The anterior most portion of the neural tube is the prosencephalon (forebrain) which is composed telencephalon and diencephalon; the middle is the mesencephalon (midbrain) and the posterior side is the rhombencephalon (hindbrain) which is subdivided into metencephalon and myelencephalon. The cerebellum is a derivative of the metencephalon, but its induction also involves the mesencephalon. At E7.5, two reciprocally repressive genes, *Otx2* and *Gbx2*, express complementarily in and mark the anterior and posterior regions of the neural tube respectively (Simeone et al., 1992; Wassarman et al., 1997). The meeting point of these two gene expression domains is the mes-metencephalon junction, or the mid-hindbrain boundary (MHB) which later develops into an important structure known as isthmic organizer (IsO) which induces the formation of the cerebellum. At E8 when somitogenesis starts, the transcription factor paired box 2 (*Pax2*) is expressed across the *Otx2/Gbx2* border (Rowitch and McMahon, 1995) and the signaling molecule Wnt1 is expressed mainly in the *Otx2*+ region of the mes-metencephalon junction (Bally-Cuif et al., 1995). Slightly later, transcription factor engrailed 1 (*En1*) is expressed at the 1-somite stage, followed by the expression of *En2* and *Pax5* at the 3–5-somite stage. The expression domains of

these 3 genes are similar to that of *Pax2* which crosses the *Otx2/Gbx2* border (Wurst and Bally-Cuif, 2001; Davis and Joyner, 1988; Davis et al., 1988; Asano and Gruss, 1992). The secreted molecule fibroblast growth factor 8 (Fgf8) is also expressed at the 3–5-somite stage, and is restricted to the *Gbx2+* side of the *Otx2/Gbx2* border (Crossley and Martin, 1995).

An organizer is a tissue of the embryo which is capable of inducing the patterning of the neighbouring region into different identities with the release of morphogens. The IsO is a local organizer (secondary organizer) that patterns the mes-metencephalic region by the morphogen Fgf8 (Sotelo, 2004). While the positioning of IsO requires *Otx2* and *Gbx2*, the maintenance of IsO is dependent on the positive regulatory loop formed by Fgf8, Wnt1, En1/2 and Pax2/5/8, which mutually induce each other's expression.

1.5.2.2 Neurogenesis from the ventricular zone

After the specification of the cerebellar region in the hindbrain, the next step of cerebellar development is the differentiation and migration of neurons. Two germinal zones are responsible for the generation of cerebellar neurons (Millen and Gleeson, 2008). The first one is the ventricular zone (VZ) which resides at the base of the cerebellar primordium. Neurogenesis in VZ is marked by the expression of the bHLH transcription factor *Ptf1a* (pancreas transcription factor 1a, Hoshino et al., 2005; Glasgow et al., 2005; Pascual et al., 2007; Sotelo, 2004). Ptf1a-expressing progenitor cells in VZ give rise to all GABAergic neurons in the cerebellum, including Purkinje, Golgi, stellate, basket cells and DCN of GABAergic subtypes. The first neurons that emerge from VZ are DCN and Purkinje cells, with DCN being born slightly earlier than Purkinje cells (Sotelo, 2004). In mouse, Purkinje cells are generated from VZ within 3 days from E11 to E13, and migrate immediately

(between E12 and E15) upward to the cerebellar plate where they are positioned underneath the already migrated DCN and later the external granular layer (Sotelo, 2004). After that, Purkinje cells start to mature and acquire their characteristic appearance.

The interneurons are born much later. Production of Golgi cells begins on E19 and ends on P3 in rat (Altman and Bayer, 1997). Basket and stellate cells are born postnatal from P1 to P15 (Miale and Sidman, 1961). However, at that time, the VZ is no longer proliferative. Indeed, some progenitors from VZ migrate into the white matter and remain mitotically active (Schilling et al., 2008). These precursors are marked by the expression of the transcription factor Pax2 and migrate upward through to the cortex to form the interneurons (Maricich and Herrup, 1999; Sotelo, 2004).

Ptf1a can be considered as the master regulator of GABAergic neuron development as knockout of this gene will cause the neurons in VZ to adopt a glutaminergic fate (Pascual et al., 2007).

The migration of Purkinje cells is dependent on the glycoprotein Reelin which is secreted first by prospective DCN near the pial surface on E13.5, then by granule cells in the EGL (Miyata et al., 1996). In *reeler* mice in which the *reelin* gene is mutated, Purkinje cells fail to migrate upward to form a Purkinje plate (Yuasa et al., 1993). Reelin acts through the receptors very low-density lipoprotein receptor (VLDLR) and apolipoprotein E receptor 2 (apoER2). Upon binding of Reelin, the adaptor protein mammalian disabled (mDab1) is phosphorylated and binds to VLDLR and apoER2. This activates the Reelin signaling pathway essential for proper neuronal migration (Trommsdorff et al., 1999). A recent report suggested that Reelin is required for the orientation change of Purkinje cells necessary for the formation of Purkinje plate (Miyata et al., 2010).

After migration, Purkinje cells start to align into a monolayer and their development is restricted to the projection of axon to DCN or vestibular nuclei (Eisenman et al., 1991) and not until shortly before birth, dendritic differentiation of Purkinje cells begins and leads to the formation of the characteristic dendritic tree (Kapfhammer, 2004).

The dendritic differentiation of Purkinje cells can be divided into four stages (Boukhtouche et al., 2006; Tao et al., 2010). In stage I which is about postnatal day 0, the cells are described as "fusiform", i.e. appear as bipolar shape (Armengol and Sotelo, 1991; Ramon y Cajal, 1926). In stage II, the dendrites regress and the cells start to align into a monolayer. In stage III which is in the first postnatal week, the dendrites elongate again and occupy a perisomatic position. In stage IV which persists from the first postnatal week to the first postnatal month, the dendrites undergo rapid and extensive growth and branching that the characteristic dendritic trees are formed. In the meantime, the circuitry and morphology of the cerebellum also develop, changes include restriction of the dendritic tree of Purkinje cells to its plane of orientation; formation of synapses between Purkinje cell and parallel fibre and inhibitory interneurons; shift of climbing fibre synapses from perisomatic to peridendritic position; elimination of multiple innervation of Purkinje cells from climbing fibre and; maturation of electrophysiological properties of Purkinje cells (Boukhtouche et al., 2006; Kapfhammer, 2004).

The nuclear receptor retinoid-related orphan receptor α (RORα), the protein product of the gene *Rora*, plays an important role in the early stages of dendritic development and functioning of Purkinje cells. In homozygous *staggerer* mice where both alleles of the *Rora* gene are mutated, the number of Purkinje cells is greatly reduced, and the remaining cells are in a primitive state and fail to develop dendrites with spines (Boukhtouche et al., 2006; Vogel et al., 2000). In addition, RORα binds

to the promoter of and activates the expression of *Shh* and *Pcp2* (Gold et al., 2003; Serinagaoglu et al., 2007). Shh from Purkinje cells is a mitogen that stimulates the proliferation of granule cells in the EGL, as evidenced by the rescue of granule cell proliferation in *staggerer* mice with exogenous Shh (Gold et al., 2003). *Pcp2* is involved in signal transduction pathway and encodes a GoLoco domain protein that binds to G-proteins and serves as a guanine nucleotide dissociation inhibitor (Natochin et al., 2001; Willard et al., 2006). Moreover, the expressions of *Pcp4* (a calmodulin inhibitor), *Itpr1* (IP_3 receptor), *Cals* (an *Itpr1* binding partner) and *Calb1* (calbindin, a calcium buffer), which are genes implicated in calcium signaling, are also dependent on RORα (Gold et al., 2003).

The LIM-homeobox genes *Lhx1* and *Lhx5* encode two functionally redundant transcription factors implicated in the differentiation of Purkinje cells. These genes are expressed in precursors that just exit cell cycle and migrate out of VZ. Inactivation of both genes results in severe loss of Purkinje cells, but the specification of granule cells appears normal as indicated by expression of *Math1*. Lhx1 and Lhx5 require the transcriptional coactivator Ldb1 for normal functioning as deletion of *Ldb1* results in similar phenotype with Lhx1/5 double mutant mice (Zhao et al., 2007).

1.5.2.3 Neurogenesis from the rhombic lip

The second germinal zone is the rhombic lip (RL) which is situated at the tip of the posterior end of the cerebellar primordium. It is the region from which all glutamatergic neurons in the cerebellum, including granule cells, unipolar brush cells and a subclass of DCN, are derived (Carletti and Rossi, 2008; Fink et al., 2006).

Between E10.5 and E12.5, DCN are the first to emerge from RL followed by UBCs starting from E13.5 to neonatal period in mice (Hevner et al., 2006). Granule

cells are not actually born in RL, rather, only their precursors are produced, which later migrate tangentially upward to form a secondary germination zone called external granular layer (EGL), where they continue to proliferate until after 2 weeks of postnatal life when this structure disappears (Sotelo, 2004). When they exit cell cycle, they migrate downward to the internal granular layer (IGL).

The development of granule cell can be divided into proliferation phase and differentiation phase. The signaling molecule sonic hedgehog (Shh) is an important requirement for the proliferation of granule cells. The role of Shh is evidenced by the fact that its inhibition results in a great reduction in the production of granule cells and treatment with Shh promotes division of granule cell precursors and prevents them from differentiation (Dahmane and Ruiz i Altaba, 1999; Wallace, 1999; Wechsler-Reya and Scott, 1999). The source of Shh is from Purkinje cells as they express Shh (Traiffort et al., 1998, 1999) under the control of *Rora* (Gold et al., 2003), and the number of granule cells generated is greatly compromised in mutant mice that have impaired Purkinje cells (Das, 1977; Mallet et al., 1979; Sotelo, 2004). The transcription factors *Gli1* and *Gli2*, which are downstream targets of Shh signaling pathway, are expressed in granule cell precursors (Sotelo, 2004).

Besides Shh, the proliferation of granule cell precursors is also controlled by the transcription factors *Zipro1* (formerly known as *Ru49* and *Zfp38*), *Zic1* and *Zic2*. *Zipro1* elevates the proliferation of granule cells and mice overexpressing *Zipro1* were shown to have a larger IGL (Yang et al., 1999). *Zic1* and *Zic2* cooperatively regulate cerebellar development by promoting proliferation and inhibiting differentiation of granule cells, so as to increase the cell population (Ebert et al., 2003). Heterozygous mutant of either *Zic1* or *Zic2* caused a slight reduction of area of granular layer and the combined mutant showed a significant reduction of area of both granular layer and molecular layer. Premature neuronal differentiation was also

observed in the mutant mice (Aruga et al., 2002a). In fact, *Zic1* prevents precursor cells from cell cycle exit (Inoue et al., 2007) and differentiation by activating Notch signaling (Aruga et al., 2002b). It also directly represses the transcription factor *Math1*, which is required for granule cell differentiation, via interaction with the *Math1* enhancer (Ebert et al., 2003).

The switch of proliferation to differentiation of granule cell precursors is mediated by extracellular matrix (ECM) glycoproteins (Pons et al., 2001). In the superficial EGL where precursors are actively dividing, laminin and its integrin receptor subunit α6 are expressed and confer responsiveness to Shh on the cells. On the other hand, vitronectin and its integrin receptor subunit αv are expressed in the inner EGL where post-mitotic granule cells dwell. Vitronectin phosphorylates the transcription factor cyclic-AMP responsive element binding protein (CREB) which induces the differentiation programme of granule cells. Therefore, when the granule cells migrate downward towards the IGL, they interact with ECM of different glycoproteins. Upon interaction with vitronectin, they quickly switch from proliferation to differentiation (Sotelo, 2004).

The migration of granule cells occurs along Bergmann radial glia (Rakic, 1971). Granule cells and Bergmann glia interact through ligand-receptor binding. Migrating granule cells and their precursors in EGL express neuregulin and its receptor erbB4 is expressed in Bergmann fibres (Rio et al., 1997). Activation of erbB4 receptor induces the formation and maintenance of radial glial phenotype of Bergmann glia and thus migration of granule cells (Sotelo, 2004).

After that, the differentiation of granule cells starts and this process is mediated by the bone morphogenesis protein (BMP) signaling (Alder et al., 1999; Qin et al., 2006). In particular, BMP2 antagonizes the proliferative action of Shh and induces the phosphorylation of its signal transducer Smad5 to direct granule cell

differentiation (Rios et al., 2004).

The differentiation of granule cells is also dependent on the bHLH transcription factor *Math1* (mouse atonal homolog 1, also known as *Atoh1*). *Math1* does not only control granule cell differentiation, it is also expressed in neural progenitors in RL (Wang et al., 2005) starting from E10.5 in mice (Akazawa et al., 1995). Thus it can be considered as the master regulator of RL neurogenesis.

During granule cell differentiation, *Math1* directly activates the Bar-class homeobox gene *Mbh1* (also known as *Barhl2*) which is first detected in posterior EGL in E14.5 (Kawauchi and Saito, 2008). *Math1* also activates *Mbh1* in the spinal cord (Saba et al., 2005). A closely related gene *Mbh2* (also known as *Barhl1*) is expressed in the cerebellum starting from E11.5 in the rhombic lip (Kawauchi and Saito, 2008). *Mbh1* and *Mbh2*, which show functional redundancy when co-express, are required at the stage when granule cells migrate from upper RL to form the EGL. In addition, these two genes are required for granule cell differentiation and the activation of the adhesion molecule TAG-1, and the repression of Purkinje cell-specific transcription factor *Lhx5* (Kawauchi and Saito, 2008).

In addition, the transcription factor Paired-box 6 (*Pax6*) is important in the differentiation of granule cells. Beginning from their emergence from the rhombic lip, the granule cells and their progenitors express *Pax6* and persist to maturity (Hevner et al., 2006). Loss of *Pax6* expression results in the failure of granule cell migration and formation of parallel fibres (Hevner et al., 2006; Yamasaki et al., 2001). Interestingly, *Pax6* has two alternatively spliced isoform Pax6 and Pax6-5a, with the latter have an additional 14 amino acids. Pax6 is more abundant in early stages of neurogenesis and the Pax6 : Pax6-5a ratio decreases through development in all parts of the brain (Pinson et al., 2005).

Besides that, the bHLH factor *Neurod1* (also known as *NeuroD*) is required for

the development of granule cells by acting as a switch of proliferation to differentiation (Pan et al., 2009) and as a factor of maintenance of the differentiated state (Miyata et al., 1999).

Differentiation of granule cells is marked by the expression of molecular markers and the projection of their axons, the parallel fibres, which have a characteristic T-shape. Interestingly, the arrangement of parallel fibres in the molecular layer is not random, but is related to the timing of migration of the granule cell progenitors. In particular, the granule cells from the same progenitor will project their axons to a specific narrow stripe in the molecular layer (Zong et al., 2005).

1.6 Scope of the thesis

Regenerative medicine represents a major discipline of modern scientific research which aims to provide long term and complete cure to diseases by replacing damaged tissues and organs. The major challenge in this field is the production of functional target cell types. Transdifferentiation is a promising candidate that provides a direct and technically easy solution suitable for virtually all cell types. Given the importance of the cerebellum in motor, language and cognitive functions, investigation into regeneration of cerebellar neurons is worthwhile and has high medical value. In addition, it will contribute insights into the mechanism of transdifferentiaton which is applicable to other systems.

The work presented in this thesis focuses on the generation of cerebellar Purkinje neurons and granule neurons. Although transdifferentiation of neurons from other somatic cells has been achieved, generation of subtype specific neurons has not been reported at commencement of this thesis.

One approach to derive Purkinje and granule neurons from other somatic cells is by ectopic expression of a cocktail of factors. Most of the reprogramming and

transdifferentiation studies were conducted by exploiting transfection of fibroblasts with exogenous factors. Thus in this study, transdifferentiation is carried out on mouse embryonic fibroblasts by transfection with retroviruses.

To this end, the following aims were designated:

1. To construct expression vectors of Purkinje and granule cell-specific genes for retroviral transfection.
2. To screen for genes that are able and sufficient to induce Purkinje and granule neuronal fate from mouse embryonic fibroblasts.
3. To characterize the molecular properties of the induced cells.

Construction of expression vectors allows the ectopic expression of candidate genes in the fibroblasts. Following identification of combinations of genes that are able and sufficient to induce Purkinje and granule neuronal fate, molecular and morphologic analyses were conducted to determine the extent of transdifferentiation of the induced cells and their resemblance to the target cell types.

CHAPTER 2

MATERIALS

2.1 Materials for Molecular Biological Work

2.1.1 Enzymes

Restriction endonucleases were purchased from New England Biolabs, Inc., USA.

Calf intestinal alkaline phosphatase was purchased from Roche Applied Science, Switzerland.

T4 DNA ligase was purchased from Takara Bio Inc., Japan.

Pfu DNA polymerase was purchased from Promega Corp., USA.

KAPA HiFi DNA polymerase was purchased from Kapa Biosystems, USA.

Reverse transcriptase SuperScript III and LR clonase were purchased from Invitrogen Inc., USA.

2.1.2 Chemicals and others

Bacto-agar, Bacto-tryptone (BD Biosciences, USA)

Yeast extract (USB, Affymetrix, USA)

dNTP (GE Healthcare, USA)

QIAGEN column for plasmid DNA preparation and nucleotide purification (QIAGEN Inc., USA)

Ethidium bromide (EtBr)

Other chemicals and organic solvent of analytical and general purpose grade (Merck & Co., Germany)

Oligonucleotide primers (Integrated DNA Technologies, USA and Tech Dragon Ltd.,

HK)

2.1.3 Plasmid vectors and plasmid

pENTR vector was purchased from Invitrogen Inc., USA

pMXs-Oct4, pMXs-Sox2, pMXs-Klf4 and pMXs-cMyc were kindly given by Dr R. Behringer (M.D. Anderson Cancer Center, The University of Texas, Houston, USA)

2.1.4 Solutions and media

Luria Broth (LB)

0.5% (w/v) Bacto yeast extract

1% (w/v) Bacto tryptone

1% (w/v) NaCl

LB-Kan

LB with 5% (w/v) Kanamycin

LB-Amp

LB with 10% (w/v) Ampicillin

LB-Agar

LB with 1.5% (w/v) Bacto-agar

LB-Amp-Agar

LB-Kan-Agar

LB-Amp-Cm-Agar

GTE

50mM glucose

10mM Na_2EDTA

25mM Tris-HCl, pH 8.0

Lysis Buffer

0.2N NaOH

1% (w/v) SDS

KAc (for alkaline acetate)

5M K^+

3M Ac^-

(60ml of 5M KAc + 11.5ml of glacial acetic acid + 28.5ml of water)

Phenol

Phenol/Chloroform

1X TAE Buffer for electrophoresis

40mM Tris-acetate

2mM Na_2EDTA

(adjusted pH to 7.85 with glacial acetic acid)

PBS

170mM NaCl

3.4mM KCl

4.0mM Na_2HPO_4

2.3mM KH_2PO_4

(adjusted to pH 7.2)

2.2 Materials for Tissue/Cell Culture

2.2.1 Chemicals

DMEM, DMEM/F12, PBS, penicillin/streptomycin (P/S, 100X stock), glutamine, non-essential amino acid (NEAA, 10mM, 100X stock) were purchased from Invitrogen Inc., USA.

Fetal bovine serum was purchased from Biosera Ltd, UK.

2-mercaptoethanol, gelatin, insulin, transferrin, sodium selenite, progesterone, putrescine, FGF2, puromycin, blasticidin were purchased from Sigma-Aldrich Co., USA

Poly-D-lysine was purchased from Millipore, USA.

2.2.2 Culture media and solutions

DMEM for culture of MEF

DMEM

10% FBS

1mM L-glutamine

1X NEAA

1X P/S

DMEM for culture of Plat-E cells

DMEM

10% FBS

1mM L-glutamine

1μg/mL puromycin

10μg/mL blasticidin

1X P/S

DMEM for transfection of Plat-E cells

DMEM

10% FBS

1mM L-glutamine

1X NEAA

N3 medium for culture of neurons

DMEM/F12

25μg/ml Insulin

50μg/ml Transferrin

30nM Sodium selenite

20nM Progesterone

100nM Putrescine

10ng/ml FGF2

1X P/S

2X Freezing medium

DMEM

20% DMSO

40% FBS

2.2.3 Culture cells

Plat-E cells were purchased from Cell Biolabs Inc., USA

2.3 Animals

Mice used in this research were supplied by Laboratory Animal Service Centre, The Chinese University of Hong Kong.

2.4 Materials for Immunocytochemistry

Mouse monoclonal antibody against Tuj1 was purchased from Covance Inc., USA.

Mouse monoclonal antibodies against GAD67 and MAP2, rabbit polyclonal antibodies against calbindin D28-K, Lhx1 and brain lipid binding protein (BLBP) were purchased from Millipore, USA.

Rabbit polyclonal antibody against Pax2 was purchased from Invitrogen Inc., USA.

Goat polyclonal antibody against $GABA_AR\alpha6$ was purchased from Santa Cruz Biotechnology, Inc., USA.

Alexa 488-goat anti-mouse Ig, Alexa 568-goat anti-rabbit Ig, Alexa 488-donkey anti-goat Ig were purchased from Invitrogen Inc., USA.

2.5 Oligonucleotide Primers

Primer	Sequence (5' to 3')	Position[a]	Purpose
Ptf1a fw	TTTGTCGACATGGACGCCGTACTCC TGGA	199-218	Cloning
Ptf1a rv	TTTCTCGAGCTCAGGACACAAACT CAAAGGGTGGT	1149-1174	Cloning
Lhx1 fw	TTTGTCGACATGGTGCACTGTGCGG GCTGCAAAA	1360-1384	Cloning
Lhx1 rv	TTTCTCGAGCTACCACACGGCTGCC TCGTTCATTTCA	2553-2580	Cloning
Lhx5 fw	TTTGTCGACATGATGGTGCACTGTG CTGGCTGTGA	396-420	Cloning
Lhx5 rv	TTTCTCGAGAACCCACGAGAGGAC TCTTGAGGCTT	1663-1688	Cloning
Ldb1 fw	TTTGTCGACACCATGCTGGATCGGG ATGT	648-667	Cloning
Ldb1 rv	TTTCTCGAGTTCACTGGGAAGCCT GTGACGT	1758-1779	Cloning
Ebf2 fw	TTTGTCGACATGTTTGGGATTCAAG ATACGCTAGG	970-995	Cloning
Ebf2 rv	TTTCTCGAGTTACATCGGGGGAACA ACAAGTC	2675-2697	Cloning
Rora fw	TTTGTCGACAAAACATGGAGTCAG CTCCGGCA	1-23	Cloning
Rora rv	TTTGATATCTTACCCATCGATTTGCA TGGCTGG	1554-1577	Cloning
Math1 fw	TTTGTCGACAGCCATTGCAGTGCGA TGT	163-181	Cloning
Math1 rv	TTTCTCGAGCTAACTGGCCTCATCA GAGTCACT	1210-1233	Cloning
Mbh1 fw	TTTGTCGACGAAATGACAGCAATG GAAGGGGCCA	323-347	Cloning
Mbh1 rv	TTTCTCGAGTGCCTCTATTCCAGTT GGTTTGGTGC	1559-1584	Cloning
Mbh2 fw	TTTGTCGACATGGAAGGCTCTAATG GCTTTGGG	743-766	Cloning
Mbh2 rv	TTTCTCGAGAGCCTCAGTGAATTTC TCCCACAC	1841-1864	Cloning

Pax6 fw	TTTGTCGACTCCAGCATGCAGAAC AGTCACA	520-541	Cloning
Pax6 rv	TTTCTCGAGCCACATAGTCATTGGC AGAGTGAACAC	1875-1901	Cloning
Zipro1 fw	TTTGTCGACTCTGTGATGACTAAGG TGGTGGGCATGG	266-293	Cloning
Zipro1 rv	TTTCTCGAGAGACGAGAATGGACC GTTACTGGACT	1930-1955	Cloning
En2 fw	TTTGGATCCATGGAGGAGAAGGAT TCCAAGCCCA	832-856	Cloning
En2 rv	TTTCTCGAGATTGCATTGTTTCTCG CGGCCCTA	1845-1868	Cloning
Foxp2 fw	TTTGTCGACATGATGCAGGAATCTG CGACAGAG	660-683	Cloning
Foxp2 rv	TTTCTCGAGTCATTCCAGGTCCTCA GATAAAGGC	2780-2804	Cloning
Sox4 fw	TTTGGATCCATGGTACAACAGACCA ACAACGC	662-684	Cloning
Sox4 rv	TTTCTCGAGTCAGTAGGTGAAGAC CAGGTTAGAG	1960-1984	Cloning
Neurog2 fw	TTTGTCGACCCGCGTAGGATGTTCG TCAAATCTGA	306-331	Cloning
Neurog2 rv	TTTCTCGAGAGCTCTAGATACAGTC CCTGGCGA	1087-1110	Cloning
Neurod6 fw	TTTGTCGACATGTTAACACTACCGT TTGACGAGTCTGTC	322-351	Cloning
Neurod6 rv	TTTCTCGAGAATTACGCAGCCCACA AGCATCTG	1392-1415	Cloning
Aes fw	TTTGTCGACATGATGTTTCCGCAAA GCCGG	83-103	Cloning
Aes rv	TTTCTCGAGCTAATCCGACTTCTCT CCGTCATCCT	651-676	Cloning
Zic1 fw	TTTGTCGACATGCTCCTGGACGCCG GACCCCAGTAT	783-809	Cloning
Zic1 rv	TTTGATATCACCCCCTTCCGCCCTTC AGCTACCAA	2396-2421	Cloning
Zic2 fw	TTTGTCGACGCGCTGGCCATGCTTC TGGA	284-303	Cloning

Zic2 rv	TTTCTCGAGGGCCCCTCACACGTAC CATTCATTGAAGT	1860-1888	Cloning
Csrp2 fw	TTTGTCGACATGCCTGTCTGGGGCG GTGGAAATAA	81-106	Cloning
Csrp2 rv	TTTCTCGAGTCTCTGTCGTGCTTAC TGGGTTCACACC	664-691	Cloning
Ascl1 fw	TTTGTCGACATGGAGAGCTCTGGC AAGATGGA	573-595	Cloning
Ascl1 rv	TTTCTCGAGTCAGAACCAGTTGGTA AAGTCCAGCAG	1242-1268	Cloning
Myt1l fw	TTTGTCGACATGGACGTGGACTCTG AGGAGAA	907-929	Cloning
Myt1l rv	TTTGATATCTCAGACCTGAATTCCT CTCACAGCCT	4439-4464	Cloning
Brn2 fw	TTTGTCGACATGGCGACCGCAGCG TCTAACCACTA	1-26	Cloning
Brn2 rv	TTTCTCGAGTCACTGGACGGGCGT CTGCAC	1318-1338	Cloning
Neurod1 fw	TTTGTCGACATGACCAAATCATACA GCGAGAGCGG	98-123	Cloning
Neurod1 rv	TTTCTCGAGCTAATCGTGAAAGATG GCATTAAGCTGGGC	1142-1171	Cloning
Pax6-5a fw	TCCCGAATTCTGCAGACCCATGCA	652-675	Cloning
Pax6-5a rv	CAGCACCTGGACTTTTGCATCTGC	673-696	Cloning
Pax6 rv new	TTTCTCGAGCTCCTTCTCTCTTTACT GTAATCGAGGCCAGT	1817-1848	Cloning
pMXs-1624	TCTCTACTTAGTCCAGCACGAAGT	1624-1647[b]	Sequencing
pENTR rev seq	GTAACATCAGAGATTTTGAGACAC	2106-2129[c]	Sequencing
pENTR fw seq	CCAGGCATCAAACTAAGCAGAAGG	263-286[c]	Sequencing
Recomb confirm	TGAATTGGTTCCTTTAAAGCCTGCT	1942-1966[b]	Recombination confirmation

a: Position in the reference sequence of mRNA unless otherwise specified

b: Position with reference of the sequence of pMXs-X vector.

c: Position with reference of the sequence of pENTR1A vector

2.6 RNA Extraction

Total RNA was extracted from mouse tissue by TRIZOL reagent according to manufacturer's instructions. Tissues were dissected out and weighed. Every 50-100mg tissue was homogenized in 1ml of TRIZOL reagent by pipetting up and down or using a homogenizer. The homogenized tissues were incubated at room temperature for 5 min. 0.2ml of chloroform per 1ml TRIZOL reagent was added to the mixture. The samples were shaken vigorously by hand for 15 seconds and were incubated at room temperature for 2-3 min. The samples were centrifuged at 12000× *g* for 15 min at 4℃.

After centrifugation, the aqueous supernatant was transferred to a new tube and the RNA was precipitated using 0.5ml of isopropanol per 1ml TRIZOL reagent used. The samples were incubated at room temperature for 10 min followed by centrifugation at 12000× *g* for 10 min at 4℃.

After centrifugation, the supernatant was discarded and the RNA pellet was washed once with 1ml of 75% ethanol per 1ml TRIZOL reagent used. The samples were centrifuged at 7500× *g* for 5 min at 4℃. The supernatant was discarded and the pellet was air dried for 5-10 min. The RNA was dissolved in DEPC-treated water and the concentration was determined by measuring the absorbance at 260nm. RNA samples were stored at –80℃.

2.7 Generation of cDNA from mRNA

First strand of cDNA was synthesized using SuperScript III First-Strand Synthesis System (Invitrogen) according to manufacturer's instructions. Briefly, 4μg of RNA was reverse transcribed using oligo$(dT)_{20}$ primer (2.5μM) with 200 units of SuperScript III reverse transcriptase at 50℃ for 50 min in 20μl buffer containing 20mM Tris-HCl (pH 8.4), 50mM KCl, 5mM $MgCl_2$, 10mM DDT, 40 units of

RNaseOUT and 0.5mM dNTP. The reverse transcriptase activity was stopped by heating the reaction mixture at 85℃ for 5 min. The cDNA generated was stored at –20℃.

2.8 Preparation of Recombinant Plasmid DNA

Recombinant DNA isolation from transformed bacterial cultures was based on the alkaline lysis method, with different modifications for different purposes.

2.8.1 Small scale preparation of DNA

Rapid and crude isolation method

This method was used to isolate DNA for restriction endonuclease digestion analysis and to check the identity of a single transformed bacterial colony.

Bacterial culture (1ml) was centrifuged at maximum speed and the pellet was resuspended in GTE (0.1ml), and then lyzed by lysis buffer (0.2ml) followed by precipitation by KAc (0.15ml) on ice. The lysate was centrifuged and the supernatant was collected. DNA was precipitated from the supernatant with 2.5 volume of 100% ethanol, pelleted by centrifugation, then washed once with 70% ethanol, air dried and dissolved in water.

QIAGEN Plasmid miniprep kit method

This method was used to isolate DNA for sequencing analysis.

Experimental procedures were done according to manufacturer's instructions. Briefly, a single bacteria colony was cultured in LB (3ml) with antibiotics for overnight until saturation. The culture was centrifuged and the pellet was resuspended in Buffer P1 (0.25ml) and lyzed with Buffer P2 (0.25ml) followed by

precipitation by Buffer N3 (0.35ml). The lysate was centrifuged at maximum speed for 10 min and the supernatant was transferred to a QIAGEN spin column. The DNA was isolated by binding to the silica membrane in the column by centrifugation, and then washed once with Washing Buffer containing 75% ethanol. The DNA was eluted in 30μl water.

2.8.2 QIAGEN Plasmid midiprep kit method

This method was used to prepare DNA in large amount and for transfection.

Experimental procedures were carried out according to manufacturer's instructions. Briefly, a single bacteria colony was first cultured in LB (5ml) with antibiotics for 6 hours and then transferred to 100ml LB for overnight culture until saturation. The culture was centrifuged at 6000× *g* for 15 min at 4℃ and the pellet was resuspended in Buffer P1 (4ml). The cells were then lyzed with 4ml Buffer P2 and incubated at room temperature for 5 min. The lysate was precipitated by chilled Buffer P3 and incubated on ice for 15 min. After that, the lysate was centrifuged at ≥20000× *g* for 30 min at 4℃. The supernatant was centrifuged again at ≥20000× *g* for 15 min at 4℃. The supernatant was allowed to flow through and bind to the QIAGEN Anion Exchange Resin by gravity before the DNA was washed twice with Buffer QC and eluted in 5ml Buffer QF. The eluted DNA was precipitated in 3.5ml isopropanol before centrifuged at ≥15000× *g* for 30 min at 4℃. The supernatant was decanted and the pellet was washed once with 2ml 70% ethanol and centrifuged at ≥15000× *g* for 10 min. The DNA pellet was dissolved in 200μl water.

2.9 Preparation of Specific DNA Fragment from Agarose Gel

DNA digested with specific restriction endonucleases was electrophoresized in 1% (w/v) agarose gel in 1X TAE buffer. The desired DNA fragment was cut out with

the size of the agarose gel slice minimized. DNA was purified by using Gel Extraction Kit (QIAGEN) according to manufacturer's instructions. Briefly, the agarose gel slice was melted in PB buffer at 50℃. The solution was made acidic by adding 10μl NaAC (pH 5) if necessary. The DNA was purified by binding to the silica membrane of the spin column by centrifugation, and then washed once with Washing Buffer containing 75% ethanol. The DNA was eluted in 30μl water. The concentration of the DNA was estimated by loading 1μl sample in agarose gel.

2.10 Subcloning of DNA Fragments

2.10.1 Preparation of cloning vectors

Vector DNA was completed digested by specific restriction endonucleases to produce unique cuttings in the multiple cloning sites of the vector. The reaction mixture was gel electrophoresized and the desired DNA fragment was purified as described in Section 3.4.

In case of end-filling of sticky ends was needed, Klenow fragment (1 unit/1μg of vector DNA) with 0.3mM dNTP in buffer containing 50mM Tris (pH 7.5), 10mM $MgCl_2$, 1mM DDT, 50μg/ml BSA was added to the digested vector DNA and incubated at 37℃ for 30 min.

The vector DNA obtained was dephosphorylated by incubating with 3 units of calf intestine alkaline phosphatase in buffer containing 50mM Tris-HCl (pH8.5), 0.1mM EDTA at 37℃ for 1 hour. The reaction was heat inactivated by adding 1μl of 0.5M EDTA and incubating at 75℃ for 10 min. The reaction mixture was then made up to at least 100μl. The DNA was purified by mixing vigorously with equal volume of phenol/chloroform and then centrifuged at maximum speed for 5 min. DNA was precipitated from the supernatant by mixing with 1/10 volume of 3M NaAc (pH 5.2)

and 2.5 volume of 100% ethanol and incubating at –20℃ for overnight. The reaction mixture was centrifuged at maximum speed for 5 min and the supernatant was discarded. The pellet was washed once with 70% ethanol and air dried before being dissolved in 30μl water.

2.10.2 Subcloning of DNA fragment

Ligation between dephosphorylated DNA vector and insert DNA was performed with Takara DNA ligation kit by incubating at 16℃ for 18 hours. The volume ratio of total DNA and ligation kit was 1:1 and the molecular ratio of vector DNA to insert DNA was maintained at 1:3 for sticky end-sticky end ligation, 1:5 for sticky end-blunt end ligation and 1:10 for blunt end-blunt end ligation.

2.10.3 Transformation of DNA into competent cells

The ligation mixture was mixed with the competent cells and incubated on ice for 30 min. Competent cells-DNA mixture was heat shocked at 42℃ for 1 min to allow the entry of exogenous DNA into the cells, and then incubated on ice for 3 min before 1ml LB medium was added and incubated at 37℃ for 1 hour. The transformed cells were pelleted by centrifugation at 4000× *g* for 1 min. The pellet was resuspended in 0.1ml LB medium and plated onto LB agar plate with antibiotics. Plates were incubated at 37℃ for 18 hours.

2.11 Preparation of Competent Cells

Saturated bacteria culture (100ml) was prepared from a single bacterial colony. It was subcultured 1:50 in 50ml of LB medium and was grown until OD_{550} reached 0.45. The culture was incubated on ice for 10 min and then centrifuged at 1000× *g* at 4℃ for 10 min. The pellet was resuspended in 12.5ml of ice-cold 0.1M $MgCl_2$.

The suspension was centrifuged again at 1000× *g* at 4℃ for 10 min, and the pellet was resuspended in 12.5ml of 0.1M $CaCl_2$. The suspension was then centrifuged in the same conditions and the pellet was finally resuspended in 0.1M $CaCl_2$ with 14% glycerol (25ml). The bacterial suspension was aliquoted (150μl) and stored in –70℃.

CHAPTER 3

GENERATION AND CHARACTERIZATION OF INDUCED NEURONS

3.1 Introduction

A key area of research into the healing of neuronal diseases is regenerative medicine. This strategy of therapy can, for instance, help patients suffering from neural injuries such as stroke and neurodegenerative diseases such as Parkinson's and Alzheimer's diseases to recover from the damage by transplanting functional neurons generated *in vitro*. Regenerative medicine is regarded as a promising therapy because unlike the traditional drug treatments and training which only relieve and slow down the development of some of the symptoms for a limited time frame, it allows long term cure to the diseases and better improvement to patients' cognitive and motor abilities. The success of this regenerative medicine is limited by the amount and specificity of neuronal tissues that can be generated. Moreover, since most neurons in mammals are quiescent and neural stem cells are only found in limited regions of the nervous system, the mammalian nervous system basically lacks regenerative capacity. Thus, it is necessary to adopt sources of cells outside the nervous system for this cell-based therapy.

Several reports have described the generation of specific cerebellar neurons from embryonic stem (ES) cells (Muguruma et al., 2010; Salero and Hatten, 2007; Su et al., 2006; Tao et al., 2010). However, the use of ES cells is controversial, and many of these reports used serum and co-culture system which made the culture conditions highly variable. Although induced pluripotent stem (iPS) cells can help bypass some controversies over ES cells, this technology is not well established,

hindering its full application. Another way to generate neurons is by direct differentiation (Vierbuchen et al., 2010). However, the neurons generated were a mixed population composed of different subtypes, with the majority being excitatory neurons. Thus, there is a great need to discover new methods to, on one hand, avoid ethical controversy, and on the other hand, produce neurons that are patient specific and subtype specific.

The work presented in this thesis focused on the generation of specific neuronal subtypes, cerebellar Purkinje cells and granule cells, from mouse embryonic fibroblasts (MEF) by direct transdifferentiation. We have identified some essential factors for cell fate switch from MEF to cerebellar neural cells and their effects on the extent of transdifferentiation. The mechanism of transdifferentiation is also addressed. Based on the present findings, we propose that *Ptf1a* and *Rora* are essential for transdifferentiation from MEF to Purkinje cells with characteristics of early phase of development.

3.2 Experimental Procedure

3.2.1 Construction of expression vectors

3.2.1.1 Preparation of insert DNA

Open reading frame (ORF) of the target genes were obtained from cDNA of E13.5, P0 or 8 weeks old mice's forebrain, midbrain and cerebellum by PCR using high fidelity DNA polymerases (*Pfu* (Promega), *Phusion* (Finnzymes) and KAPA HiFi (Kapa Biosystems)).

3.2.1.2 Construction of entry vectors

The vector pENTR1A (Invitrogen) was cut with either *Sal*I/*Xho*I, *Sal*I/*Eco*RV or *Bam*HI/*Xho*I. The 2260 bp backbone fragment containing kanamycin resistance gene, pUC replication origin and attL1/attL2 recombination sites was purified from agarose gel and then dephosphorlyated. Insert DNA of target genes were cut with either *Sal*I/*Xho*I, *Sal*I/*Eco*RV or *Bam*HI/*Xho*I and was ligated to pENTR1A vector to produce the entry vector pENTR-X (Fig. 3.1). Selection of successfully ligated clones were done by transforming the ligation mixture into DH5α *E. coli* and the cells were plated onto LB-Kan agar plates.

3.2.1.3 Construction of destination vectors

Moloney Murine Leukemia Virus (MMLV)-based retroviral vector (pMXs) was employed in the current study. To construct the destination vector pMXs-gwRfA (Gateway Reading Frame Cassette A), pMXs-Oct4 vector which was a pMXs vector available in our laboratory was cut with *Bam*HI/*Not*I restriction endonucleases to remove the original Oct4 gene. The 4.6 kb fragment containing ampicillin resistance gene, pBR332 replication origin and MoMuLV LTR was gel purified and end-filled. Gateway Reading Frame Cassette A (Invitrogen) was ligated to the vector to complete the construction (Fig. 3.2). This vector was propagated in special *E. coli* strain (One Shot® ccdB Survival™ 2 T1^{R} Competent Cells, Invitrogen) which were resistant to *ccdB*.

3.2.1.4 Construction of expression vectors

To construct expression vectors pMXs-X, LR-recombination was performed between 75ng of entry vectors and 75ng of destination vector with LR clonase

(Invitrogen) according to manufacturer's instructions (Fig. 3.3). Briefly, entry vector and destination vector were mixed and the volume of reaction was made up to 4μl. 1μl of LR clonase was added and the reaction mixture was incubated at room temperature for 2 hours. The reaction was inactivated by incubating with 0.5μl of proteinase K at 37℃ for 10 min. The reaction mixture was then transformed into DH5α *E. coli* and the cells were plated onto LB-Amp agar plates. Only bacteria containing the expression vector could survive on ampicillin containing plates. Cells containing the destination vector (pMXs-gwRfA) and donor vector would be killed by the *ccdB* gene while cells containing the entry vector (pENTR-X) could not survive in the presence of ampicillin. The production of expression vector was confirmed by PCR.

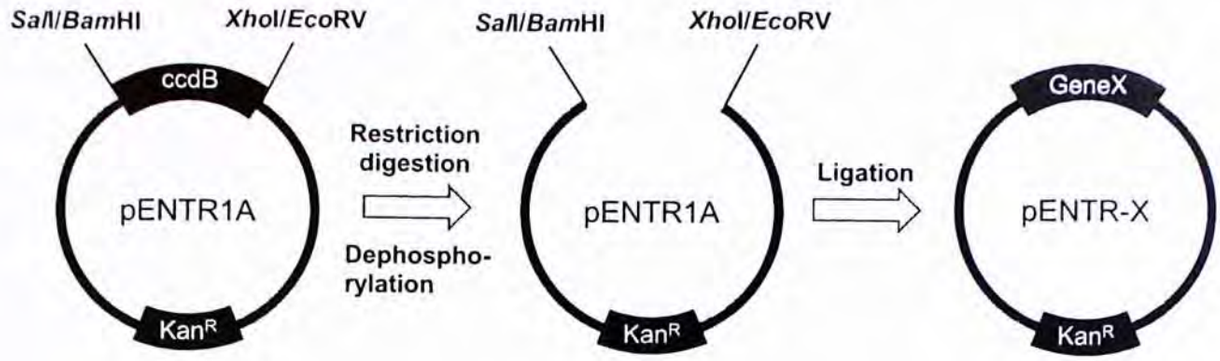

Fig. 3.1 Construction of entry vector. pENTR1A vector was cut with *SalI*/*Xho*I, *SalI*/*Eco*RV or *Bam*HI/*Xho*I and the fragment containing *ccdB* gene was removed. *ccdB* targets DNA gyrase and is toxic in common *E. coli* strain such as DH5α. The vector backbone was dephosphoylated before ligation with the ORF of the candidate genes. Kan^R, kanamycin resistance gene; X, candidate gene.

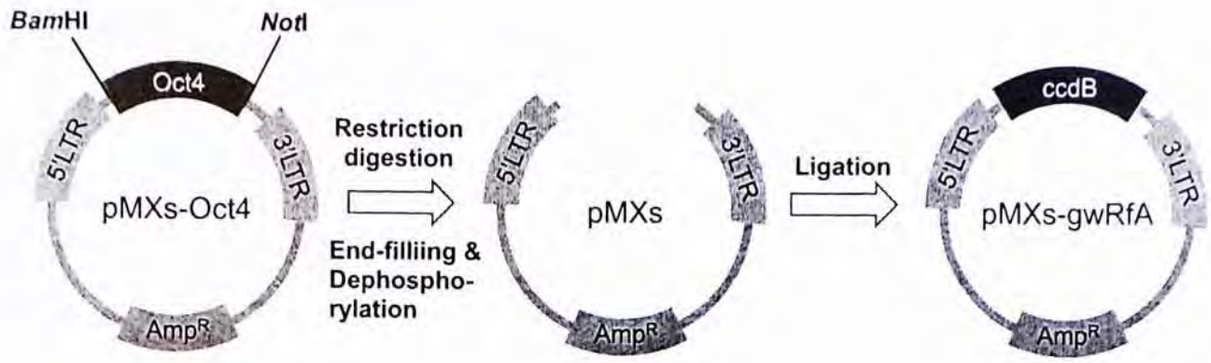

Fig. 3.2 Construction of destination vector. pMXs-Oct4 was cut with *Bam*HI and *Not*I to release the Oct4 ORF. The restriction sites were end-filled and dephosphorylated before ligation with the Gateway Reading Frame Cassette A (Invitrogen) which contains *ccdB* gene for negative selection. The long terminal repeat (LTR) functions as the promoter to drive gene expression. Amp^R, ampicillin resistance gene.

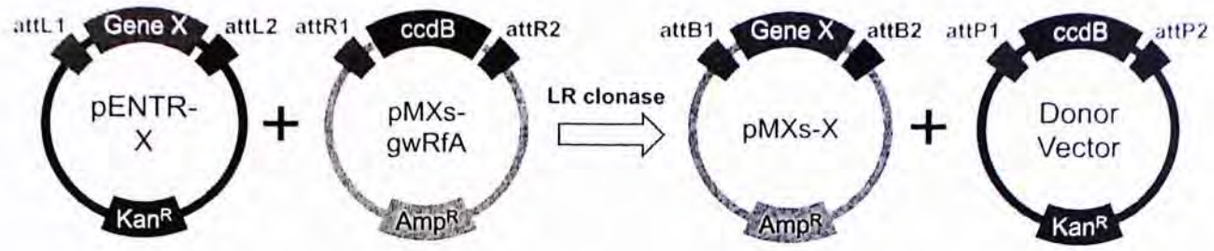

Fig. 3.3 Construction of expression vector. The expression vector pMXs-X was produced from the site specific recombination of entry vector pENTR-X and destination vector pMXs-gwRfA. In the presence of LR clonase, recombination occurred between attL1 and attR1 as well as between attL2 and attR2 such that the ORF of candidate genes on entry vector exchanged position with the Gateway cassette on the destination vector. The whole reaction mixture was transformed into DH5α *E. coli* and the cells were plated onto LB-Amp agar plates. Only bacteria containing the expression vector could survive on ampicillin containing plates. Cells containing the destination vector (pMXs-gwRfA) and donor vector would be killed by the *ccdB* gene while cells containing the entry vector (pENTR-X) could not survive in the presence of ampicillin. attL1/2, attR1/2, attB1/2 and attP1/2 are sites for recombination. Amp^R, ampicillin resistance gene; Kan^R, kanamycin resistance gene; X, ORF of candidate genes.

3.2.2 Generation of induced neural cells

3.2.2.1 Culture of mouse embryonic fibroblasts (MEF)

Mouse embryos of age E13.5 from cross between C57BL6 mice were collected. The head, spinal cord and visceral mass of the embryos were removed to prevent contamination of neurons or neural progenitors. The remaining tissues were minced in the presence of 0.25% trypsin to isolate single cell. MEF from 1 embryo were seeded on one 10-cm culture dish. The MEF were allowed to grow to 90% confluent and then split once before being frozen. After thawing, the MEF were cultured on 10-cm plates until confluent before splitting onto plates for transfection.

3.2.2.2 Production of expression vector containing retroviruses

Retrovirus packaging Platinum-E (Plat-E) cells (Morita et al., 2000) were grown to 70-80% confluence without antibiotics. To transfect Plat-E cells, 27μl of Fugene 6 transfection reagent (Roche) was equilibrated in 300μl DMEM at room temperature for 5 min. 9μg of expression vectors of target transgenes was then mixed with the Fugene 6-DMEM mixture and incubated at room temperature for 15 min. The DNA-Fugene 6 mixture was then applied to Plat-E cells drop by drop. After one day, the media of Plat-E cells were discarded and new media were added. After one day, the media containing retrovirus were collected and filtered through a 0.45μm syringe filter. For every 10ml filtered media, 5μl of 8mg/ml polybrene was added before applying to the MEF. New media were added to Plat-E cells for second collection of medium in the next day.

3.2.2.3 Transfection and induction of neural fate of MEF

MEF were thawed and cultured on 10-cm plates until confluent before being

harvested and plated onto wells of 6-well plates or onto 10-cm plates pre-coated with poly-D-lysine at density of 1.33×10^5 cells/well or 8×10^5 cells/10-cm plate respectively. Media containing retroviruses with expression vectors prepared as described in section 3.2.2.2 were applied to the MEF twice in two days. After one day of the final transfection, medium of MEF was changed to MEF medium without antibiotics. After one day, the medium was changed to complete MEF medium. After one day and onwards, transfected MEF were cultured in N3 medium (Wernig, et al. 2002). The medium was changed every 2-3 days.

3.2.3 Immunocytochemcial anaylsis

For immunostaining, induced neural cells were washed twice in PBS for 5 min before fixed in 4% PFA in PBS for 10 min. The samples were washed in PBS and made permeable by incubating in 0.2% Trition-X in PBS for 5 min at room temperature. The samples were then blocked in 4% BSA and 1% sheep serum (or horse serum in case the antibody is of goat origin) in PBS for 30 min at room temperature and probed with primary antibodies overnight at 4 ℃. Mouse monoclonal antibodies used: anti-Tuj1 (diluted 1:500 in 4% BSA/1% serum, Covance). Rabbit polyclonal antibodies used: anti-calbindin D-28K (1:500, Millipore) and anti-Lhx1 (1:500, Millipore). Goat polyclonal antibody used: anti-$GABA_AR\alpha6$ (1:150, Santa Cruz). After incubation, the samples were washed three times in PBS, and probed with Alexa 488 or 576 conjugated goat anti-mouse or rabbit antibodies, or donkey anti-goat antibody (diluted 1:1000 in 4% BSA/1% serum, Invitrogen) for 30 min at room temperature in dark. The samples were then washed three times in PBS and counter stained with Hoechst 33342 (diluted 1:1000 in PBS) in dark for 5 min at room temperature. The samples were finally washed in PBS three times and

mounted with glycerol. The staining signals were observed under a fluorescence microscope (Olympus).

3.2.4 Efficiency calculation

The performance of induction by different factor combinations was evaluated in two aspects. The first aspect was the neuronal conversion efficiency which quantified the conversion of fibroblasts into cells showing neuronal properties by the factor combinations. The definition of neuronal properties was that cells were stained positive for Tuj1 and displayed morphology with processes at least 3 times longer than the cell body (for simplicity, these cells were called Tuj1+ cells). To calculate the efficiency of neuronal conversion from fibroblasts for each factor combination, photos were taken from 30 randomly selected ×10 fields. The total number of cells showing neuronal properties and the total number of cells present, determined by the number of nuclei stained by Hoechst were determined in all 30 photos. The conversion efficiency was calculated by $\frac{\text{Total number of Tuj1+cells counted}}{\text{Total number of nuclei counted}}$.

The second aspect was the Purkinje cell induction efficiency which quantified the induction of Purkinje cell properties in the induced neurons by the factor combinations. The expression of calbindin and Lhx1 was used as an indicator for the display of Purkinje cell properties in the evaluation. To calculate the induction efficiency of Purkinje cell properties in induced neuronal cells, the number of cells that co-expressed Tuj1 and calbindin or Lhx1 was determined from the same 30 photos. In the 30 photos, 15 were cells stained with calbindin and 15 were cells stained with Lhx1. The individual induction efficiency of each calbindin and Lhx1 was determined by $\frac{\text{Total number of calbindin+or Lhx1+cells}}{\text{Total number of Tuj1+cells in 30 fields}}$. The combined induction

efficiency of both calbindin/Lhx1+ cells was determined by $\frac{\text{Total number of calbindin+ and Lhx1+cells}}{\text{Total number of Tuj1+cells in 30 fields}}$.

Fig. 3.4 summarizes the experimental procedures of expression vector construction, retrovirus production and neural fate induction in MEF.

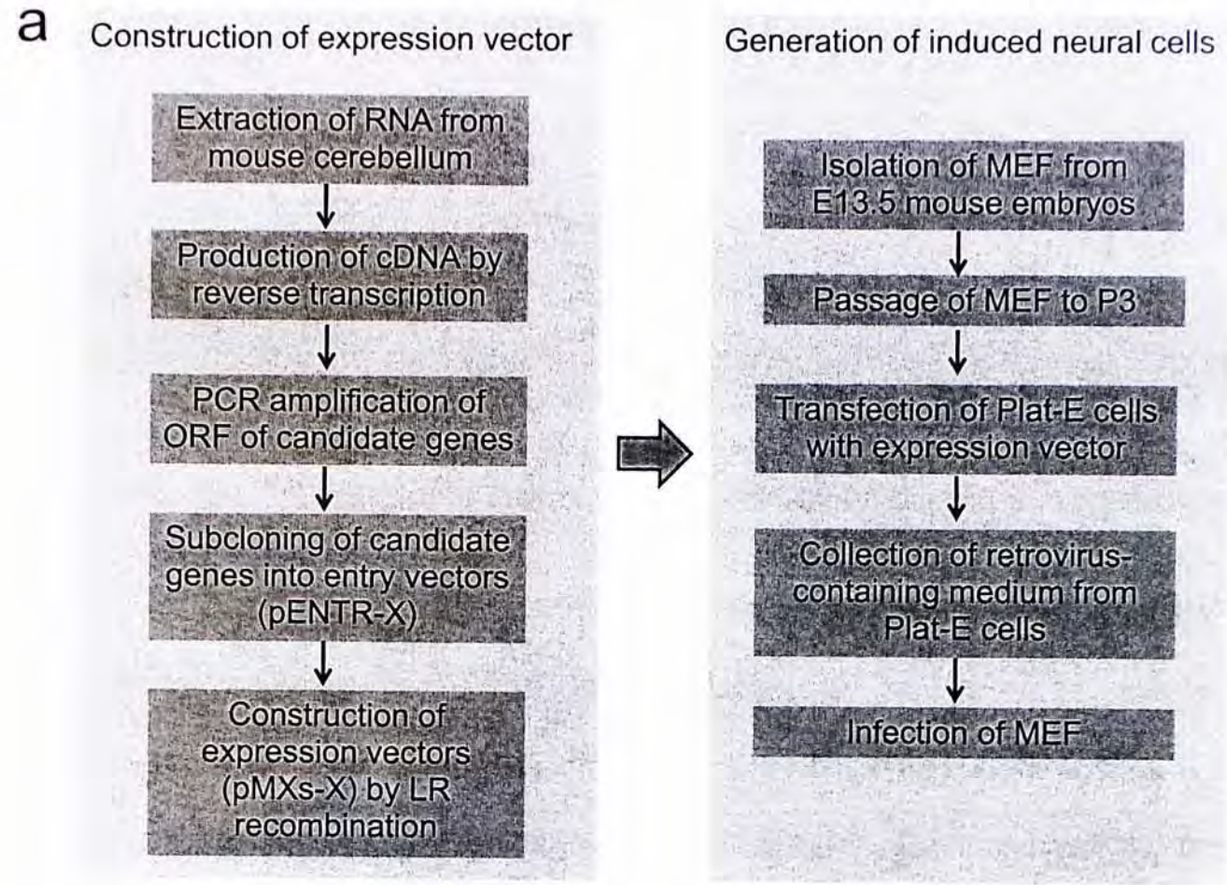

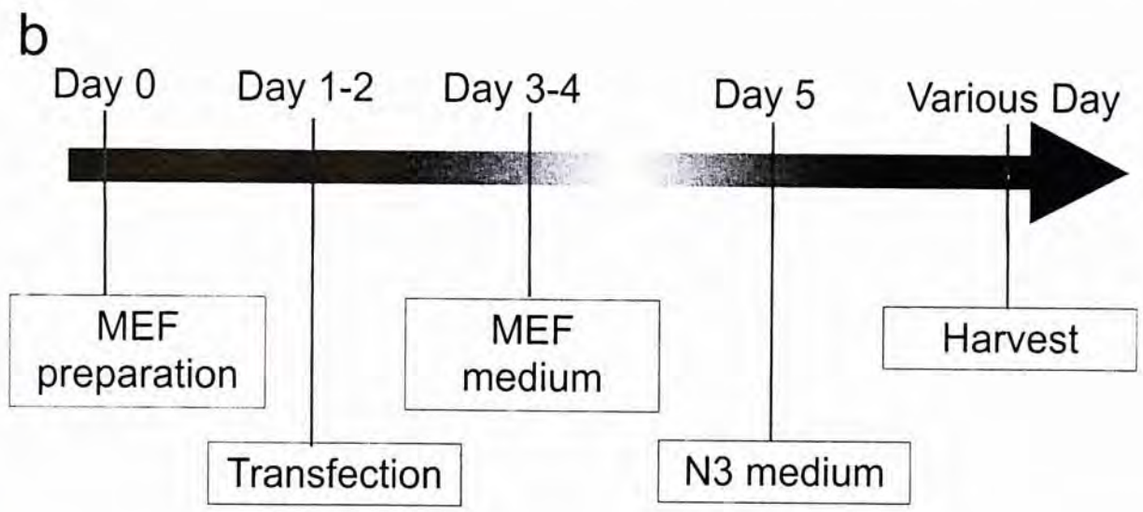

Fig. 3.4 Summary of the experimental procedures. (a) Procedures for preparatory work for generation of induced neural cell, including construction of expression vectors for candidate genes expression and production of retrovirus-containing medium for MEF infection. (b) Timeline for induction of neural fate in MEF. The time line is applicable for both Purkinje cell and granule cell induction.

3.3 Results

3.3.1 A screen for cerebellar Purkinje and granule cell fate-inducing factors

In light of generation of iPS cells (Takahashi and Yamanaka, 2006) and previous experiments demonstrating that expression of transcription factors could induce cell fate switch of differentiated cell types (Davis et al., 1987; Xie et al., 2004; Vierbuchen et al., 2010; Ieda et al., 2010), it is hypothesized that ectopic expression of core transcription factors characteristic to Purkinje and granule cells can also induce the transdifferentiation of differentiated fibroblasts to the desired cell types. In order to identify the transcription factors that are essential for the induction, a pool of candidate factors was first set up for each of Purkinje cells and granule cells. The candidate factors were selected mainly based on the gene annotation from Gene Ontology. The transcription factors that are under the annotation "cerebellar Purkinje cell differentiation" or "cerebellar granule cell differentiation" (retrieved on October 2009) were included in the initial pool of candidate genes (Table 3.1). Transcription factors that have been shown to be specifically expressed in Purkinje or granule cells in other literatures, and the 3 genes that have been shown to directly convert somatic cells to neurons, *Ascl1*, *Brn2* and *Myt1l*, were also included (Vierbuchen et al., 2010).

6 factors were included in the candidate pool for Purkinje cell induction. Among these, 5 factors came from Gene Ontology and one, *Ptf1a*, was selected because it was shown to a play important role in Purkinje cell development (Glasgow et al., 2005; Pascual et al., 2007). For granule cell induction, 15 factors were included in the candidate pool. Among these, 11 factors came from Gene Ontology and 3 factors, *Zic1*, *Csrp2* and *Neurod1*, were included because they were shown to be specifically expressed in the cerebellum (Schuller et al., 2006). The last one, *Math1*, was selected

because it was shown to control granule cell differentiation (Gazit et al., 2004).

At the start of the experiment, cDNA of 4 factors for Purkinje cells and 14 factors for granule cells were successfully subcloned into expression vector and were used for induction. For Purkinje cell induction, all possible combinations of the 4 factors were tested (Table 3.2). Meanwhile, because the granule cell pool contained a larger number of genes, besides an all-factor induction, only several factors that were thought to be more important based on literature review were selected (Table 3.3).

Table 3.1 Candidate factor pool for Purkinje cell and granule cell transdifferentiation

For Purkinje cell transdifferentiation			
Gene	**RefSeq ID**	**Reference**	**Subcloned in expression vector**
Ptf1a	NM_018809.2	Glasgow et al., 2005	Yes
Lhx1	NM_008498.2	Gene Ontology	No
Lhx5	NM_008499.5	Gene Ontology	Yes
Ldb1	NM_010697.1	Gene Ontology	No
Ebf2	NM_010095.5	Gene Ontology	Yes
Rora	NM_013646.1	Gene Ontology	Yes
For granule cell transdifferentiation			
Gene	**RefSeq ID**	**Reference**	**Subcloned in expression vector**
Math1	NM_007500.4	Gazit et al., 2004	Yes
Mbh1	NM_001005477.1	Gene Ontology	Yes
Mbh2	NM_019446.4	Gene Ontology	Yes
Pax6	NM_013627.4	Gene Ontology	Yes
Zipro1	NM_011757.2	Gene Ontology	Yes
En2	NM_010134.3	Gene Ontology	Yes
Foxp2	NM_053242.4	Gene Ontology	No
Sox4	NM_009238.2	Gene Ontology	Yes
Neurog2	NM_009718.2	Gene Ontology	Yes
Neurod6	NM_009717.2	Gene Ontology	Yes
Aes	NM_010347.3	Gene Ontology	Yes
Zic1	NM_009573.3	Schuller et al., 2006	Yes
Zic2	NM_009574.3	Gene Ontology	Yes
Csrp2	NM_007792.4	Schuller et al., 2006	Yes
Neurod1	NM_010894.2	Schuller et al., 2006	Yes
Genes that have been shown to directly convert MEF to neurons			
Gene	**RefSeq ID**	**Reference**	**Subcloned in expression vector**
Ascl1	NM_008553.4	Vierbuchen et al., 2010	Yes
Brn2	NM_008899.1	Vierbuchen et al., 2010	No
Myt1l	NM_008666.3	Vierbuchen et al., 2010	No

Table 3.2 Factor combinations tested for Purkinje cell transdifferenatiaton

4-factor	**3-factor**	**2-factor**	**1-factor**
Ptf1a, Ebf2, Rora, Lhx5 (PERL)[a]	Ptf1a, Ebf2, Rora (PER)[a]	Ptf1a, Ebf2	Ptf1a
	Ptf1a, Ebf2, Lhx5 (PEL)[a]	Ptf1a, Rora	Ebf2
	Ptf1a, Rora, Lhx5 (PRL)[a]	Ptf1a, Lhx5	Rora
	Ebf2, Rora, Lhx5 (ERL)[a]	Ebf2, Rora	Lhx5
		Ebf2, Lhx5	
		Rora, Lhx5	
Total: 15 combinations			

a: Letter codes in brackets were abbreviations of the factor combinations.

Table 3.3 Factor combinations tested for granule cell transdifferentiation

Math1, Mbh1, Mbh2, Pax6, En2, Sox4, Neurog2, Neurod1, Neurod6, Aes, Zic1, Csrp2, Ru49, Zic2 (14F)[a]
Math1, Mbh1, Mbh2, En2, Sox4, Neurog2, Neurod1, Neurod6, Aes, Zic1, Csrp2, Ru49, Zic2 (14F without Pax6) (13F)[a]
Math1, Pax6, Neurog2, En2, Zic1 (5F)[a]
Pax6, Neurog2, En2, Zic1 (PGEZ)[a]
Math1, Pax6 Neurog2, En2 (MPGE)[a]
Pax6, Neurog2, En2 (PGE)[a]
Math1, Pax6, Neurog2 (MPG)[a]
Pax6, Neurog2 (PG)[a]
Total: 8 combinations

a: Letter codes in bracket were abbreviations of factor combinations

3.3.2 Characterization of the induced neurons

The characterization of induced neurons aimed to determine the neuronal and subtype properties based on morphological and molecular criteria. The induced cells in both experimental sets of Purkinje and granule cell induction were considered to have neuronal properties if they possessed processes at least 3 times longer than the cell body and expressed the pan-neuronal marker Tuj1 (Chatzi et al., 2011; Morikawa et al., 2009).

The induced cells were considered to have mature Purkinje cell properties if they had a large number of outgrowths from the cell bodies, because genuine Purkinje cells have an extensive dendritic tree, and if they expressed the marker proteins calbindin, a cytoplasmic calcium binding protein, and Lhx1, a transcription factor. Meanwhile, possession of T-shaped axons and the expression of α6 subunit of the ionotropic $GABA_A$ receptor ($GABA_A\alpha6$) were the criteria for characterization of granule cells.

3.3.2.1 Granule cell induction

Immunostaining on 20 days after transgene transfection showed that 5 out of 8 combinations of candidate factors (14F, 13F, 5F, *Pax6-Neurog2-En2* (PGE), *Pax6-Neurog2* (PG), see Table 3.3 for abbreviations; n=1) could induce the fibroblasts to express Tuj1 and adopt neuronal morphology, with the combination "*Pax6- Neurog2- En2- Zic1*" (PGEZ), "*Math1- Pax6- Neurog2- En2*" (MPGE) and "*Pax6- Neurog2- Math1*" (PGE) being the exceptions (Fig. 3.5). The majority of Tuj1+ cells from all combinations displayed simple neuronal morphology with a central cell body and 2-4 processes. However, none of the cells stained positive for $GABA_A\alpha6$, nor did they display the characteristic T-shaped axon of granule cells.

This indicated that the induction of granule cell fate from fibroblasts was incomplete. The efficiency of conversion to Tuj1+ cells from MEF was only recordable in the combination 5F which attained 0.310%. Since the induction of granule cell fate was not satisfactory, we only focused on the generation of Purkinje cells in further experiments.

14F
13F
5F
a
b
c
d
e
f
g
h
i
j
k
l
m
n
o
p
Tuj1
GABA$_A$Rα6
Hoechst
Tuj1/GABA$_A$Rα6/Hoechst

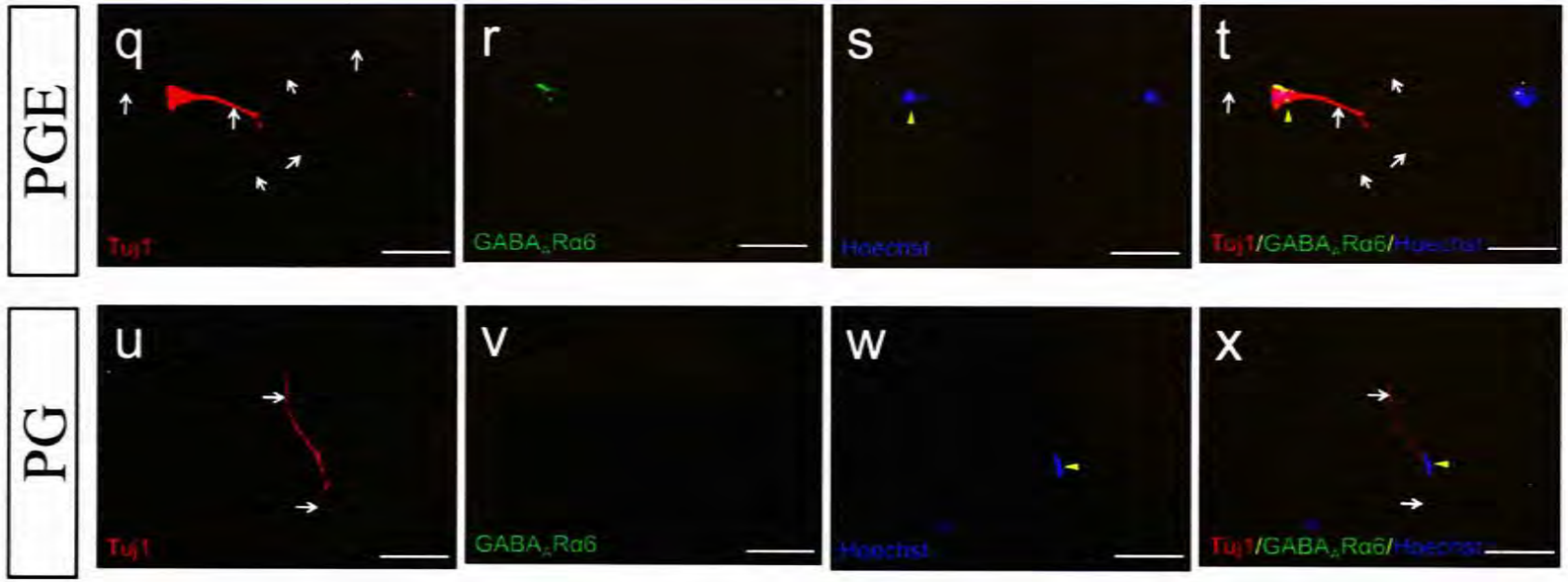

Fig. 3.5 Conversion of Tuj1+ from MEF by candidate factors of granule cell's pool. The induced cells were stained with pan-neuronal marker Tuj1 (a,e,i,m,q,u) and granule cell marker $GABA_AR\alpha6$ (b,f,j,n,r,v). The nuclei were visualized by Hoechst 33342 (H33342) (c,g,k,o,s,w). Only 4 out of 8 factor combinations demonstrated induction of Tuj1+ cells. (a-d) A Tuj1+ cell with simple morphology induced by 14F. (e-h) A Tuj1+ cell with 4 neurite outgrowths induced by 13F. (i-p) 5F achieved the highest efficiency of Tuj1 induction in MEF among all experimental groups of factors of granule cell's pool. (q-t) A Tuj1+ cell induced by *Pax6-Neurog2-En2* (PEG) displayed outgrowths with branches. (u-x) A bipolar-shaped Tuj1+ cell induced by *Pax6-Neurog2* (PG). Combinations not shown here were unable to induce the expression of Tuj1. No combination could induce the expression of $GABA_AR\alpha6$ or production of a characteristic T-shaped axon. Arrows depict the neurites and arrowheads depict the nuclei. Scale bar: 50μm.

3.3.2.2 Purkinje cell induction

4-factor induction

For Purkinje cell induction, immunostaining was carried out on 17, 20 and 28 days after transfection (each time point n=1). The ability of the factors to induce the expression of the Tuj1, and thus the ability to drive the MEF to neuronal lineage, was first assessed. When all four factors (*Ptf1a*, *Ebf2*, *Rora* and *Lhx5*) were transfected, a small number of cells (0.055%±0.048%) were stained Tuj1+ with various degree of complexity (Table 3.4, Fig. 3.6 and 3.7). This indicated that some factors in this pool could induce expression of Tuj1 and adoption of neuronal morphology in MEF. In order to deduce the relative importance of neuronal induction of each factor, omission of one factor from the pool was performed.

3-factor induction

Interestingly, the removal of any one of the 4 factors led to an increase in the conversion efficiency, indicating that the 4 factors together might have an inhibitory effect on neuronal induction. The most efficient conversion was achieved by the omission of *Ebf2* (PRL, 0.674%±0.218%). Omission of *Lhx5* achieved the second highest efficiency among all 3-factor groups (PER, 0.350%±0.185%), but was nearly half the value of that of PRL. The conversion efficiencies of ERL and PEL were 0.268% ±0.218% and 0.173%±0.122% respectively (Table 3.4, Fig. 3.6 and Fig. 3.8-3.11). Both PRL and PER contained the factors *Ptf1a* and *Rora*, their relatively high conversion efficiencies might indicate the importance of these 2 factors in neuronal induction.

2-factor induction

To further evaluate the contribution of each factor, all 2-factor combinations were tested. Consistent with the above observation, the highest conversion efficiency among the 2-factor induction was attained by *Ptf1a-Rora* (0.441%±0.263%). *Ptf1a-Ebf2* attained the second highest efficiency (0.259%±0.146%), followed by *Ebf2-Lhx5* (0.205% ± 0.084%), *Rora-Lhx5* (0.159% ± 0.080%), *Ptf1a-Lhx5* (0.132%±0.102%) and *Ebf2-Rora* (0.037%±0.052%) (Table 3.4, Fig. 3.6 and 3.12-3.17).

1-factor induction

Next, the ability of single factor to induce neuronal fate switch was tested. Surprisingly, all the 4 factors alone could induce the MEF to show some neuronal properties. Among them, *Ptf1a* was the best inducer with conversion efficiency reaching 0.384%±0.160%. *Rora* followed with efficiency of 0.184%±0.155%. *Ebf2* and *Lhx5* achieved efficiencies of 0.145% ± 0.074% and 0.070% ± 0.058% respectively (Table 3.4, Fig. 3.6 and 3.18-3.21).

Control experiments were set up to validate the results. Some MEF were left uninfected to confirm the phenotypes observed in experimental groups were due to the ectopic expression of the transgenes. Controls without primary antibody were also set up for each secondary antibody used (Alexa 488 conjugated goat anti-mouse Ig and Alexa 576 conjugated anti-rabbit Ig). In this control experiment set, PRL was used as this factor combination gave rise to cells with neuronal characteristics at highest efficiency. Only secondary antibodies were applied to determine whether they specifically bind to primary antibodies. No Tuj1+ cell or cell displaying

neuronal morphology was observed in uninfected MEF and no positive staining was observed when primary antibodies were absent (Fig. 3.22).

Induction of neuronal properties

The most efficient conversion was achieved by PRL. When *Lhx5* was also omitted, or when *Lhx5* was replaced by *Ebf2*, the efficiencies only dropped slightly. This indicated that both *Ptf1a* and *Rora* were important in the induction of neuronal fate. Consistent with this, the omission of either *Ptf1a* or *Rora* caused a more significant reduction in neuronal conversion. In fact, 3 out of the top 4 combinations with the most efficient Tuj1 induction included both *Ptf1a* and *Rora*. The dependence on *Ptf1a* and *Rora* was also reflected in the fact that *Ptf1a* and *Rora* alone induced Tuj1 expression better than the other 2 factors.

Lhx5 alone or with one more factor showed relatively low conversion efficiency, but displayed the highest efficiency together with *Ptf1a* and *Rora*. The improvement was also noticed in *Ebf2-Rora* (a 7.29-fold increase in ERL). This indicated that *Lhx5* alone was not sufficient or essential to induce neuronal fate, but acted synergistically to enhance the effect of other factors, especially *Rora*.

The effect of *Ebf2* in neuronal induction was ambiguous. In some cases, the omission of *Ebf2* resulted in an improvement in conversion efficiency, implying an inhibitory effect exerted by this gene (compare PRL vs PERL; *Ptf1a-Rora* vs PER; *Rora* vs *Ebf2-Rora*; *Ptf1a* vs *Ptf1a-Ebf2*). However, in the presence of *Lhx5*, the omission of *Ebf2* caused a decrease in the conversion (compare *Ptf1a-Lhx5* vs PEL; *Rora-Lhx5* vs ERL; *Lhx5* vs *Ebf2-Lhx5*). This might suggest cooperation in function between *Ebf2* and *Lhx5*. Therefore, other parameters had to be assessed to determine the suitability of *Ebf2* in Purkinje cell induction.

Induction of Purkinje cell properties

The expression of pan-neuronal marker Tuj1 only indicated the fate switch from mesodermal MEF to ectodermal neurons. However, the subtypes of the induced cells were not implicated. In an attempt to determine the similarity of induced Tuj1+ cells to Purkinje cells in terms of molecular marker expression, calbindin and Lhx1 were stained. The efficiency of induction of expression of these two proteins was only recordable in 7 groups. Surprisingly, *Ebf2*, which did not have a prominent effect in neuronal conversion, achieved the highest induction efficiency of Purkinje cell markers in Tuj1+ cells. About 83.3%±23.57% of the Tuj1+ cells were also stained positive for calbindin or Lhx1. The second highest was *Rora-Lhx5* which attained 75%±35.36%, followed by *Ptf1a* (50%±40.82%), *Rora* and *Ptf1a-Ebf2* (both 33.3%±47.14%), *Ptf1a-Lhx5* (22.2%±31.43%) and PRL (4.76%±6.734%) (Table 3.4 and Fig. 3.23). It is intriguing to note that the efficiencies were higher with less factor transfected. Only 3 out of 6 2-factor groups and 1 out of 4 3-factor groups showed recordable induction. When calbindin and Lhx1 were separately considered, it can be seen that all combinations showed expression of Lhx1, but only *Ebf2*, *Ptf1a*, *Rora* and *Rora-Lhx5* showed expression of calbindin (Table 3.4 and Fig. 3.23). The ratio of calbindin and Lhx1 expression was similar, with Lhx1 being slightly higher. Although the efficiency of calbindin/Lhx1 induction was not recorded in the other 8 groups, cells double-stained with Tuj1 and calbindin/Lhx1 were still occasionally noticed in those groups. In general observation, more Tuj1- and calbindin/Lhx1-doubly stained cells arose from those combinations containing the gene *Rora*. In fact, all combinations consisting *Rora* could give rise to Tuj1 and calbindin/Lhx1 double positive cells (Fig. 3.7-3.21).

Induction of complexity

Different factor combinations did not only induce neuronal transdifferentiation at varying efficiencies, but also with different complexities in morphology and organization. The complexity of morphology refers to the number and branching of neuronal processes (Fig. 3.24). Most Tuj1+ cells displayed simple morphology of "fusiform", that is, bipolar shaped (Fig. 3.25). However, some patterns were observed when each factor was analyzed individually. In general, all combinations containing the factor *Ptf1a*, whether 1-,2-, 3-factor, tended to give rise to Tuj1+ cells with more processes extending from the cell bodies, and the processes were more branched than those cells from combinations that did not include *Ptf1a* (Fig. 3.7-3.21). On average, Tuj1+ cells induced by *Ptf1a*-containing combinations produced 3.922 ± 2.583 processes while 3.194 ± 1.656 were produced in non-*Ptf1a*-containing combinations. Interestingly, the presence of *Ebf2*, *Rora* or *Lhx5* tended to cause a reduction in number of processes produced (Table 3.5 and Fig. 3.26). Tuj1+ cells in *Ebf2*-containing combinations produced 3.296 ± 1.876 processes compared to 3.854 ± 2.500 in non-*Ebf2*-containing groups. Cells induced by *Rora*-containing groups produced 3.368 ± 1.788 processes compared to 4.187 ± 3.001 in groups without *Rora*. 3.452 ± 1.933 processes were produced in *Lhx5*-containing groups while 3.897 ± 2.693 were produced in combinations without *Lhx5*. The combination PERL was not included in the statistics as the contribution of each factor could not be compared.

On the other hand, the complexity of organization can be revealed by the number of cells interacting with each other (Fig. 3.24). Again, when *Ptf1a* was in pool, more Tuj1+ cells appeared as cluster rather than solitary. An average of 1.941 ± 1.934 cells appeared together when *Ptf1a* was present while 1.479 ± 1.070

cells appeared when it was absent. *Ebf2* also tended to increase the complexity of organization. An average of 2.011 ± 2.008 cells was contacting each other *Ebf2*-containing induction while the number was 1.610 ± 1.402 when *Ebf2* was omitted. 1.902 ± 2.005 cells were in contact with each other in *Lhx5*-containing combinations while 1.575 ± 1.037 cells were recorded in non-*Lhx5*-containing groups. *Rora* had no effect on the complexity as 1.753 ± 1.507 and 1.783 ± 1.958 cells were in contact when it was present or absent respectively (Table 3.5 and Fig. 3.27).

Although the "fusiform" made up the majority of Tuj1+ cells, some cells displaying more mature Purkinje cells morphology with the extensive neurite outgrowths were occasionally observed. One cell induced by *Ptf1a* alone and one by *Lhx5* were similar to Purkinje cells at stage III of dendritic development, with several highly branched processes extending from the somata (Fig. 3.18i-l and Fig. 3.21i-l). They were not classified as stage IV as the branches did not come from a single outgrowth from the soma. A cell from *Ptf1a-Rora* group showed characteristics of early stage IV, but had degenerated before the time of fixation (Fig. 3.28).

From the above results, *Ptf1a* and *Rora* were the most important factors in Purkinje cell induction. Combinations containing these 2 factors attained higher efficiency of conversion to Tuj1+ cells with higher complexity and better Purkinje cell properties. *Lhx5* had a synergistic effect on *Ptf1a* and *Rora*, thus this gene may also be included. Although *Ebf2* had a prominent effect in calbindin/Lhx1 induction, it showed an inferior effect in the induction of Tuj1 and morphological complexity. As Tuj1 expression is the prerequisite for neuronal fate acquisition, to strike a balance, *Ebf2* seemed to be dispensable.

Table 3.4 Conversion efficiency (%) of Tuj1+ cells and calbindin/Lhx1+ cells (out of Tuj1+ cells) by candidate factors for Purkinje cell transdifferentiation

Combination of factors	Tuj1+		calbindin+		Lhx1+		calbindin/Lhx1+	
	%[a]	SEM[d]	%[b]	SEM[d]	%[b]	SEM[d]	%[c]	SEM[d]
PERL	0.055	0.048	0	0	0	0	0	0
PER	0.350	0.185	0	0	0	0	0	0
PEL	0.173	0.122	0	0	0	0	0	0
PRL	0.674	0.218	0	0	4.762	6.734	4.762	6.734
ERL	0.268	0.218	0	0	0	0	0	0
Ptf1a-Ebf2	0.259	0.146	0	0	33.33	47.14	33.33	47.14
Ptf1a-Rora	0.441	0.263	0	0	0	0	0	0
Ptf1a-Lhx5	0.132	0.102	0	0	22.22	31.43	22.22	31.43
Ebf2-Rora	0.037	0.052	0	0	0	0	0	0
Ebf2-Lhx5	0.205	0.084	0	0	0	0	0	0
Rora-Lhx5	0.159	0.080	41.67	42.49	33.33	47.14	75.00	35.36
Ptf1a	0.384	0.160	16.67	23.57	33.33	23.57	50.00	40.82
Ebf2	0.145	0.074	33.33	47.14	50.00	40.82	83.33	23.57
Rora	0.184	0.155	16.67	23.57	16.67	23.57	33.33	47.14
Lhx5	0.070	0.058	0	0	0	0	0	0

a: See Section 3.2.4 for calculation of conversion efficiency of Tuj1+ cells.

b: See Section 3.2.4 for calculation of conversion efficiency of calbindin+ and Lhx1+ cells.

c: See Section 3.2.4 for calculation of conversion efficiency of calbindin/Lhx1+ cells.

d: SEM, standard error of the mean.

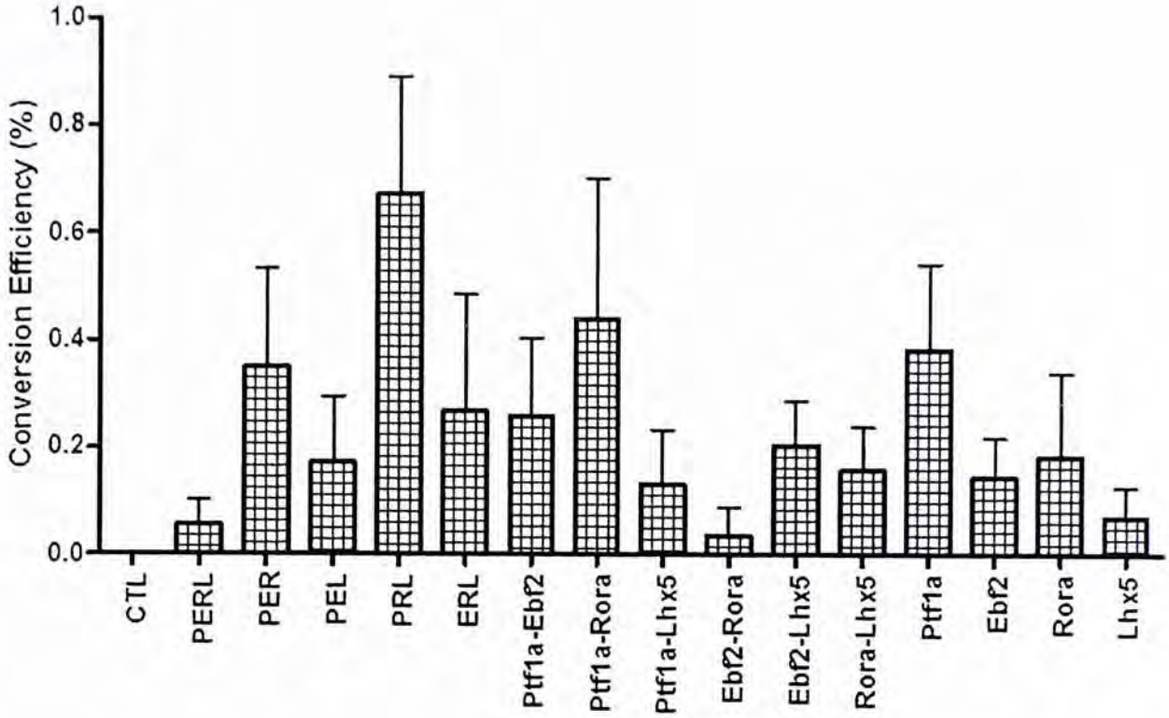

Fig. 3.6 Conversion efficiency of Tuj1+ cells from MEF by candidate factors of the Purkinje cell pool. All combinations of factors could induce the expression of the pan-neuronal marker Tuj1, and those with *Ptf1a* and *Rora* tended to have a higher efficiency. Lhx5 had a weak inducing power but acted synergistically with *Rora*. Effect of *Ebf2* was ambiguous. Uninfected MEF (CTL) did not show Tuj1 expression. n=3; Error bar: SEM

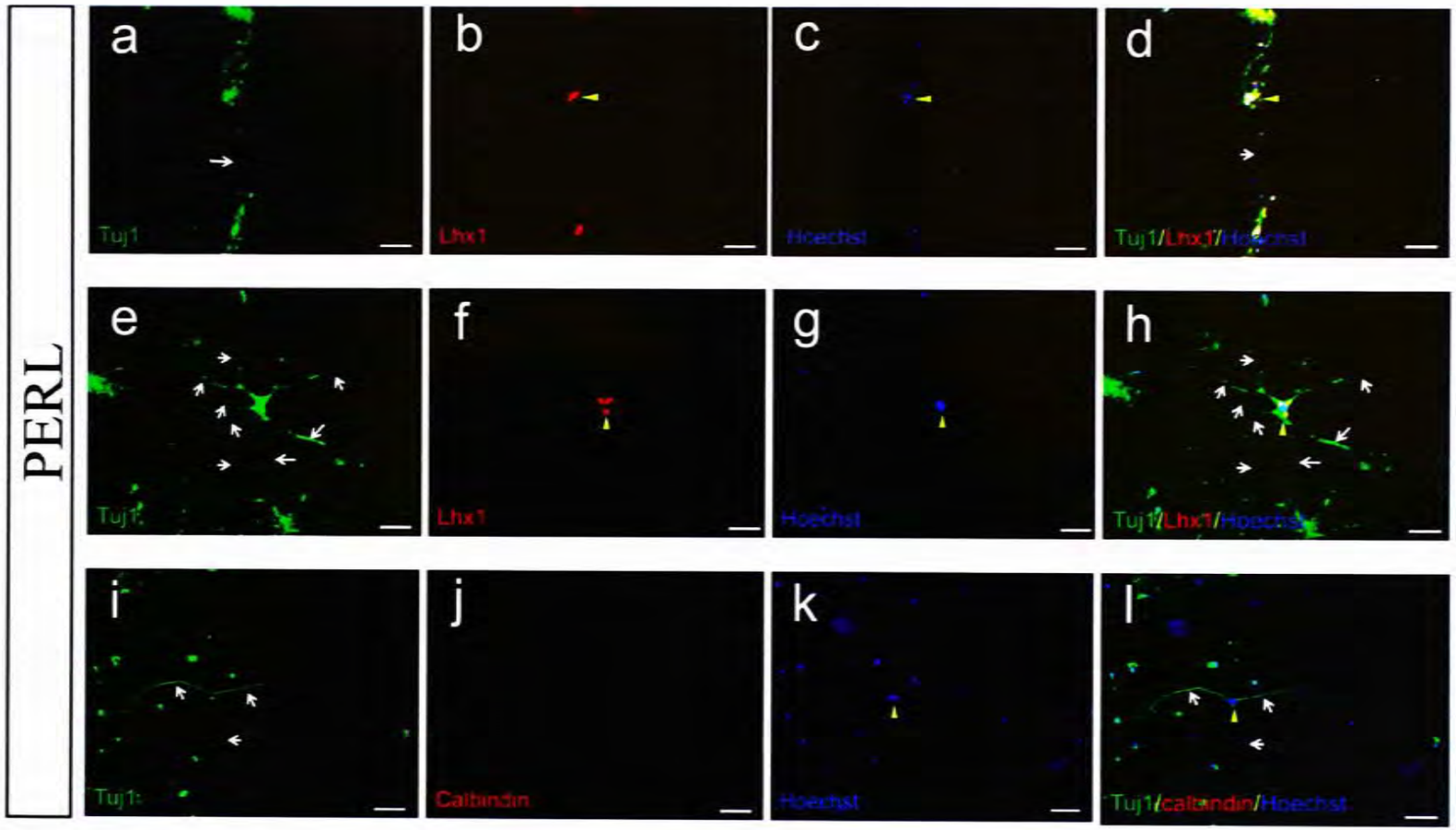

Fig. 3.7 Conversion of MEF to Tuj1+ cells displaying neuronal morphology by PERL. The induced cells were stained with pan-neuronal marker Tuj1 (a,e,i) and Purkinje cell marker calbindin or Lhx1 (b,f,j). The nuclei were visualized by Hoechst 33342 (H33342) (c,g,k). (a-d) A Tuj1/Lhx1 double positive cell with simple morphology. (e-h) A Tuj1/Lhx1 double positive cell with more complex morphology, showing 8 processes and branches (arrows) extending from the cell body. (i-l) A Tuj1+ cell with simple morphology, but failed to express calbindin in the processes. Arrows depict the neurites and arrowheads depict the nuclei. Scale bar: 50μm.

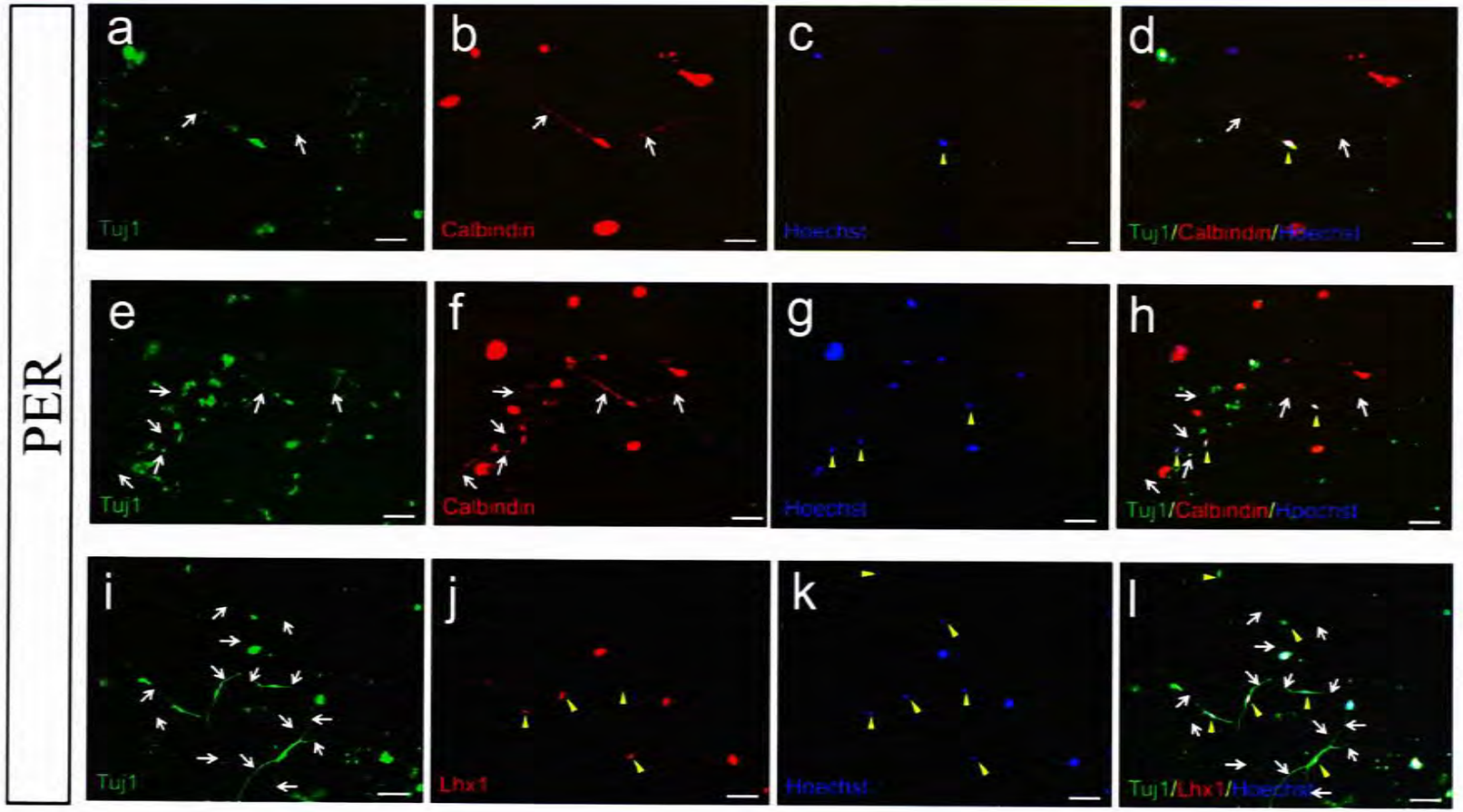

Fig. 3.8 Conversion of MEF to Tuj1+ cells displaying neuronal morphology by PER. The induced cells were stained with Tuj1 (a,e,i) and calbindin or Lhx1 (b,f,j). The nuclei were visualized by H33342 (c,g,k). Co-expression of Tuj1 and calbindin (a-h) or Lhx1 (i-l) demonstrated the efficient induction of Purkinje cell properties in *Rora*-containing factor combination. (e-h) High complexity of organization in *Ptf1a*-containing factor combination exemplified by the presence of 3 cells (e-h, arrowheads) and 6 cells (i-l, arrowheads) contacting each other. Arrows depict the neurites and arrowheads depict the nuclei. Scale bar: 50μm.

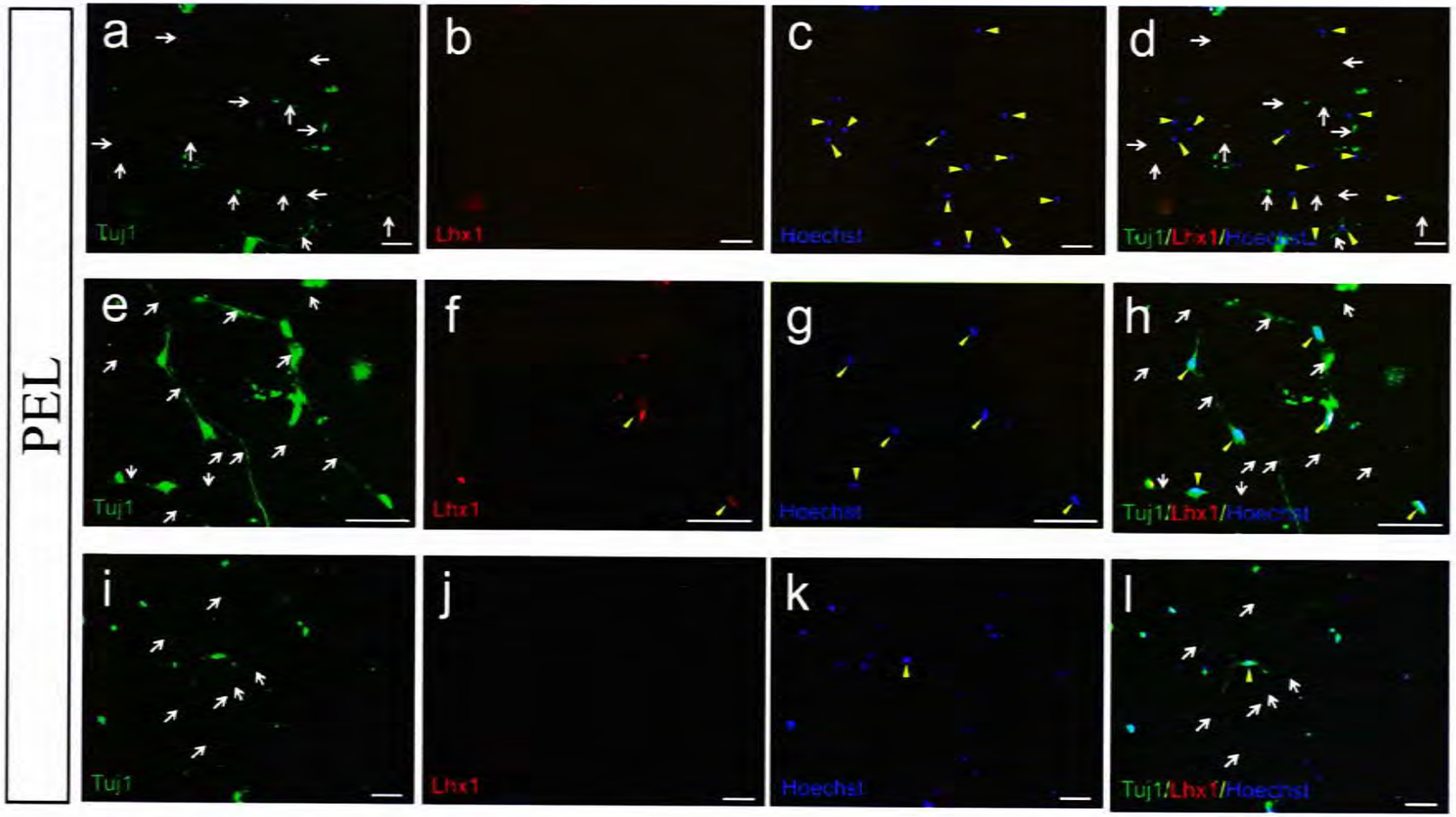

Fig. 3.9 Conversion of MEF to Tuj1+ cells displaying neuronal morphology by PEL. The induced cells were stained with Tuj1 (a,e,i) and Lhx1 (b,f,j). The nuclei were visualized by H33342 (c,g,k). Calbindin+ cells were undetected. Absence of *Rora* might cause the failure of induction of Purkinje cell markers. Induction of high complex of organization (a-h) and morphology (i-l) by *Ptf1a*-containing factor combination. (a-d) 12 cells (arrowheads) were in contact and formed a network-like organization. (e-h) 6 cells (arrowheads) were contacting each other. (i-l) 7 neurite outgrowths (arrows) extending from the soma of a Tuj1+ cell. Arrows depict the neurites and arrowheads depict the nuclei. Scale bar: 50μm.

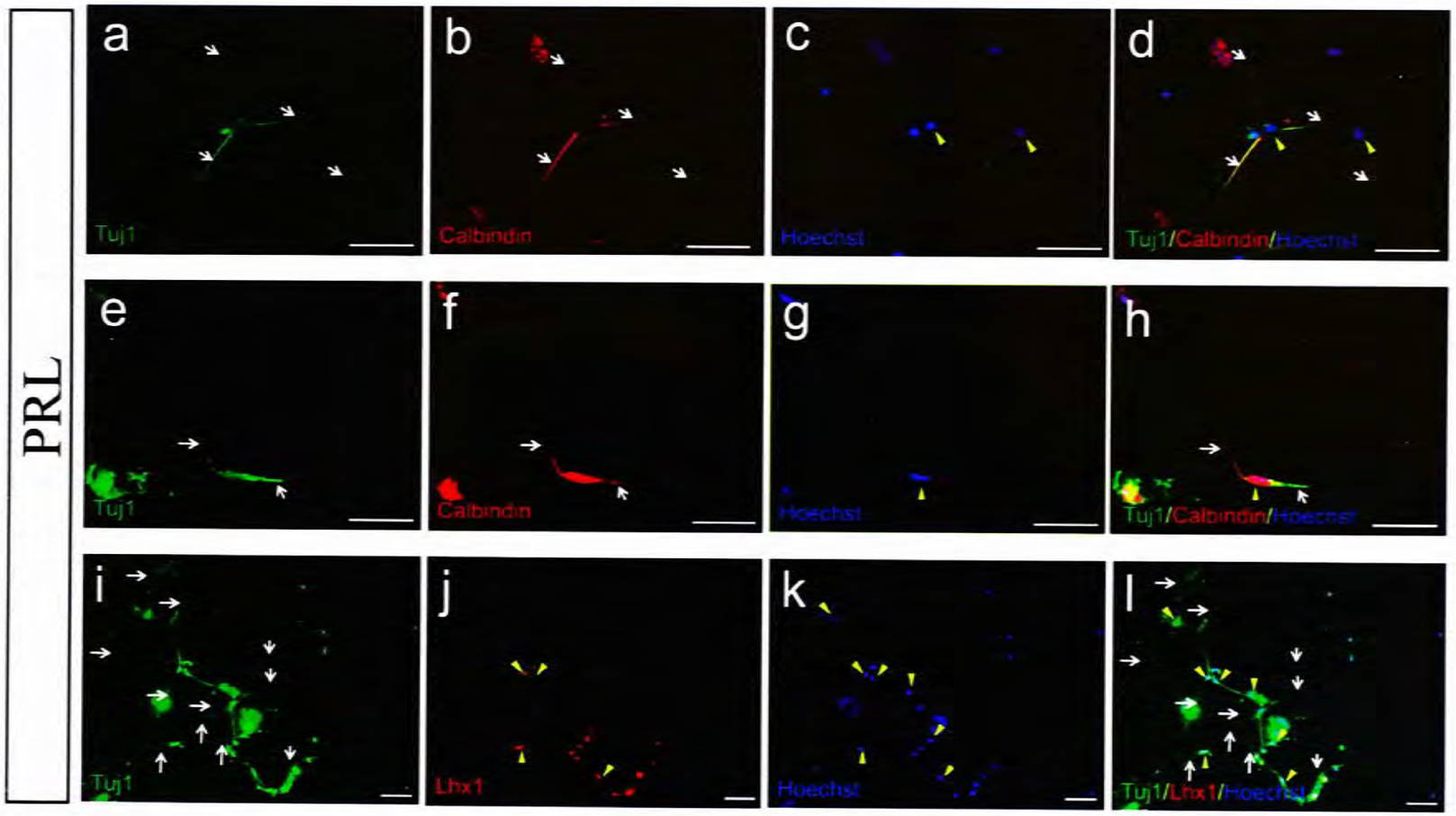

Fig. 3.10 Conversion of MEF to Tuj1+ cells displaying neuronal morphology by PRL. The induced cells were stained with Tuj1 (a,e,i) and calbindin or Lhx1 (b,f,j). The nuclei were visualized by H33342 (c,g,k). Co-expression of Tuj1 and calbindin (a-h) or Lhx1 (i-l) demonstrated the efficient induction of Purkinje cell properties in *Rora*-containing factor combination. High complexity of organization in *Ptf1a*-containing factor combination exemplified by the presence of 2 cells (a-d, arrowheads) and 7 cells (i-l, arrowheads) contacting each other. Arrows depict the neurites and arrowheads depict the nuclei. Scale bar: 50μm.

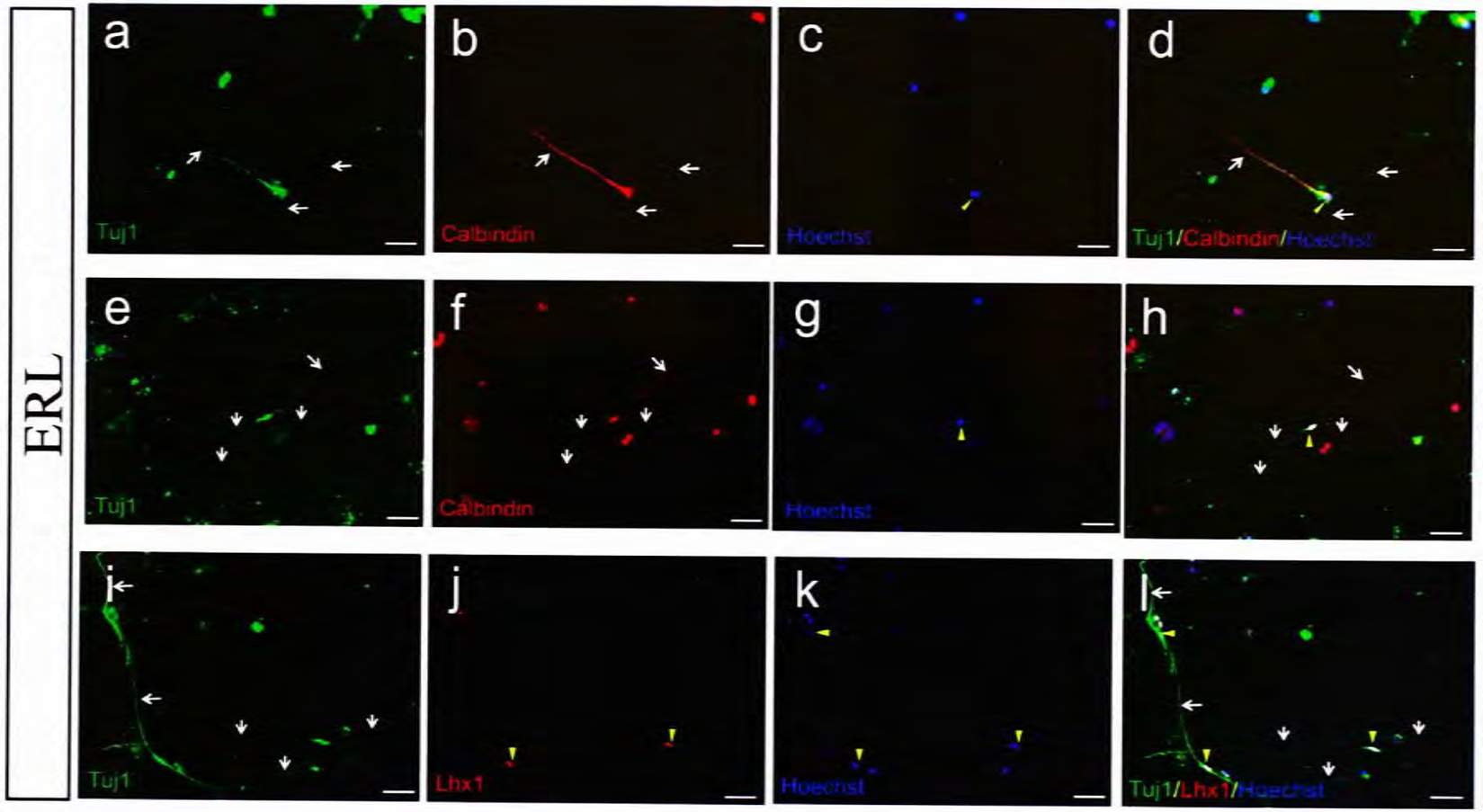

Fig. 3.11 Conversion of MEF to Tuj1+ cells displaying neuronal morphology by ERL. The induced cells were stained with Tuj1 (a,e,i) and calbindin or Lhx1 (b,f,j). The nuclei were visualized by H33342 (c,g,k). Co-expression of Tuj1 and calbindin (a-h) or Lhx1 (i-l) demonstrated the efficient induction of Purkinje cell properties in *Rora*-containing factor combination. (e-h) Complexity of morphology exemplified by the production of 4 processes (arrows) from soma. (i-l) Complexity of organization illustrated by 3 cells (arrowheads) in contact with each other. Arrows depict the neurites and arrowheads depict the nuclei. Scale bar: 50μm.

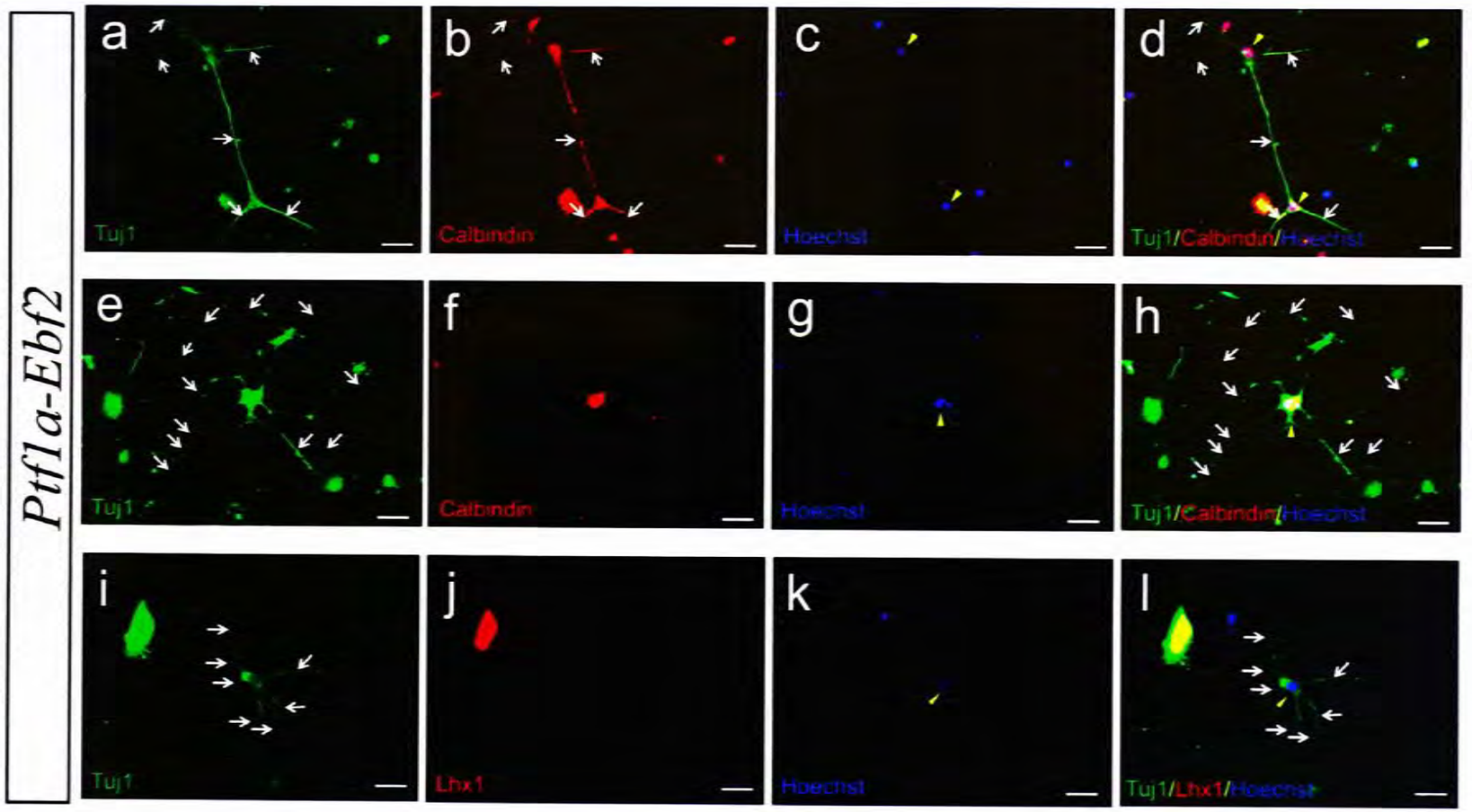

Fig. 3.12 Conversion of MEF to Tuj1+ cells displaying neuronal morphology by *Ptf1a-Ebf2*. The induced cells were stained with Tuj1 (a,e,i) and calbindin or Lhx1 (b,f,j). The nuclei were visualized by H33342 (c,g,k). Co-expression of Tuj1 and calbindin (a-d) demonstrated the induction of Purkinje cell properties, but was weaker in the absence of *Rora* (i-l). High complexity of morphology in *Ptf1a*-containing group exemplified by the extension of 11 (e-h, arrows) and 7 (i-l, arrows) processes from soma. (e-h) Calbindin expression should be in periphery instead of nucleus. (i-l) Lhx1 staining did not coincide with the nucleus. Arrows depict the neurites and arrowheads depict the nuclei. Scale bar: 50μm.

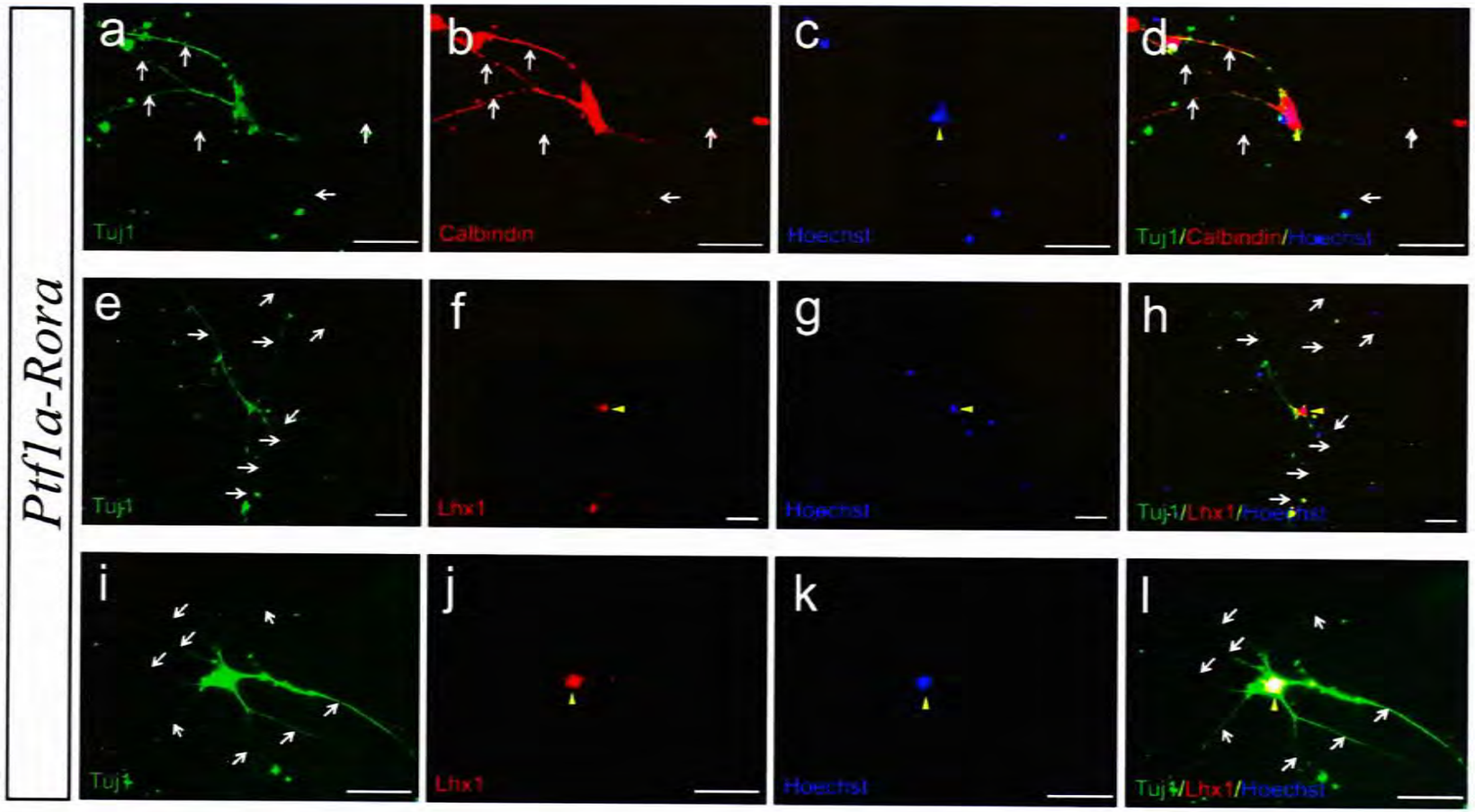

Fig. 3.13 Conversion of MEF to Tuj1+ cells displaying neuronal morphology by *Ptf1a-Rora*. The induced cells were stained with Tuj1 (a,e,i) and calbindin or Lhx1 (b,f,j). The nuclei were visualized by H33342 (c,g,k). Co-expression of Tuj1 and calbindin (a-d) or Lhx1 (e-l) demonstrated the efficient induction of Purkinje cell properties in *Rora*-containing factor combination. High complexity of morphology in *Ptf1a*-containing factor combination illustrated by the production of 6 (a-d, arrows) and 8 (e-h and i-l, arrows) processes and branches from the somata. Arrows depict the neurites and arrowheads depict the nuclei. Scale bar: 50μm.

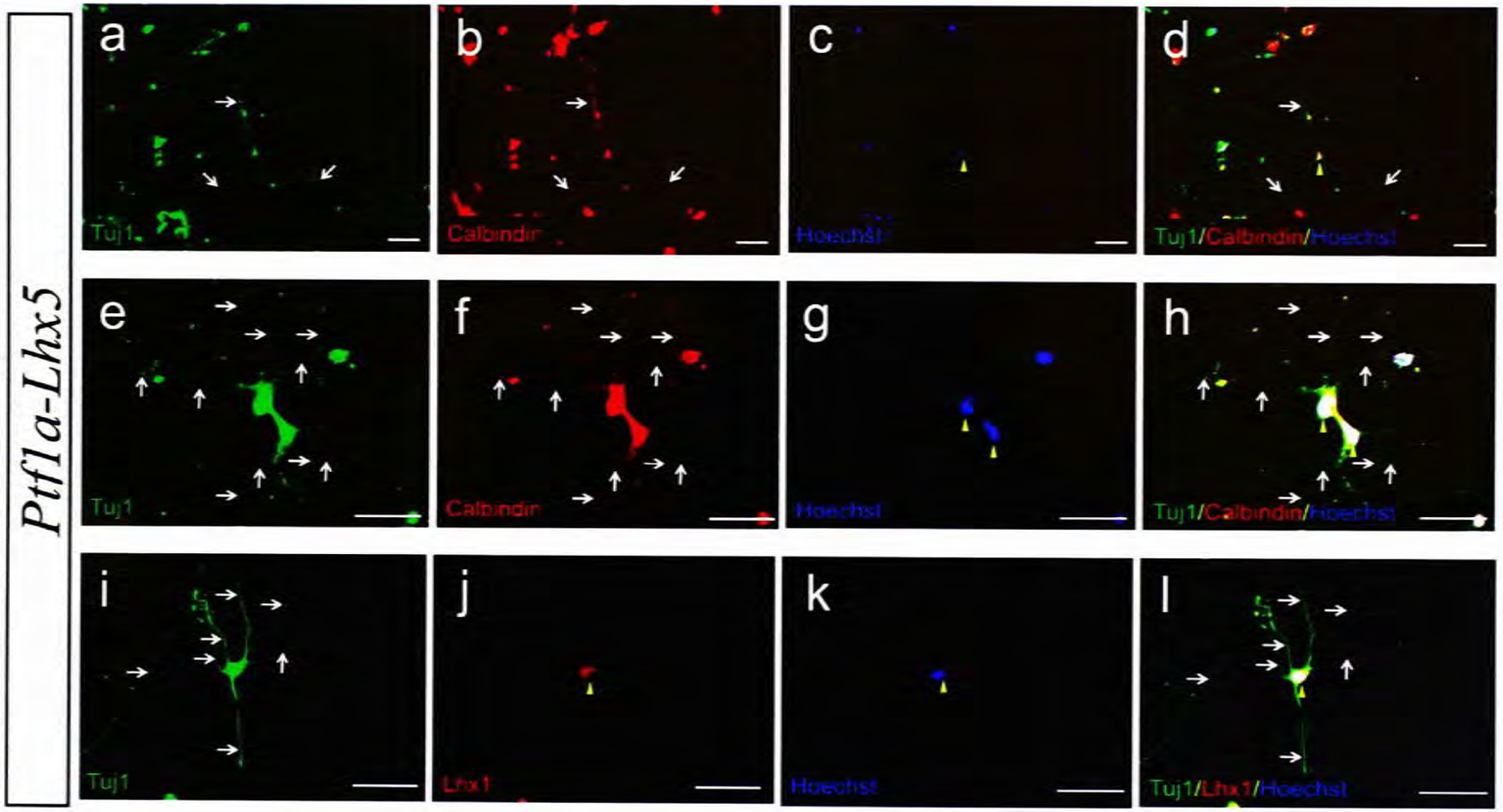

Fig. 3.14 Conversion of MEF to Tuj1+ cells displaying neuronal morphology by *Ptf1a-Lhx5*. The induced cells were stained with Tuj1 (a,e,i) and calbindin or Lhx1 (b,f,j). The nuclei were visualized by H33342 (c,g,k). Co-expression of Tuj1 and calbindin (a-h) or Lhx1 (i-l) demonstrated the induction of Purkinje cell properties. Complexity of morphology in *Ptf1a*-containing factor combination exemplified by the production of 10 processes and branches (e-h, arrows) from 2 cells and 7 neurite outgrowths (i-l, arrows) from the somata. Arrows depict the neurites and arrowheads depict the nuclei. Scale bar: 50μm.

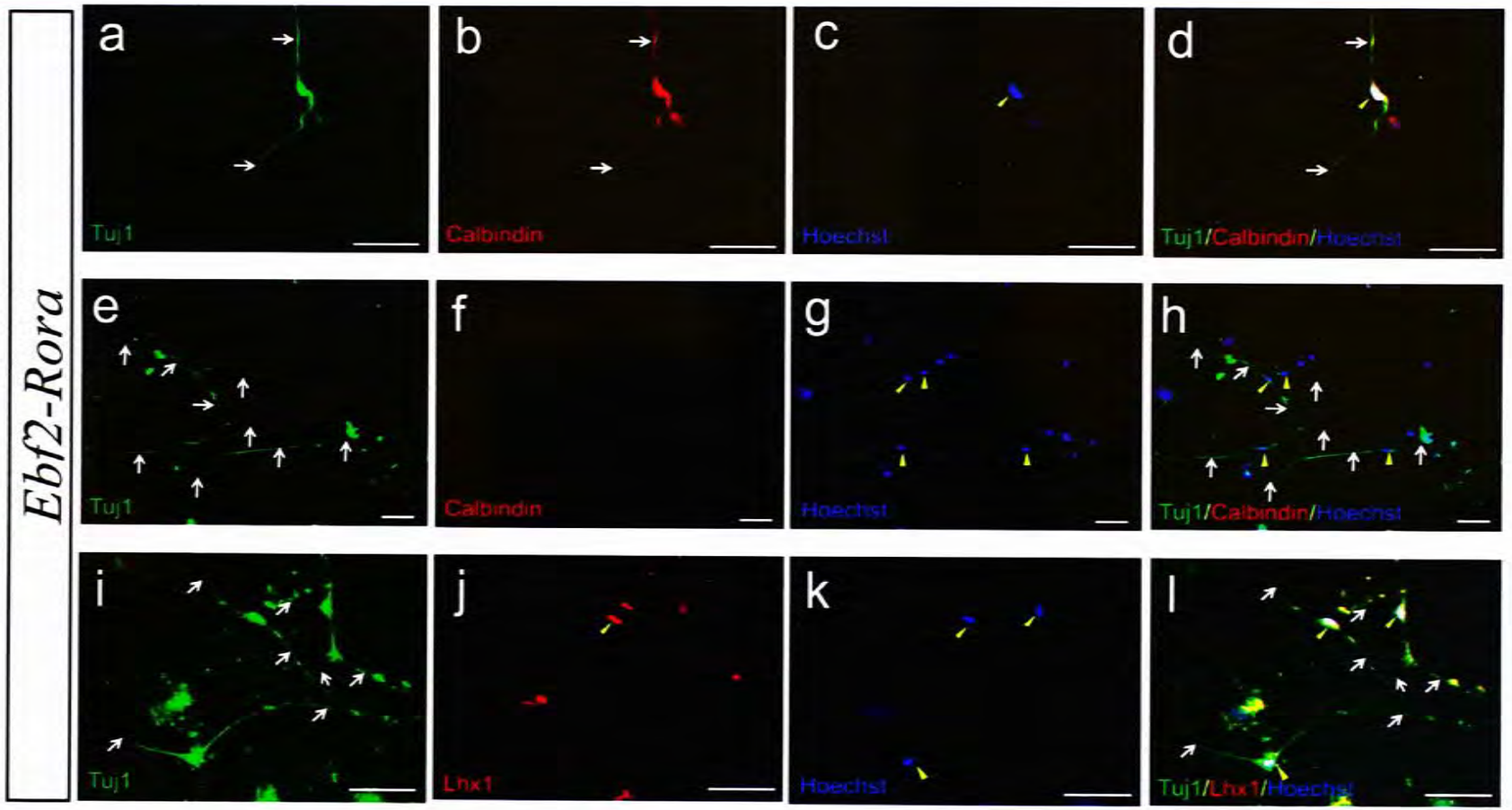

Fig. 3.15 Conversion of MEF to Tuj1+ cells displaying neuronal morphology by *Ebf2-Rora*. The induced cells were stained with Tuj1 (a,e,i) and calbindin or Lhx1 (b,f,j). The nuclei were visualized by H33342 (c,g,k). Co-expression of Tuj1 and calbindin (a-d) or Lhx1 (i-l) demonstrated the induction of Purkinje cell properties. Complexity of organization was illustrated by 4 (e-h, arrowheads) and 3 cells (i-l, arrowheads) in contact with each other. Arrows depict the neurites and arrowheads depict the nuclei. Scale bar: 50μm.

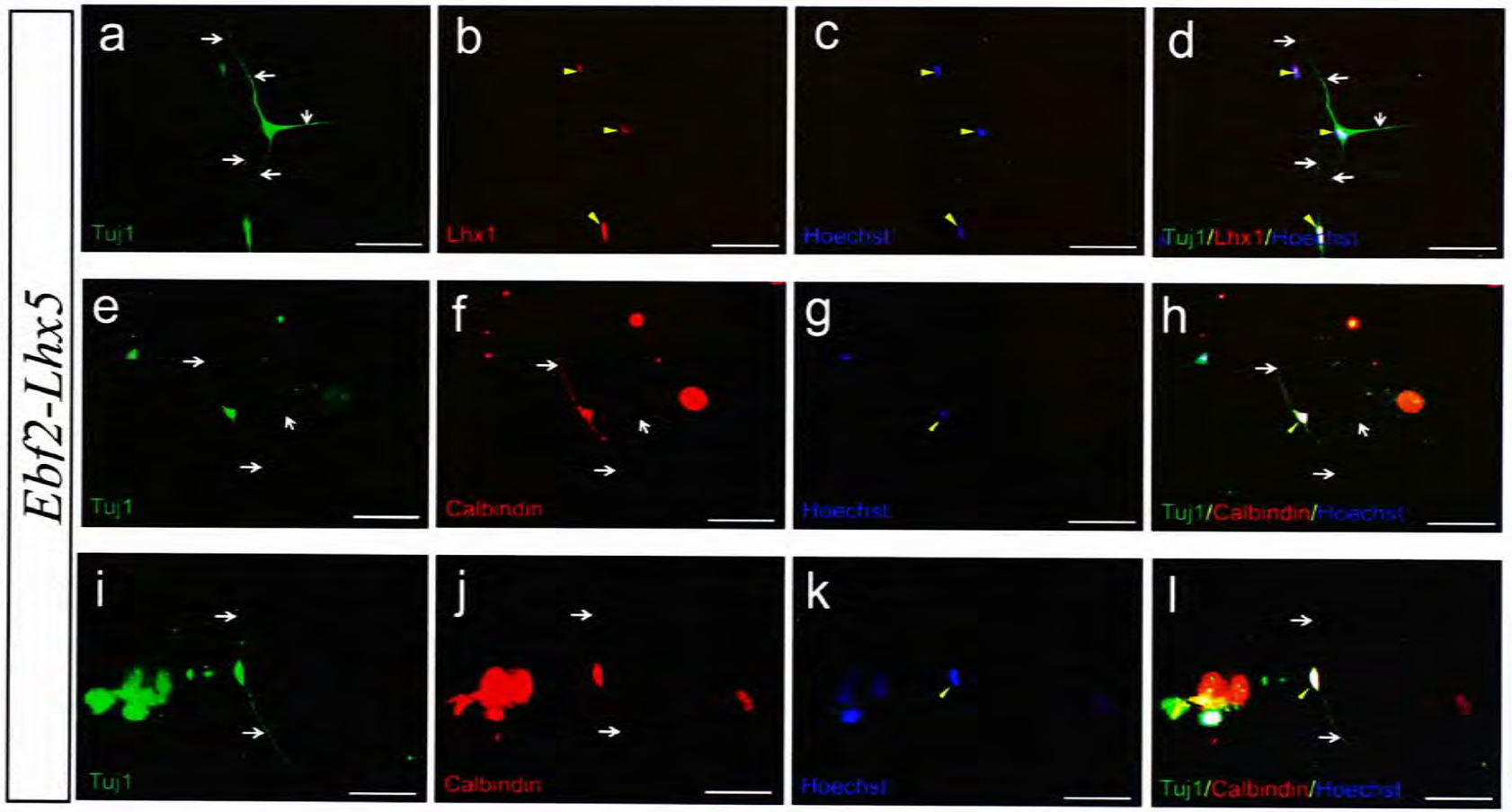

Fig. 3.16 Conversion of MEF to Tuj1+ cells displaying neuronal morphology by *Ebf2-Lhx5*. The induced cells were stained with Tuj1 (a,e,i) and calbindin or Lhx1 (b,f,j). The nuclei were visualized by H33342 (c,g,k). Co-expression of Tuj1 and Lhx1 (a-d) or calbindin (e-l) demonstrated the induction of Purkinje cell properties. Complexity of organization was illustrated by 3 cells (a-d, arrowheads) in contact with each other. (a-l) The complexity seemed to be compromised in the absence of *Ptf1a*. Arrows depict the neurites and arrowheads depict the nuclei. Scale bar: 50μm.

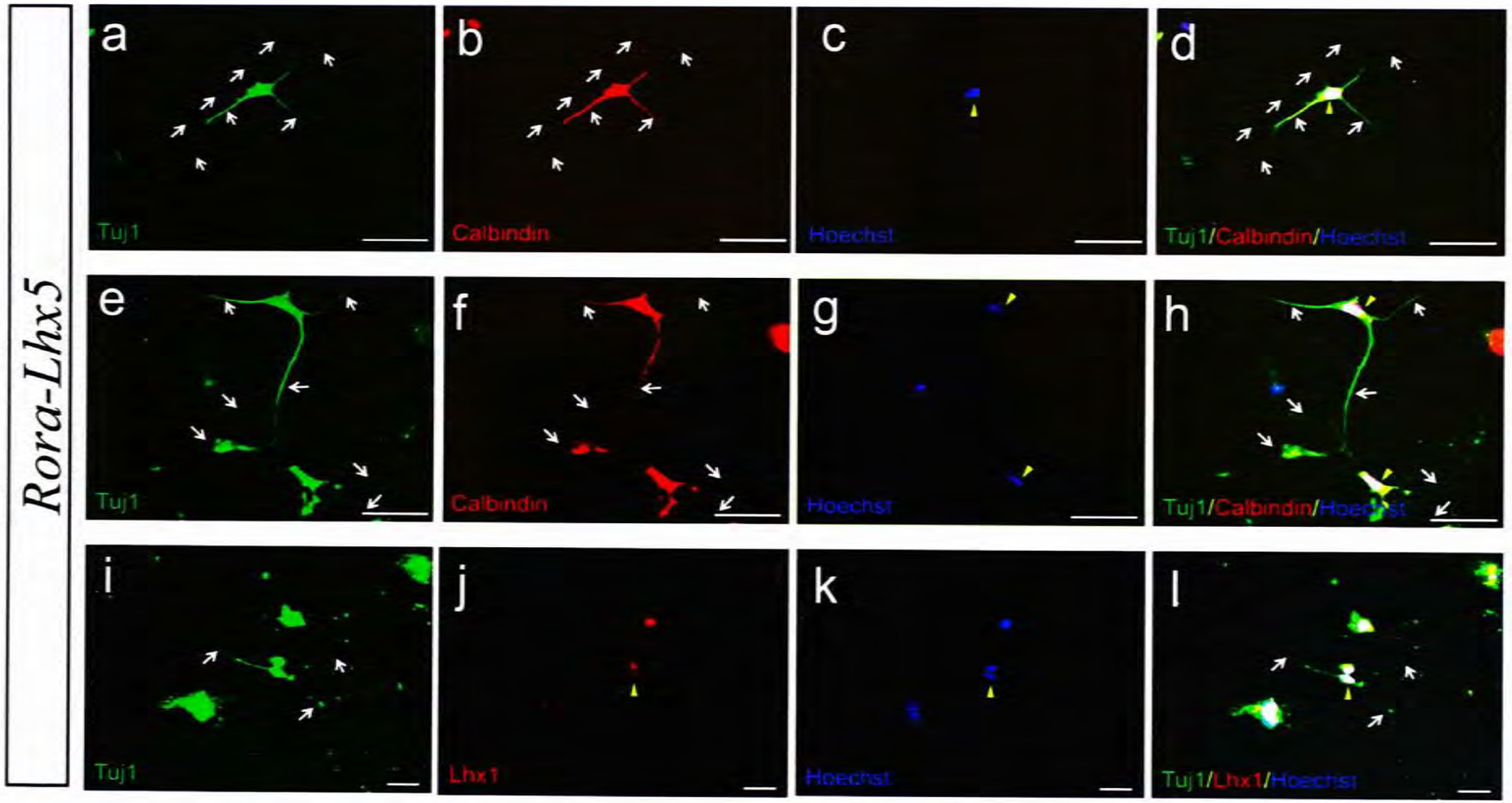

Fig. 3.17 Conversion of MEF to Tuj1+ cells displaying neuronal morphology by *Rora-Lhx5*. The induced cells were stained with Tuj1 (a,e,i) and calbindin or Lhx1 (b,f,j). The nuclei were visualized by H33342 (c,g,k). Co-expression of Tuj1 and calbindin (a-h) or Lhx1 (i-l) demonstrated the efficient induction of Purkinje cell properties in *Rora*-containing factor combination. Complexity of morphology was illustrated by extension of 8 neurite outgrowths from the soma (a-d, arrows). Complexity of organization was demonstrated by the 2 cells contacting each other (e-h, arrowheads). Arrows depict the neurites and arrowheads depict the nuclei. Scale bar: 50μm.

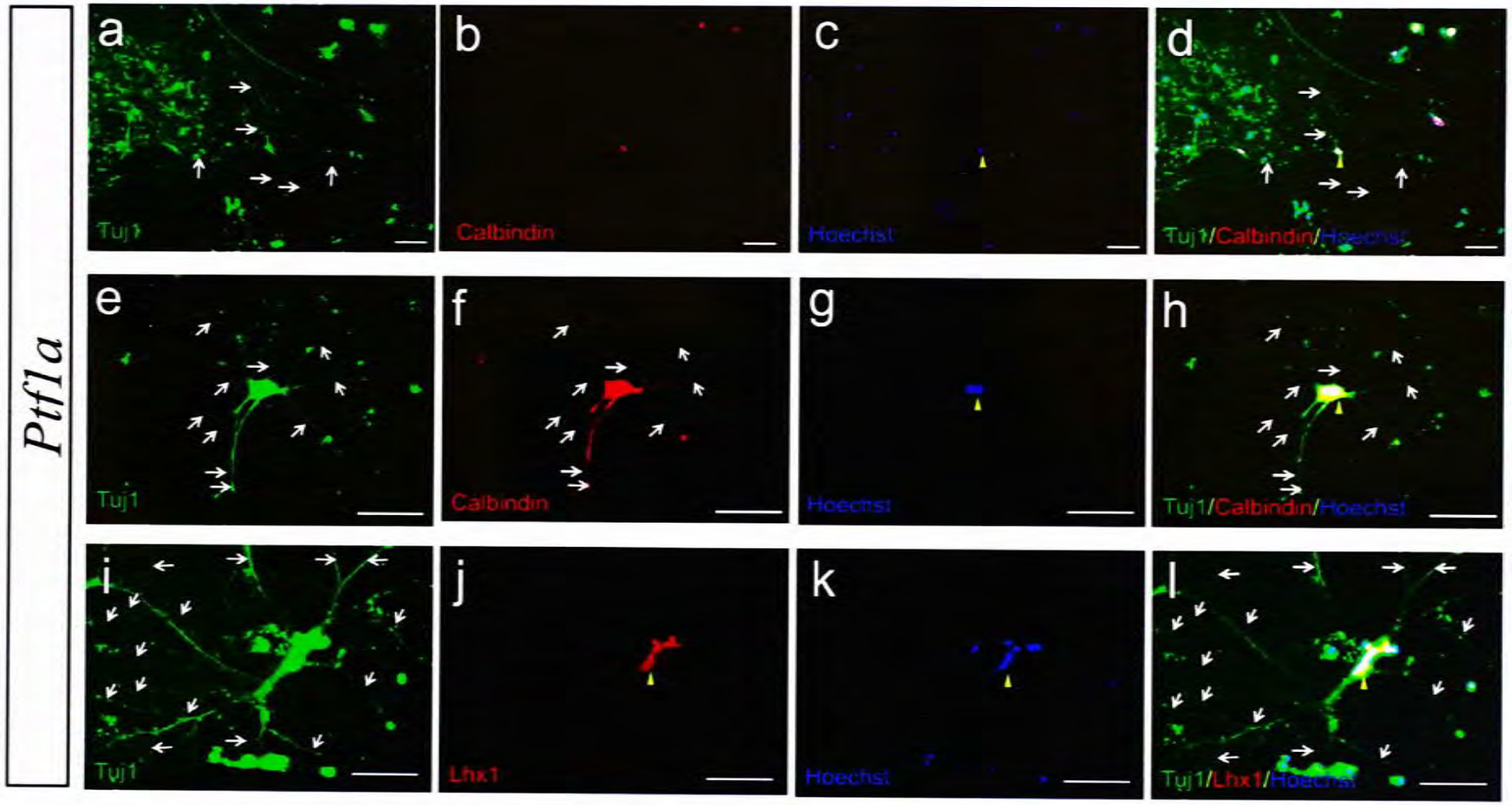

Fig. 3.18 Conversion of MEF to Tuj1+ cells displaying neuronal morphology by *Ptf1a*. The induced cells were stained with Tuj1 (a,e,i) and calbindin or Lhx1 (b,f,j). The nuclei were visualized by H33342 (c,g,k). Co-expression of Tuj1 and calbindin (e-h) or Lhx1 (i-l) demonstrated the induction of Purkinje cell properties. Complexity of morphology in *Ptf1a*-containing factor combination was illustrated by extension of 6 (a-d, arrows), 10 (e-h, arows) and 16 (i-l, arrows) neurite outgrowths and/or branches from the somata. (i-l) Occasional exhibition of complex morphology similar to Purkinje cells in stage III. Arrows depict the neurites and arrowheads depict the nuclei. Scale bar: 50μm.

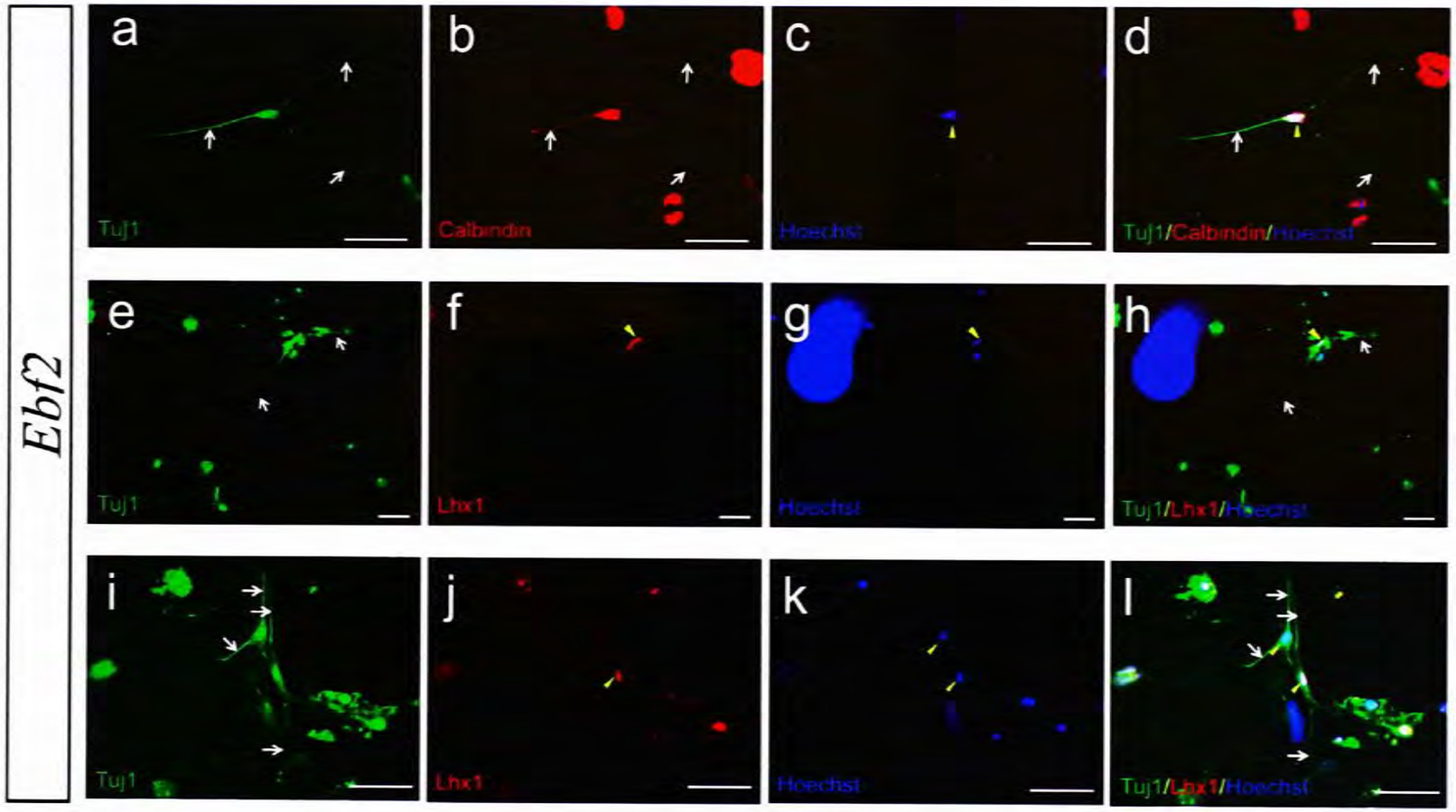

Fig. 3.19 Conversion of MEF to Tuj1+ cells displaying neuronal morphology by *Ebf2*. The induced cells were stained with Tuj1 (a,e,i) and calbindin or Lhx1 (b,f,j). The nuclei were visualized by H33342 (c,g,k). Efficient induction of Purkinje cell properties demonstrated by the co-expression of Tuj1 and calbindin (a-d) or Lhx1 (e-l). (a-l) In the absence of *Ptf1a*, a low degree of both complexity of morphology and organization was observed. Arrows depict the neurites and arrowheads depict the nuclei. Scale bar: 50μm.

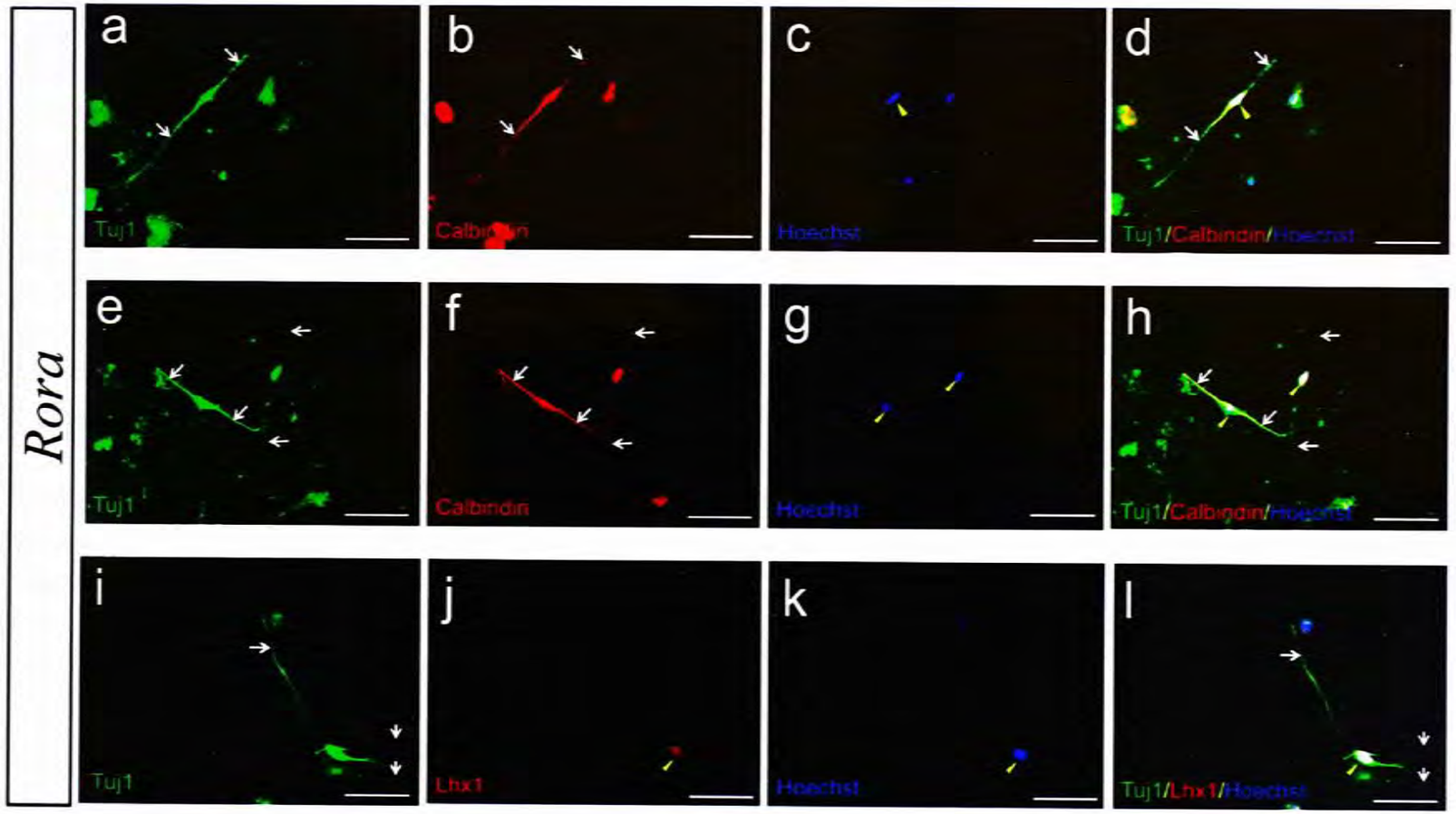

Fig. 3.20 Conversion of MEF to Tuj1+ cells displaying neuronal morphology by *Rora*. The induced cells were stained with Tuj1 (a,e,i) and calbindin or Lhx1 (b,f,j). The nuclei were visualized by H33342 (c,g,k). Efficient induction of Purkinje cell properties in *Rora*-containing factor combination demonstrated by the co-expression of Tuj1 and calbindin (a-h) or Lhx1 (i-l). (a-l) In the absence of *Ptf1a*, a low degree of both complexity of morphology and organization was observed. Arrows depict the neurites and arrowheads depict the nuclei. Scale bar: 50μm.

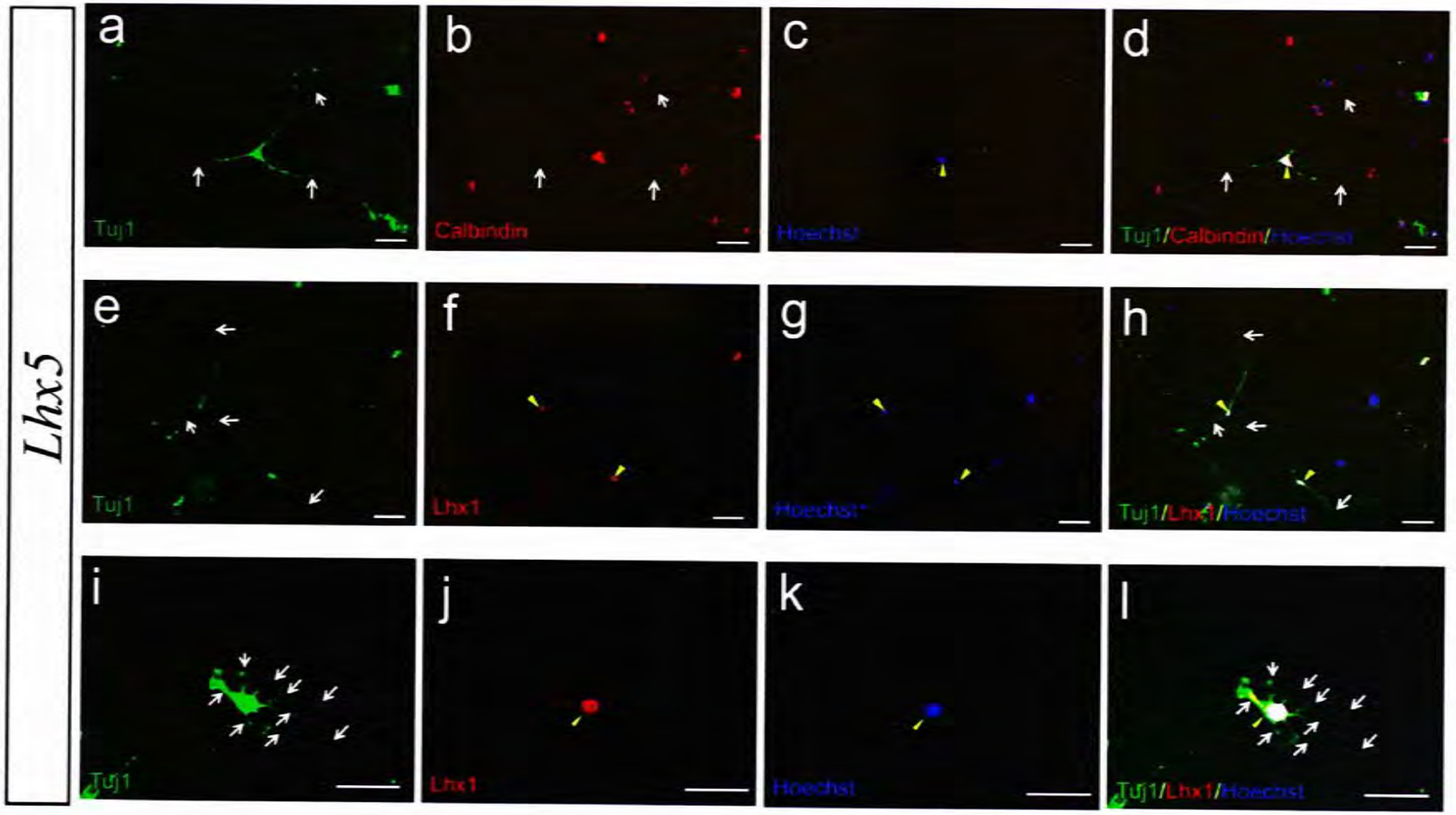

Fig. 3.21 Conversion of MEF to Tuj1+ cells displaying neuronal morphology by *Lhx5*. The induced cells were stained with Tuj1 (a,e,i) and calbindin or Lhx1 (b,f,j). The nuclei were visualized by H33342 (c,g,k). Co-expression of Tuj1 and calbindin (a-h) or Lhx1 (i-l) demonstrated the induction of Purkinje cell properties. (a-h) Typical Tuj1+ cells with simple morphology observed in non-*Ptf1a*-containing factor combination. (i-l) Occasional emergence of Tuj1+ cells with highly complex morphology, similar to Purkinje cells in stage III of dendritic development. Arrows depict the neurites and arrowheads depict the nuclei. Scale bar: 50μm.

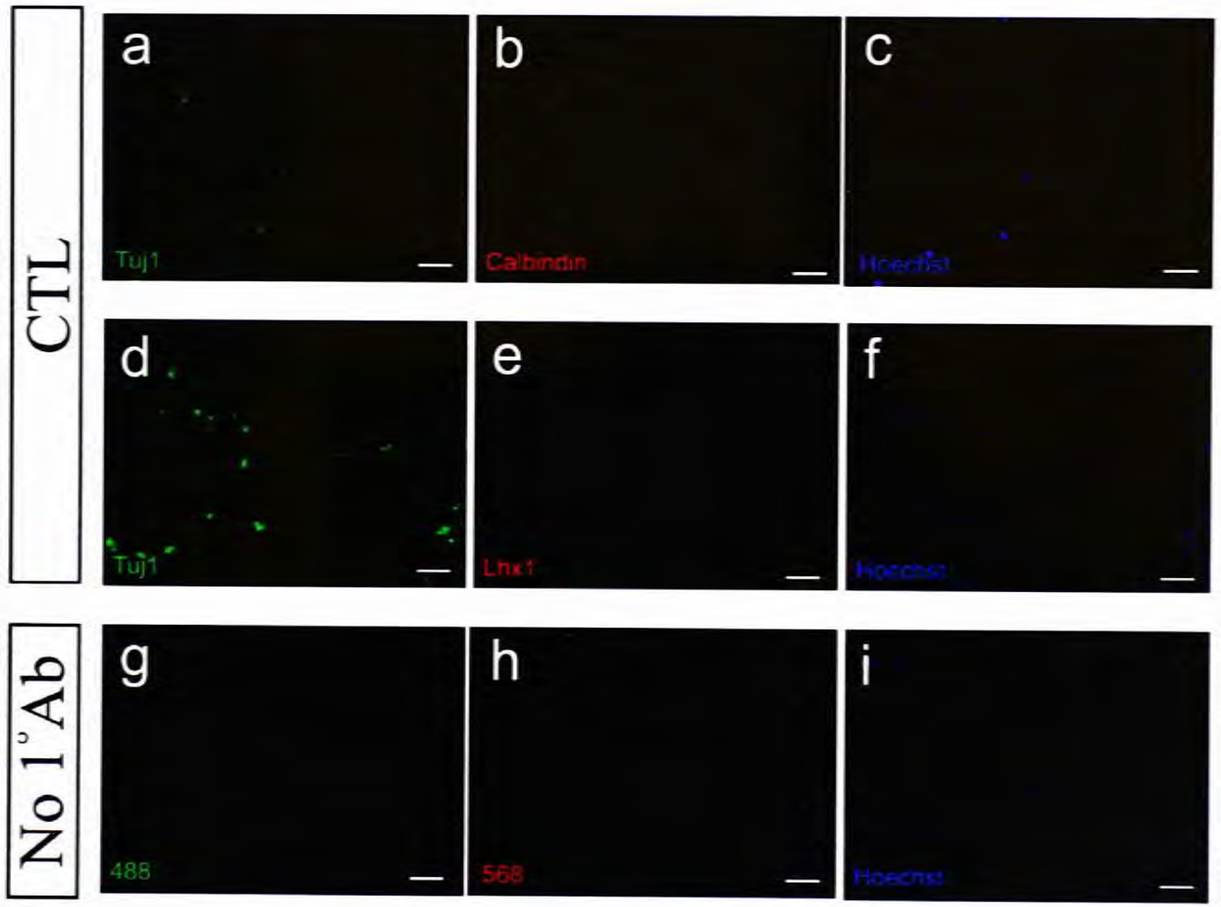

Fig. 3.22 Immunostaining on control experiments. No positive results were observed. (a-f) Uninfected MEF (CTL) did not give rise to Tuj1, calbindin or Lhx1 positive cells or adopt neuronal morphology. (g-i) No primary antibody controls (No 1°Ab) performed on cells induced by PRL. No true signal was observed for both 488nm and 568nm excitation. The signals observed in a, b, d, e and g were signals from auto-fluorescence of intracellular biomolecules. Scale bar: 50μm.

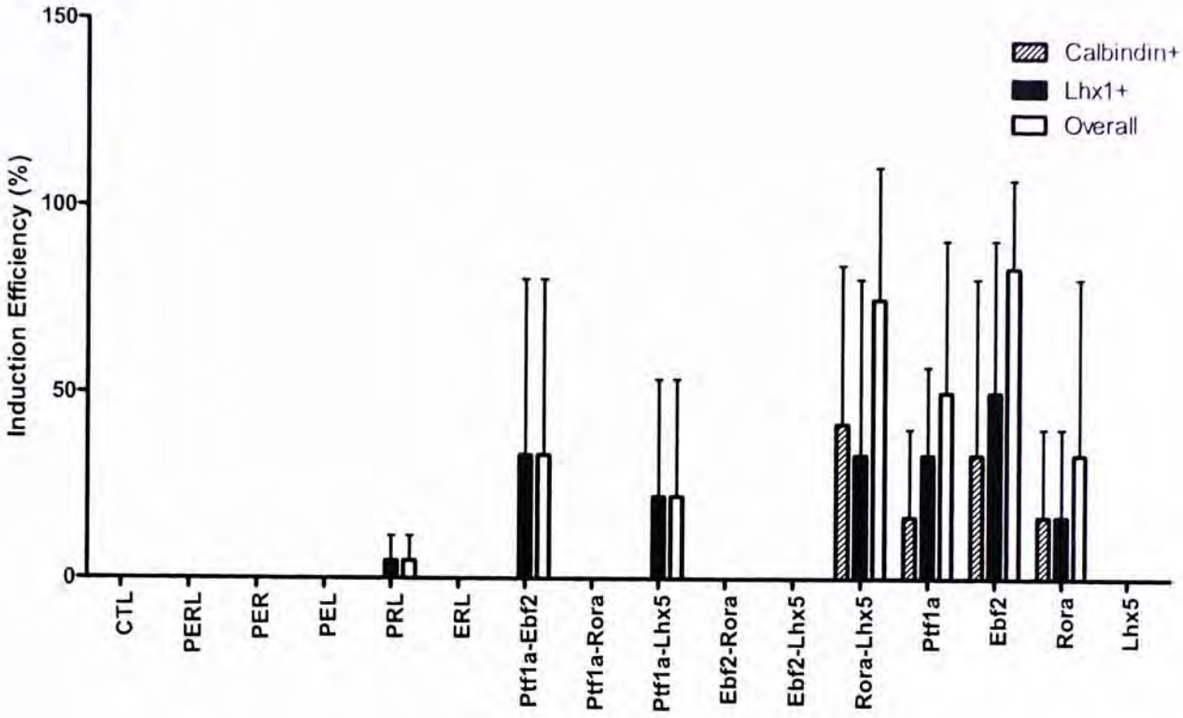

Fig. 3.23 Induction efficiency of calbindin and Lhx1 in Tuj1+ cells by candidate factors of Purkinje cell pool. Efficiency was recordable in 7 groups. Combinations with fewer factors tended to have a higher efficiency and higher incidence of calbindin expression. All 7 combinations showed Lhx1 expression. Error bar: SEM.

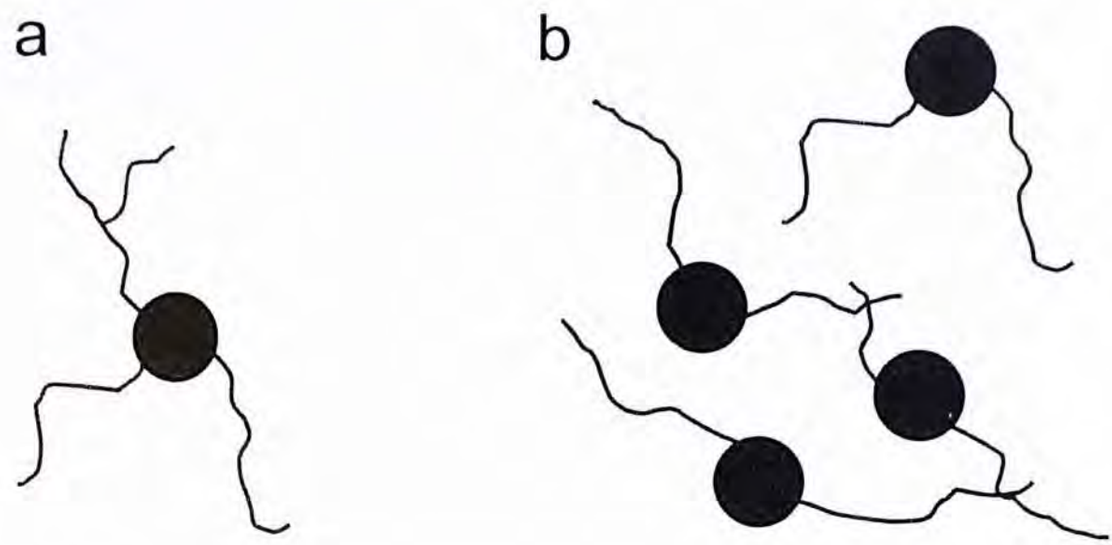

Fig. 3.24 Illustration of definition of complexity of morphology and organization. (a) The complexity of morphology is a measure of the number and branching of neuronal processes. The cell has 3 processes from the cell body and one of the processes has one branch, so the total number of outgrowths is 4. (b) The complexity of organization is a measure of the number of cells interacting with each other. 4 cells are observed but only 3 cells are interacting and in contact with each other, so the degree of complexity is 3.

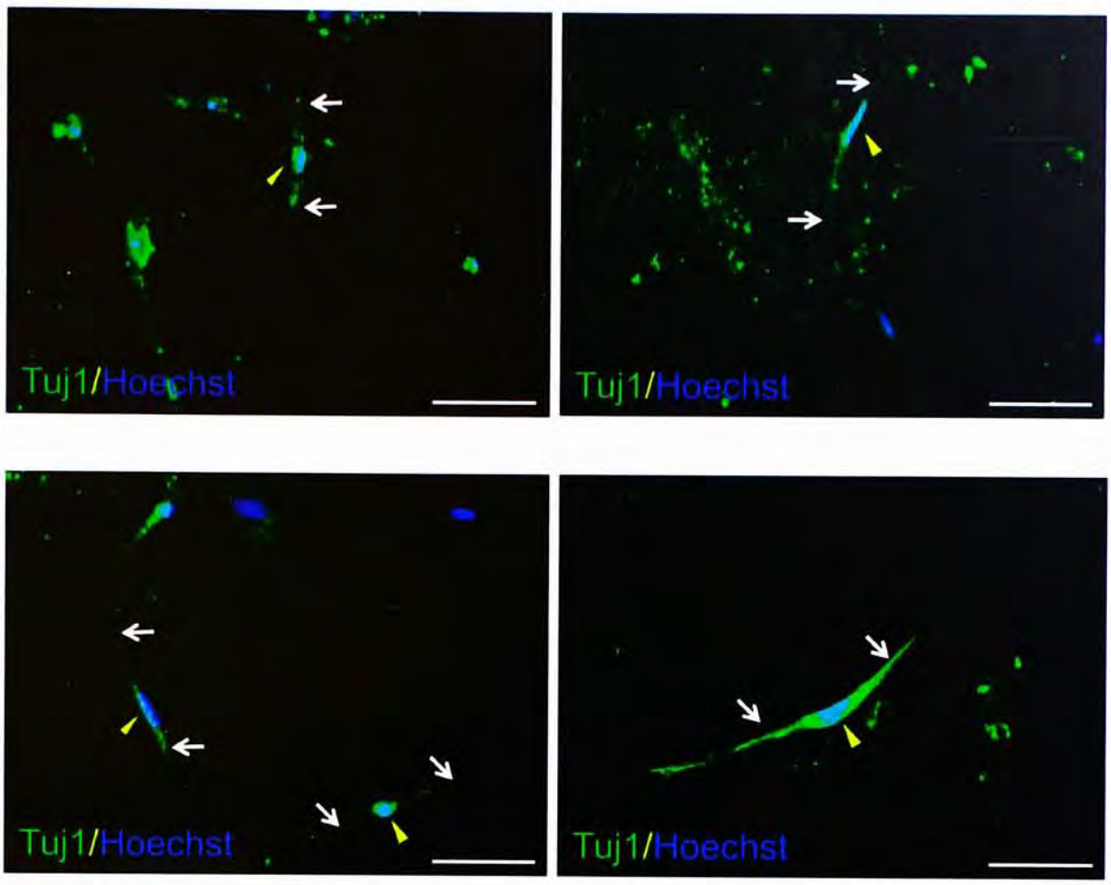

Fig. 3.25 Examples of Tuj1+ cells displaying "fusiform" morphology. Most of the induced Tuj1+ cells adopted this morphology. Arrows depict the neurites and arrowheads depict the nuclei. Scale bar: 50μm.

Table 3.5 Degree of complexity of morphology and organization of Tuj1+ cells in the present or absent of candidate factors

		No. of outgrowth and branches produced		No. of cells appearing together	
		Average	**SEM[a]**	**Average**	**SEM[a]**
Ptf1a	With	3.923	2.583	1.941	1.934
	Without	3.194	1.656	1.479	1.070
Ebf2	With	3.296	1.876	2.011	2.008
	Without	3.854	2.500	1.610	1.402
Rora	With	3.368	1.788	1.753	1.507
	Without	4.187	3.000	1.783	1.958
Lhx5	With	3.452	1.933	1.902	2.005
	Without	3.897	2.693	1.575	1.037

a: SEM, standard error of the mean.

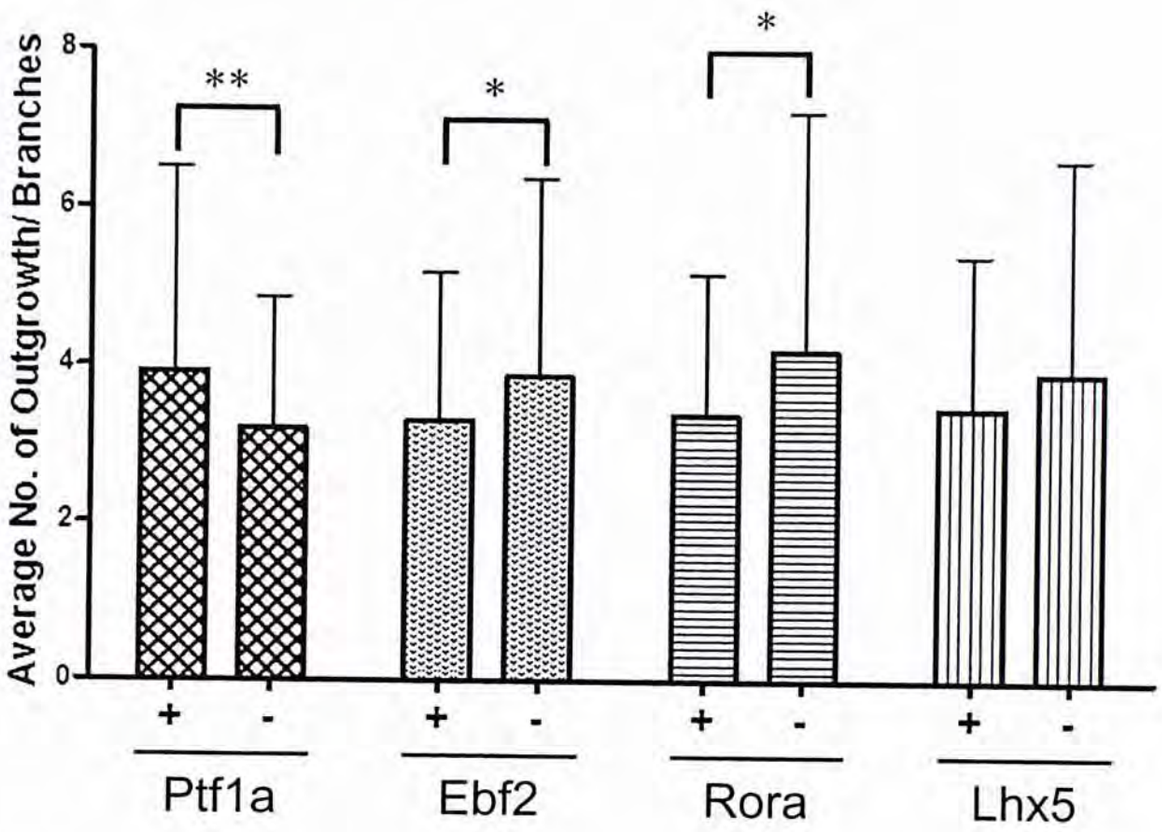

Fig. 3.26 Complexity of morphology induced in the presence and absence of each factor. The calculation was based on observing more than 400 cells. Each bar represented the average number of outgrowths and branches of the Tuj1+ cells. The "+" groups meant that the statistics was calculated from cells that were induced by combinations with that factor. For example, "Ptf1a+" meant the statistics was calculated from Tuj1+ cells induced by factor combinations PER, PEL, PRL, *Ptf1a-Ebf2*, *Ptf1a-Rora*, *Ptf1a-Lhx5* and *Ptf1a*. The "–" groups meant that the statistics was calculated from Tuj1+ cells that were induced by combinations without that factor. *Ptf1a* conferred a higher complexity of morphology on Tuj1+ cells indicated by the number of neurite outgrowth and branches produced. The presence of *Ptf1a* promoted the production of processes while the presence of the other 3 factors had an inhibiting effect on neurite generation. +, cells induced with factor combinations with the factor; –, cells induced with factor combinations without the factor; *, $p<0.05$; **, $p<0.01$, *t*-test.

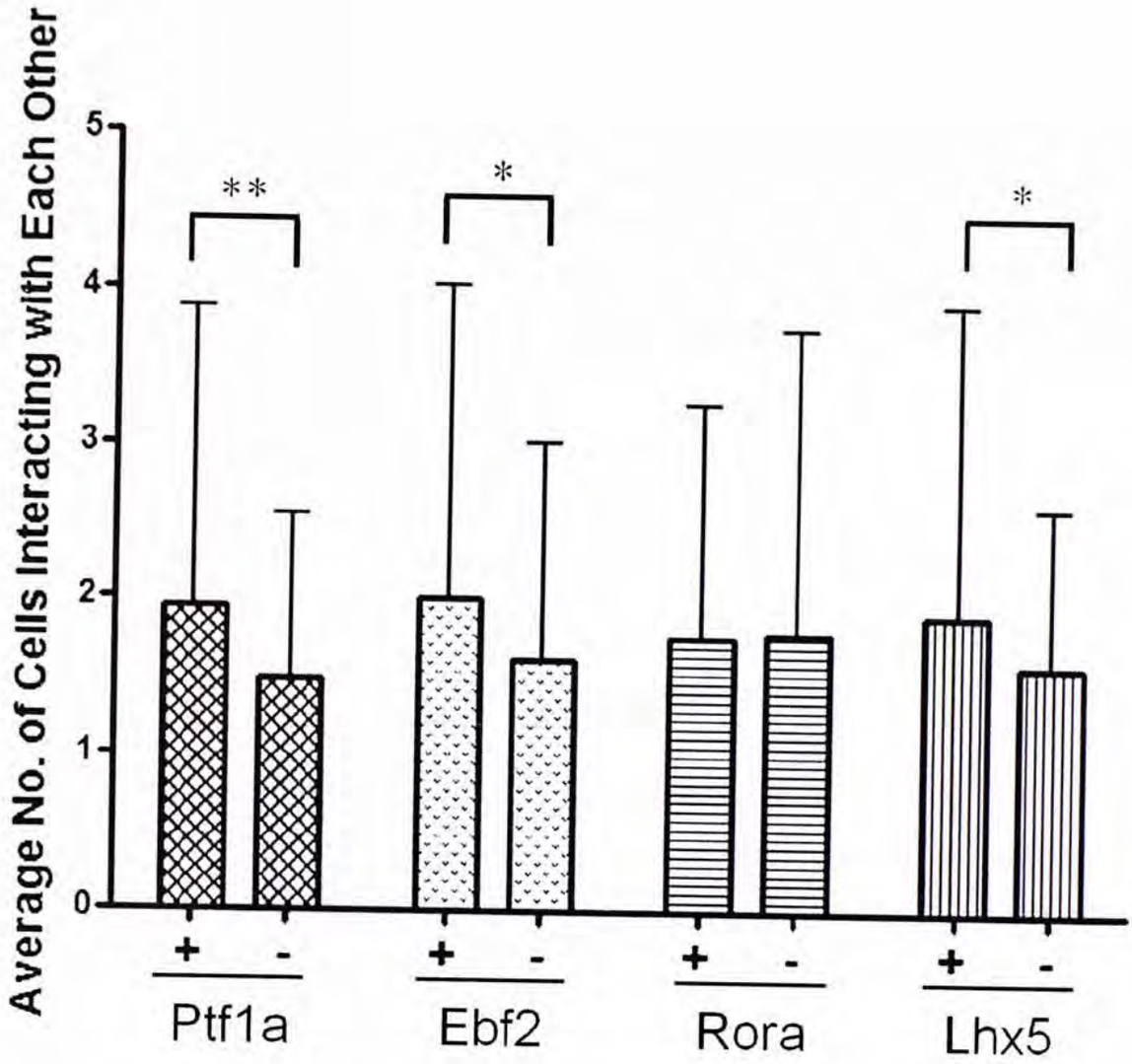

Fig. 3.27 Complexity of organization induced in the presence and absence of each factor. Each bar represented the average number of Tuj1+ cells interacting with each other. The "+" groups meant that the statistics was calculated from Tuj1+ cells that were induced by combinations with that factor. For example, "Ptf1a+" meant the statistics was calculated from cells induced by factor combinations "PER, PEL, PRL, *Ptf1a-Ebf2*, *Ptf1a-Rora*, *Ptf1a-Lhx5* and *Ptf1a*". The "–" groups meant that the statistics was calculated from Tuj1+ cells that were induced by combinations without that factor. *Ptf1a* conferred a higher complexity of organization on Tuj1+ cells indicated by the number of Tuj1+ cells contacting each other. The presence of *Ptf1a*, *Ebf2* and *Lhx5* allowed the induction of a higher complexity of organization at similar level, but the effect of Ptf1a was statistically more significant. *Rora* showed no effect on the induction of complexity of organization. +, cells induced with factor combinations with the factor; –, cells induced with factor combinations without the factor; *, $p<0.05$; **, $p<0.01$, *t*-test.

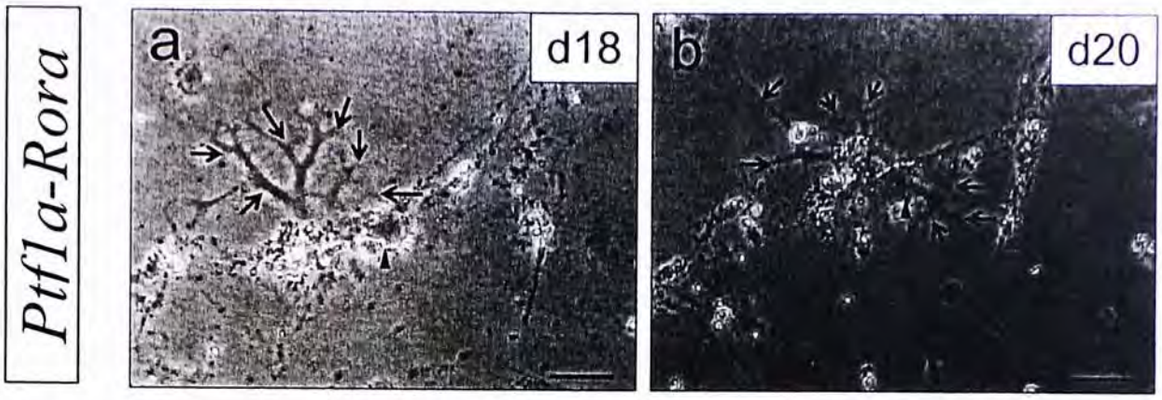

Fig. 3.28 A cell induced by *Ptf1a-Rora* displayed morphology similar to Purkinje cells at stage IV of dendritic development. (a) The cell produced an extension from the cell body and possessed several branches on 18 days (d18) after retroviral infection. (b) The cell degenerated 2 days later (d20) with shrunken processes. Arrows depict processes and arrowheads depict cell body. Scale bar: 50μm.

3.4 Discussion

3.4.1 Roles of inducing factors in Purkinje cells and granule cells development

Previous studies have demonstrated that recapitulation of the signaling environment of early development of the cerebellum can induce the differentiation of ES cells into Purkinje cells and granule cells (Muguruma et al., 2010; Su et al., 2006). Therefore, it is conceivable that the correct combinations of inducing factors allow the recapitulation of gene expression profiles of differentiation of the two cell types.

Consistent with this, we have shown that *Ptf1a* and *Rora* were important in neuronal induction. These two transcription factors play very important roles in the development of Purkinje cells. As described in Chapter 1.5.2, *Ptf1a* is expressed in progenitors in ventricular zone to determine GABAergic over glutamatergic neuronal identity (Glasgow et al., 2005; Pascual et al., 2007). Ptf1a cooperates with mammalian Suppressor of Hairless (Rbpj) to activate gene expression (Hori et al., 2008). Ptf1a and its binding partner E-protein bind to the E-box sequence (CANNTG) while Rbpj binds to the TC-box sequence ((A/T)TTCCC). One target of the Ptf1a-Rbpj transcription complex is the bHLH transcription factor Neurogenin 2 (*Neurog2*) (Henke et al., 2009). *Neurog2* has been demonstrated to control the generation of dopaminergic neurons in ventral midbrain (Kele et al., 2006), motorneurons (Mizuguchi et al., 2001), sensory neurons (Fode et al., 1998) and cortical glutaminergic neurons (Schuurmans et al., 2004). Although there is no direct evidence showing *Neurog2* has a role in the development of Purkinje cell, *in situ* hybridization data reveal that *Neurog2* and *Ptf1a* express in overlapping domain in the ventricular zone during some stages of cerebellar development (Zordan et al., 2008). These suggest that *Neurog2* may be a downstream effector of *Ptf1a* in the

generation cerebellar GABAergic neuron, possibly including Purkinje cells. Moreover, Ptf1a represses the action of Math1 and blocks the differentiation of granule cells (Kawauchi and Saito, 2008), maintaining the GABAergic identity of progenitors in VZ.

Rora plays a more specific role than *Ptf1a* in Purkinje cell development. It starts to be expressed in Purkinje cells in E13 (Ino, 2004) and controls their proliferation and dendritic differentiation (Boukhtouche et al., 2006). At DNA level, RORα binds to the promoter of Purkinje cell protein 2 (*Pcp2*), a gene that code for a guanine nucleotide dissociation inhibitor in G-protein mediated signal transduction pathway. Pcp2 induces neuronal differentiation in PC12 cells (rat pheochromocytoma cells) through the activation of $G_{\beta\gamma}$ mediated Ras and p38 MAPK (mitogen activated protein kinase). The same signaling pathways may also be used in Purkinje cells (Guan et al., 2005). Complete loss of this gene causes severe loss of Purkinje cells and renders the remnant in an immature state, displaying rudimentary dendrites without spiny branches and embryonic surface markers such as embryonic NCAM (Edelman and Chuong, 1982; Hatten and Messer, 1978; Trenkner, 1979). Consistent with this, Boukhtouche et al. (2006) demonstrated that *Rora* is required for the early phase of dendritic development of Purkinje cells. They discovered that in the absence of *Rora*, the Purkinje cells remain in "fusiform" (stage I of dendritic differentiation, see Section 1.5.2.2), and that exogenous expression of RORα can rescue the phenotype. Moreover, overexpression of RORα accelerates the progression of development of dendrites of Purkinje cells from stages I or II to stage IV *in vitro*, but this cannot be recapitulated when overexpression takes place at stage III. This may explain our results that most of the Tuj1 and calbindin/Lhx1 double positive cells were also in "fusiform" with bipolar shape and relatively simple morphology. Due to

its role in early dendritic development, RORα may induce MEF to transdifferentiate to a young stage of Purkinje cell only but fail to stimulate them to further develop. Therefore, other factors that participate in the late differentiation of dendrites may have to be included for more complete transdifferentiation.

Lhx5 was shown to have weak neuronal-inducing power but acted synergistically with other factors. This gene and its closely related gene *Lhx1* are important and show functional redundancy in development of cerebellum. When *Lhx1* and *Lhx5* were specifically knocked out in the cerebellum, a severe reduction in Purkinje cells resulted. The expression of Shh target gene *Gli1* was also missing in both Purkinje cells and granule cells (Zhao et al., 2007). In addition, *Lhx5* was shown to control the development and distribution of Cajal-Retzius cells which are important in the lamination of the cerebral cortex, and the distribution of reelin-expressing cells in the telencephalon (Miquelajauregui, et al., 2010). This gene also controls the differentiation and migration of neurons in hippocampus, as well as the production of signaling molecules such as Wnt5a, Bmp4 and Bmp7 (Zhao et al., 1999). Moreover, *Lhx5* was shown to activate the expression of two secreted Wnt antagonists to promote forebrain development in zebrafish (Peng and Westerfield, 2006). All these suggest a complex role of *Lhx5* in neuronal development. However, the precise functional role of *Lhx5* is not well established as most studies were done on *Lhx5*-null mice and therefore, the effect resulted was global rather than regional, restricted to the organ of interest.

Consistent with the hypothesis, *Ebf2* was shown to be dispensable in the induction of Purkinje cell fate. *Efb2* is expressed in a subset of Purkinje cells which is zebrin II negative and acts to suppress zebrin II+ phenotype (Chung et al., 2008). Zebrin II expression has been use to subdivide different compartments of the

cerebellum into parasagittal stripes (Brochu et al., 1990). Although strong evidence suggested that the stripe identity is established at the time when the Purkinje cell is born (Hashimoto and Mikoshiba, 2002), *Ebf2* seems to play a minor role in development because *Ebf2* null mice only showed defective morphology in restricted region of the cerebellum and a subpopulation of Purkinje cells was affected (Croci et al., 2006). In addition, from *in situ* hybridization data from Allen Brain Atlas (Lein et al., 2007), this gene is not expressed on or before E13.5 and it is expressed in a subset, rather than a broad range of Purkinje cells at E15.5 and E18.5.

It is intriguing to note the respective induction efficiency of calbindin and Lhx1 in Tuj1+ cells. All 7 combinations with recordable efficiencies showed induction of Lhx1, while only 4 combinations showed induction of calbindin. Interestingly, the efficiencies of overall calbindin/Lhx1 induction of these 4 combinations were the highest among all groups. Besides, efficiency of Lhx1 induction was generally higher that of calbindin. This may indicate that Lhx1 expression is an earlier event than that of calbindin during transdifferentiation process, and that the expression of calbindin signifies a more complete cell fate transition. Consistent with this, the *in situ* hybridization data from Allen Brain Atlas (Lein et al., 2007) showed that Lhx1 is strongly expressed in the ventricular zone of the developing cerebellum as early as E13.5, but the expression of calbindin only becomes prominent at E15.5. Thus, expression of calbindin implies a better recapitulation of Purkinje cell development.

The fact that some cells occasionally display mature Purkinje cell phenotype suggests that transdifferentiation is not a deterministic process. In most cases, the current pool of factors is not sufficient to drive the induced neuronal cells to full maturity. Nevertheless, a suitable transgene expression level and the necessary epigenetic modification might stochastically be attained such that even a single factor

could drive the transdifferentiation to mature Purkinje cells, as seen with *Ptf1a* and *Lhx5* (Fig. 3.18i-l and Fig. 3.21i-l). As the transgene expression level cannot be accurately controlled and the four factors are not directly involved in epigenetic remodeling mechanisms, these must be achieved by stochastic events (Yamanaka, 2009).

The failure of induction of granule cells might be the result of a failure of recapitulation of its development. Granule cell development can be divided into proliferation phase where progenitor cells replicate to increase the cell number and differentiation phase where the progenitors exit cell cycle and develop to acquire properties of granule cells. In proliferation phase, the zinc finger proteins *Zic1*, *Zic2* and *Zipro1* promote the growth of progenitor cells' population and inhibit differentiation (Ebert et al., 2003; Yang et al., 1999, see also section 1.5.2.3). The differentiation phase is controlled by factor such as *Math1*, *Mbh1/2*, *Pax6* and *Neurod1* (Hevner et al., 2006; Kawauchi and Saito, 2008; Miyata et al., 1999; Pan et al., 2009, see also section 1.5.2.3). It has been shown that *Math1* is negatively regulated by Zic1 and Neurod1 (Ebert et al., 2003; Pan et al., 2009). Thus the pool of candidate factors contained transcription factors that have opposite actions, and they may antagonize each other's activity.

Functions of other factors in the candidate pool in cerebellum are not well characterized. *Csrp2* is specifically expressed in the EGL but knockout of this gene causes no observable change to the growth of cerebellum (Schuller et al., 2006).

Neurod6 (also known as *Nex1* and *Math2*) is a bHLH transcription factor and its neurogenic ability was demonstrated by the promotion of neuronal differentiation of PC12 cell line and regeneration of neurites even in the absence of nerve growth factor (Uittenbogaard and Chiaramello, 2002).

En2 participates in the definition of cerebellar region in the neural tube and controls the patterning of cerebellar foliation and Purkinje cell parasagittal stripes (Sillitoe et al., 2008). It also regulates genes linked to vesicle formation and transport (Holst et al., 2008).

Sox4 (SRY-box containing gene 4), a member of group C of the high mobility group (HMG)-box transcription factor, is highly expressed in the inner EGL and weakly expressed in the IGL for an extended period, which implies a role in the maturation of granule cells (Cheung et al., 2000).

There is no report on *Neurog2* (*Ngn2*) being directly involved in cerebellar development. However, *Neurog2* is shown to be regulated by Pax6, a gene enriched in granule cells (Scardigli et al., 2003) and is also a direct target of Ptf1a-Rbpj, a complex function in the specification of GABAergic neurons (Henke et al., 2009). Thus this gene may involve in the development of both granule and Purkinje cells.

There is no report on the action of *Aes* (also known as *Grg5*) in cerebellum yet, but this gene is shown to be involved in skeletal development (Wang et al., 2002, 2004).

Overall, the molecular network controlling the development of granule cells is very complicated, and the precise roles of each factor are not well established yet. This poses difficulty in the recapitulation of granule cell development and hence the selection of suitable factors for transdifferentiation.

3.4.2 Mechanism of neural transdifferentiation

The mechanism of transdifferentiation may be similar to that of reprogramming, i.e. by epigenetic remodeling. Specifically, in the case of iPS cell generation, c-Myc probably loosens the chromatin structure for easy access of other reprogramming

factors (Knoepfler et al., 2006). Oct4, Sox2 and Klf4 may recruit chromatin remodeling enzymes (such as histone demethylase and DNA demethylase) and reactivate pluripotency genes expression (such as endogenous *Oct4*, *Sox2* and *Nanog*), leading to the activation of endogenous pluripotency regulatory network, so that the pluripotent state can be maintained (Hanna et al., 2010; Hochedlinger and Plath, 2009; Plath and Lowry, 2011). In the same way, the inducing factors may also bring about epigenetic changes to activate neuronal programme and repress the fibroblast specific gene expression. Consistent with this, induced cardiomyocytes converted from cardiac fibroblasts displayed epigenetic state similar to true cardiomyocytes (Ieda et al., 2010). Currently the participation of *Ptf1a*, *Rora*, *Lhx5* and *Ebf2* in epigenetic modulation has not been reported. Nevertheless, these factors may activate downstream targets which are involved in chromatin and DNA modification, eventually leading to the remodeling of epigenetic markers.

Functionally, the factors may allow the recapitulation of development of Purkinje cells. First, Ptf1a potentiates the MEF for a switch to GABAergic neuronal lineage. This change allows Rora and Lhx5 to turn on the transcription profile specific to Purkinje cells and direct the transfected MEF to the designated fate. Temporally controlling the expression of transgenes by inducible promoters can help elucidate the requirement of factors at different times at molecular level.

Our results added evidence to the feasibility of transdifferentiation by showing that ectopic expression of core transcription factors of Purkinje cells can drive the induction of neuronal and Purkinje cell properties in MEF. An important direction for transdifferentiation is revealed in the present work. The recapitulation of developmental process is suggested as an effective route of transdifferentiation. Therefore, knowledge in developmental biology becomes essential in further

advance in regenerative medicine.

CHAPTER 4

FUTURE DIRECTIONS

The generation of neuronal cells and tissues has long been of great value in regenerative medicine. A small number of cases of recovery after neural injury by embryonic stem (ES) cells treatment have been reported in mice and rats (Cui et al., 2008; Nagai et al., 2010) and transdifferentiation of neurons from other cell types have been demonstrated (Vierbuchen et al., 2010). The mechanism of neuronal differentiation is not established and it is difficult to control the types of cell generated. More importantly, no study regarding the generation of cerebellar neurons have been reported. This thesis provides new insights into the transdifferentiation of cerebellar neurons and contributes to decipher the molecular mechanism of cell fate switch from differentiated somatic cells to neuronal cell types.

The finding that core transcription factors of Purkinje cells can induce mouse embryonic fibroblasts (MEF) to display immature Purkinje cell properties leads to the quest for new factors and culture systems for transdifferentiaiton to maturation. Nevertheless our data provides proof of principle of the feasibility of transdifferentiation by ectopic factor expression. The failure of granule cell induction prompts us to alter the strategy of factor selection for further study. The present study also opens up a direction to investigate how transcription factors bring about transdifferentiation at molecular level.

In the following section, some of the future plans for the study of generation of neural cells will be presented and discussed.

4.1 Complete Induction of Purkinje Cell Fate

After specification, the dendritic differentiation of Purkinje cells takes place in four stages (Boukhtouche et al., 2006; Tao et al., 2010). *Ptf1a* only specifies the GABAergic identity of progenitors in VZ and does not to play a role in further differentiation. Although the expression of *Rora* persists in Purkinje cells throughout the animals' lives since their emergence, it does not participate in the late development of the dendritic arbor. *Lhx5* and *Ebf2* also do not function in dendritic development. Thus, in order to induce Purkinje cell conversion to completion, other factors that control later development should be tested. One candidate may be the forkhead transcription factor *Foxp4*. *Foxp4* was shown to be dispensable for early dendritic growth, but when it was knocked down in cerebellar slices in later phase *in vitro*, a significant loss of the characteristic "dendritic tree" resulted (Tam et al., 2011). Transfection of MEF with *Ptf1a-Rora-Foxp4* will be performed to determine whether *Foxp4* has the power to drive the formation of mature dendritic arbor.

Studies of the directed differentiation of Purkinje cells from ES cells revealed that recapitulation of *in vivo* microenvironment of cerebellar development can efficiently generate Purkinje cells (Muguruma et al., 2010). Application of the growth factor Fgf2 and/or Shh antagonist cyclopamine promotes the expression of Pcp2 (Muguruma et al., 2010). Co-culture of ES cells with postnatal cerebellar feeder with the addition of Shh, brain-derived neurotrophic factor (BDNF), neurotrophin-3 (NT3) and the thyroid hormone 3,3',5-triiodo-L-thyronine (T_3) efficiently gave rise to mature Purkinje cells (Tao et al., 2010). T_3 was also shown to induce dendritic differentiation through action of RORα (Boukhtouche et al., 2010). These indicate that the culture conditions have a considerable influence on differentiation. To optimize the culture conditions for facilitating the transdifferentiation of MEF to mature Purkinje cells, different combinations of growth factors and inhibitors will be

applied in addition to the currently using N3 medium which contains Fgf2.

The present study utilized the Moloney Murine Leukemia Virus (MMLV)-based retroviral vectors for transgene delivery and expression (Takahashi and Yamanaka, 2006). However, the long terminal repeat (LTR)-driven gene expression was shown to be low, which was about 2-3 folds of the endogenous level. Moreover, this vector was easily silenced and transgene expression dropped significantly after 1-2 weeks after transfection (Berninger et al., 2007a, 2007b; Gaiano et al., 1999; Heins et al., 2001, 2002). Thus, the failure of induction of mature Purkinje cells may be a result of the use of the expression vector (Berninger et al., 2007a). A new expression construct is needed to overcome the above problems. One favorable choice is the chicken β-actin promoter-based (pCAG) vector (Heinrich et al., 2010). Heinrich et al. (2010) indicated that transgene expression was still detectable at 5-6 weeks after transfection. They also demonstrated that the forced expression of *Neurog2* and *Dlx2* could drive the complete conversion to neurons from astroglia when using pCAG vector, but the same could not be achieved when using MMLV-based vector. Therefore, the pCAG vector allows a stronger transgene expression and may enable the complete induction of Purkinje cells using the same pool of genes.

Morphological and immunostaining analysis will be used to compare the degree of specificity and maturity of the induced MEF with Purkinje cells. Electrophysiology assay will also be performed to confirm the functionality of the cells induced (see Section 1.4.3.2). These studies will contribute to the selection of essential factors and optimization of culture conditions for Purkinje cell transdifferentiation.

4.2 Induced Neurons of Different Subtypes

It has been demonstrated that the expression of core transcription factors of a

specific cell type can induce the conversion to that cell type from others (Ieda et al., 2010; Vierbuchen et al., 2010). The present study which manifested the induction of Purkinje cell properties from MEF by expression of core transcription factors specific to Purkinje cells added proof to this approach of transdifferentiation. Therefore it is conceivable that expression of other transcription factors can also induce the conversion to neurons of other subtypes. We have tried to convert MEF to cerebellar granule cells, but the result was not satisfactory. To investigate the transdifferentiation of granule cell again, the problem of low efficiency of neuronal induction observed in the present work should be overcome first. In this regard, *Ascl1* may be essential. *Ascl1* alone has been shown to induce the conversion of MEF to functional neurons (Vierbuchen et al., 2010). To test the feasibility of inclusion of *Ascl1* into the candidate pool, it was co-transfected with *Math1* and *Neurog2*. *Math1* is an important transcription factor in granule cell differentiation as discussed in previous sections (see Section 1.5.2.3 and 5.3.1) and *Neurog2* has been shown to induce the conversion of astroglia to excitatory neurons (Heinrich et al., 2010). The infection of MEF by *Ascl1* with either *Math1* or *Neurog2*, or with the 2 factors together resulted in the induction of Tuj1+cells at greater amount and higher density than all combinations tested in the present work. Therefore, *Ascl1* seems to be a potent inducer neuronal fate. Further selection of factors and characterization will be performed to achieve the efficient generation of cerebellar granule cell from MEF.

Moreover, the present study reinforces the practicability of transdifferentiation by ectopic expression of core transcription factors of the target cell types. The generation of neurons of other subtypes will be studied using the same approach. Knowledge in the developmental programme of the targets will be essential to the success of this further study.

4.3 Mechanism of Transdifferentiation

Despite the success of transdifferentiation in neurons and cardiomyocytes, the mechanism of such event is not well characterized. Epigenetic remodeling is suggested to be the key to iPS cell generation (Hanna et al., 2010; Hochedlinger and Plath, 2009; Plath and Lowry, 2011), and the same may also apply in the case of direct transdifferentiation. Specifically, histone H3 lysine 4 trimethylation (H3K4me3) is associated with active gene transcription while histone H3 lysine 9 trimethylation (H3K9me3), H3K27me3 and DNA methylation at CpG island are repressive marks (Amabile and Meissner, 2009; Plath and Lowry, 2011). It has been shown that induced cardiomyocytes exhibited similar epigenetic state to true cardiomyocytes (Ieda er al., 2010). However, the way how such changes are brought about is not resolved yet. As the epigenetic changes must be mediated by enzymes such as histone methyltransferase and DNA methyltransferase, the inducing factors must directly or indirectly interact with these enzymes. Chromatin immunoprecipitation (ChIP) assay and microarray comparing normal and knockdown of inducing factors will reveal the enzymes necessary for modifying the epigenetic state during fate switch, thus elucidating the mechanism of the event.

4.4 Transdifferentiation and Regenerative Medicine

The present work provides proof of principle of the feasibility of transdifferentiation by ectopic factor expression. However, there are still obstacles that hamper the transdifferentiation to different cell types and the application in clinical cases. One major difficulty is the identification of core factors that are necessary for cell fate switch. Selection of essential factors in our study relied on information from literatures and online databases. Genes that are shown to regulate development of the target cell types are picked into the candidate pools. However,

such information is not available for all cell types. Therefore, the sequence of events in the developmental process should be worked out before the commencement of transdifferentiation studies concerning other cell types.

Another obstacle is that target cell types of transdifferentiation are usually incapable of cell division. This poses a problem of selection and enrichment of the successfully transdifferentiated cells to obtain sufficient amount of cells for clinical applications. Studies should concentrate on the improvement of efficiency of transdifferentiation and methods for selection and enrichment before transdifferentiation can be fully utilized.

The ultimate goal of transdifferentiation is the application in regenerative medicine. At present, regenerative medicine relies on the use of ES cells and iPS cells. Direct transdifferentiation has the potential to overtake the use of these two cell types because, first, it can avoid immunorejection as hosts' own tissue is used as the source. Second, as transdifferentiaton is a direct one-step process, there is less chance to generate undesired cell types. However, ES cells and iPS cells are pluripotent which can give rise to many cell types, thus it is more difficult to control them to differentiate into the target lineages. More importantly, ES cells and iPS cells have the risk to develop into cancer cells which threatens the health of the patients.

Given the current obstacles faced in transdifferentiation experiments, it will take long before the first case of clinical trial. Nevertheless, with the accumulation of knowledge in developmental biology and advance in technology, the difficulties will be overcome and transdifferentiation will become the main stream in regenerative medicine.

BIBLIOGRAPHY

Ackermann, H. (2008). Cerebellar contributions to speech production and speech perception: psycholinguistic and neurobiological perspectives. Trends Neurosci. *31*, 265-272.

Akazawa, C., Ishibashi, M., Shimizu, C., Nakanishi, S., Kageyama, R., (1995). A mammalian helix-loop-helix factor structurally related to the product of Drosophila proneural gene atonal is a positive transcriptional regulator expressed in the developing nervous system. J. Biol. Chem. *270*, 8730-8738.

Alder, J., Lee, K.J., Jessell, T.M., and Hatten, M.E. (1999). Generation of cerebellar granule neurons *in vivo* by transplantation of BMP-treated neural progenitor cells. Nat. Neurosci. *2*, 535-540.

Allen, G.I., and Tsukahara, N. (1974). Cerebro-cerebellar communication systems Physiol. Rev. *54*, 957-1006.

Altman, J., and Bayer, S.A. (1997). Development of the Cerebellar System: In Relation to Its Evolution, Structure, and Functions (Boca Raton: CRC Press).

Amabile, G., and Meissner, A. (2009). Induced pluripotent stem cells: current progress and potential for regenerative medicine. Trends Mol. Med. *15*, 59-68.

Aoki, E., Semba, R., and Kashiwamata, S. (1986). New candidates for GABAergic neurons in the rat cerebellum: an immunocytochemical study with anti-GABA antibody. Neurosci. Lett. *68*, 267-271.

Apps, R., and Garwicz, M. (2005). Anatomical and physiological foundations cerebellar information processing. Nat. Rev. Neurosci. *6*, 297-311.

Armengol, J.A., and Sotelo, C. (1991). Early dendritic development of Purkinje cells in the rat cerebellum. A light and electron microscopic study using axonal tracing in "in vitro" slices. Brain Res. Dev. Brain Res. *64*, 95-114.

Aruga, J., Inoue, T., Hoshino, J., and Mikoshiba, K. (2002a). Zic2 controls cerebellar development in cooperation with Zic1. J. Neurosci. *22*, 218-225.

Aruga, J., Tohmonda, T., Homma, S., and Mikoshiba, K. (2002b). Zic1 promotes the expansion of dorsal neural progenitors in spinal cord by inhibiting neuronal differentiation. Dev. Biol. *244*, 329-341.

Asano, M., and Gruss, P. (1992). Pax-5 is expressed at the midbrain-hindbrain boundary during mouse development. Mech. Dev. *39*, 29-39.

Asanuma, C., Thach, W.T., and Jones, E.G. (1983). Distribution of cerebellar terminations and their relation to other afferent terminations in the ventral lateral thalamic region of the monkey. Brain Res. *286*, 237-265.

Baillieux, H., DeSmet, H.J., Paquier, P.F., DeDeyn, P.P., and Marien, P. (2008). Cerebellar neurocognition: Insights from the bottom of the brain. Clin. Neurol. and Neurosurg. *110*, 763-773.

Bally-Cuif, L., Cholley, B., and Wassef, M. (1995). Involvement of Wnt1 in the formation of the mes/metencephalic boundary. Mech. Dev. *53*, 23-34.

Bellamy, T.C. (2006). Interaction between Purkinje neurones and Bergmann glia. Cerebellum *5*, 116-126.

Beneventi, H., Tonnessen, F.E., Ersland, L., and Hugdahl, K. (2010). Working memory deficit in dyslexia: behavioral and fMRI evidence. Int. J. Neurosci. *120*, 51-59.

Berninger, B., Costa, M.R., Koch, U., Schroeder, T., Sutor, B., Grothe, B., and Gotz, M. (2007a). Functional properties of neurons derived from in vitro reprogrammed postnatal astroglia. J. Neurosci. *27*, 8654-8664.

Berninger, B., Guillemot, F., and Gotz, M. (2007b). Directing neurotransmitter identity of neurones derived from expanded adult neural stem cells. Eur. J. Neurosci. *25*, 2581-2590.

Blau, H.M., and Baltimore, D. (1991) Differentiation requires continuous regulation. J. Cell Biol. *112*, 781-783.

Blau, H.M., Chiu, C.P., and Webster, C. (1983). Cytoplasmic activation of human nuclear genes in stable heterocaryons. Cell *32*, 1171-1180.

Blau, H.M., Pavlath, G.K., Hardeman, E.C., Chiu, C.P., Silberstein, L., Webster, S.G., Miller, S.C., and Webster, C. (1985) Plasticity of the differentiated state. Science *230*, 758-766.

Boukhtouche, F., Brugg, B., Wehrle, R., Bois-Joyeux, B., Danan, J.L., Dusart, I., and Mariani, J. (2010). Induction of early Purkinje cell dendritic differentiation by thyroid hormone requires RORα. Neural Dev. *5*, 18.

Boukhtouche, F., Janmaat, S., Vodjdani, G., Gautheron, V., Mallet, J., Dusart, I., and Mariani, J. (2006). Retinoid-related orphan receptor α controls the early steps of Purkinje cell dendritic differentiation. J. Neurosci. *26*, 1531-1538.

Brochu, G., Maler, L., and Hawkes, R. (1990). Zebrin II: a polypeptide antigen expressed selectively by Purkinje cells reveals compartments in rat and fish cerebellum. J. Comp. Neurol. *291*, 538-552.

Carletti, B., and Rossi, F. (2008). Neurogenesis in the cerebellum. Neuroscientist *14*, 91-100.

Chatzi, C., Brade, T., and Duester, G. (2011). Retinoic acid functions as a key GABAergic differentiation signal in the basal ganglia. PLoS Biol. *9*, e1000609.

Cheung, M., Abu-Elmagd, M., Clevers, H., and Scotting, P.J. (2000). Roles of Sox4 in central nervous system development. Mol. Brain Res. *79*, 180-191.

Chung, S.H., Marzban, H., Croci, L., Consalez, G.G., and Hawkes, R. (2008). Purkinje cell subtype specification in the cerebellar cortex: early B-cell factor 2 acts to repress the zebrin II-positive Purkinje cell phenotype. Neuroscience *153*, 721-732.

Collin, L., Doretto, S., Malerba, M., Ruat, M., and Borrelli, E. (2007). Oligodendrocyte ablation affects the coordinated interaction between granule and Purkinje neurons during cerebellum development. Exp. Cell Res. *313*, 2946-2957.

Croci, L., Chung, S.H., Masserdotti, G., Gianola, S., Bizzoca, A., Gennarini, G., Corradi, A., Rossi, F., Hawkes, R., and Consalez, G.G. (2006). A key role for the HLH transcription factor EBF2$^{COE2,O/E-3}$ in Purkinje neuron migration and cerebellar cortical topography. Development *133*, 2719-2729.

Crossley, P. H., and Martin, G. R. (1995). The mouse Fgf8 gene encodes a family of polypeptides and is expressed in regions that direct outgrowth and patterning in the developing embryo. Development *121*, 439-451.

Cui, L., Jiang, J., Wei, L., Zhou, X., Fraser, J.L., Snider, B.J., and Yu, S.P. (2008). Transplantation of embryonic stem cells improves nerve repair and functional recovery after severe sciatic nerve axotomy in rats. Stem Cells *26*, 1356-1365.

D'Souza, C.A., Chopra, V., Varhol, R., Xie, Y.Y., Bohacec, S., Zhao, Y., Lee, L.L., Bilenky, M., Portales-Casamar, E., He, A., et al. (2008). Identification of a set of genes showing regionally enriched expression in the mouse brain. BMC Neurosci. *9*, 66.

Dahmane, N., and Ruiz i Altaba, A. (1999). Sonic hedgehog regulates the growth and patterning of the cerebellum. Development *126*, 3089-3100.

Das, G.D. (1977). Experimental analysis of embryogenesis of cerebellum in rat. I. Subnormal growth following X-ray irradiation on day 15 of gestation. J. Comp. Neurol. *176*, 419-434.

Davis, C. A., and Joyner, A. L. (1988). Expression patterns of the homeobox containing genes En1 and En2 and the protooncogene int-1 diverge during mouse development. Genes Dev. *2*, 1736-1744.

Davis, C. A., Noble-Topham, S. E., Rossant, J., and Joyner, A. L. (1988). Expression of the homeobox-containing gene En2 delineates a specific region of the developing mouse brain. Genes Dev. *2*, 361-371.

Davis, R.L., Weintraub, H., and Lassar, A.B. (1987). Expression of a single transfected cDNA converts fibroblasts to myoblasts. Cell *51*, 987-1000.

Dieudonne, S., and Dumoulin, A. (2000). Serotonin-driven long-range inhibitory connections in the cerebellar cortex. J. Neurosci. *20*, 1837-1848.

Dino, M.R., Schuerger, R.J., Liu, Y., Slater, N.T., and Mugnaini, E. (2000). Unipolar brush cell: a potential feedforward excitatory interneuron of the cerebellum. Neuroscience *98*, 625-636.

Dugue, G.P., Dumoulin, A., Triller, A., and Dieudonne, S. (2005). Target-dependent use of co-released inhibitory transmitters at central synapses. J. Neurosci. *25*, 6490-6498.

Ebert, P.J., Timmer, J.R., Nakada, Y., Helms, A.W., Parab, P.B., Liu,Y., Hunsaker, T.L., and Johnson, J.E. (2003). Zic1 represses Math1 expression via interactions with the Math1 enhancer and modulation of Math1 autoregulation. Development 130, 1949-1959.

Echelard, Y., Epsteinstar, D.J., St-Jacquesstar, B., Shen, L., Mohler, J., McMahon, J.A., and McMahon, A.P. (1993). Sonic hedgehog, a member of a family of putative signaling molecules, is implicated in the regulation of CNS polarity. Cell 75, 1417-1430.

Edelman, G.M., and Chuong, C.M. (1982). Embryonic to adult conversion of neural cell adhesion molecules in normal and staggerer mice. Proc. Natl. Acad. Sci. USA 79, 7036-7040.

Eisenman, L.M., Schalekamp, M.P., and Voogd, J. (1991). Development of the cerebellar cortical efferent projection: an in-vitro anterograde tracing study in rat brain slices. Brain Res. Dev. Brain Res. 60, 261-266.

Eminli, S., Utikal, J., Arnold, K., Jaenisch, R., and Hochedlinger, K., (2008). Reprogramming of neural progenitor cells into induced pluripotent stem cells in the absence of exogenous Sox2 expression. Stem Cells 26, 2467-2474.

Evans, M.J., and Kaufman, M.H. (1981). Establishment in culture of pluripotential cells from mouse embryos. Nature 292, 154-156.

Evarts, E.V., and Thach, W.T. (1969). Motor mechanisms of the CNS: cerebrocerebellar interrelations. Annu. Rev. Physiol. 31, 451-498.

Fink, A.J., Englund, C., Daza, R.A., Pham, D., Lau, C., Nivison, M., Kowalczyk, T., and Hevner, R.F. (2006). Development of the deep cerebellar nuclei: transcription factors and cell migration from the rhombic lip. J. Neurosci. 26, 3066-3076.

Fink, G.R., Marshall, J.C., Shah, N.J., Weiss, P.H., Halligan, P.W., Grosse-Ruyken, M., Ziemons, K., Zilles, K., and Freund, H.J. (2000). Line bisection judgments implicate right parietal cortex and cerebellum as assessed by fMRI. Neurology 54, 1324-1331.

Fode, C., Gradwohl, G., Morin, X., Dierich, A., LeMeur, M., Goridis, C., and Guillemot, F. (1998). The bHLH protein NEUROGENIN 2 is a determination factor for epibranchial placode-derived sensory neurons. Neuron *20*, 483-494.

Gaiano, N., Kohtz, J.D., Turnbull, D.H., and Fishell, G. (1999). A method for rapid gain-of-function studies in the mouse embryonic nervous system. Nat. Neurosci. *2*, 812-819.

Gazit, R., Krizhanovsky, V., and Ben-Arie, N. (2004). Math1 controls cerebellar granule cell differentiation by regulating multiple components of the Notch signaling pathway. Development *131*, 903-913.

Geurts, F.J., De Schutter, E., and Dieudonne, S. (2003). Unraveling the cerebellar cortex: cytology and cellular physiology of large-sized interneurons in the granular layer. Cerebellum *2*, 290-299.

Ghosh, S., Basu, A., Kumaran, S.S., and Khushu, S. (2010). Functional mapping of language networks in the normal brain using a word-association task. Indian J. Radiol. Imaging *20*, 182-187.

Glasgow, S.M., Henke, R.M., MacDonald, R.J., Wright, C.V.E., and Johnson, J.E. (2005). Ptf1a determines GABAergic over glutamatergic neuronal cell fate in the spinal cord dorsal horn. Development *132*, 5461-5469.

Gold, D.A., Baek, S.H., Schork, N.J., Rose, D.W., Larsen, D.D., Sachs, B.D., Rosenfeld, M.G., and Hamilton, B.A. (2003). RORα coordinates reciprocal signaling in cerebellar development through Sonic hedgehog and calcium-dependent pathways. Neuron *40*, 1119-1131.

Guan, J., Luo, Y., and Denker, B.M. (2005). Purkinje cell protein-2 (Pcp2) stimulates differentiation in PC12 cells by Gβγ -mediated activation of Ras and p38 MAPK. Biochem. J. *392*, 389-397.

Hanna, J.H., Saha, K., and Jaenisch, R. (2010). Pluripotency and cellular reprogramming: facts, hypotheses, unresolved issues. Cell *143*, 508-525.

Hashimoto, M., and Mikoshiba, K. (2002). Mediolateral compartmentalization of the cerebellum is determined on the "birth date" of Purkinje cells. J. Neurosci. *23*, 11342-11351.

Hatten, M.E., and Messer, A. (1978). Postnatal cerebellar cells from staggerer mutant mice express embryonic cell surface characteristic. Nature *276*, 504-506.

Heinrich, C., Blum, R., Gascon, S., Masserdotti, G., Tripathi, P., Sanchez, R., Tiedt, S., Schroeder, T., Gotz, M., and Berninger, B. (2010). Directing astroglia from the cerebral cortex into subtype specific functional neurons. PLoS Biol. *8*, e1000373.

Heins, N., Cremisi, F., Malatesta, P., Gangemi, R.M., Corte, G., Price, J., Goudreau, G., Gruss, P., and Gotz, M. (2001). Emx2 promotes symmetric cell divisions and a multipotential fate in precursors from the cerebral cortex. Mol. Cell. Neurosci. *18*, 485-502.

Heins, N., Malatesta, P., Cecconi, F., Nakafuku, M., Tucker, K.L., Hack, M.A., Chapouton, P., Barde, Y.A., and Gotz, M. (2002). Glial cells generate neurons: the role of the transcription factor Pax6. Nat. Neurosci. *5*, 308-315.

Henke, R.M., Savage, T.K., Meredith, D.M., Glasgow, S.M., Hori, K., Dumas, J., MacDonald, R.J., and Johnson, J.E. (2009). Neurog2 is a direct downstream target of the Ptf1a-Rbpj transcription complex in dorsal spinal cord. Development *136*, 2945-2954.

Hevner, R.F., Hodge, R.D., Daza, R.A.M., Englund, C. (2006). Transcription factors in glutamatergic neurogenesis: Conserved programs in neocortex, cerebellum, and adult hippocampus. Neurosci. Res. *55*, 223-233.

Hochedlinger, K., and Plath, K. (2009). Epigenetic reprogramming and induced pluripotency. Development *136*, 509-523.

Holst, M.I., Maercker, C., Pintea, B., Masseroli, M., Liebig, C., Jankowski, J., Miething, A., Martini, J., Schwaller, B., Oberdick, J., et al. (2008). Engrailed-2 regulates genes related to vesicle formation and transport in cerebellar Purkinje cells. Mol. Cell. Neurosci. *38*, 495-504.

Hong, H., Takahashi, K., Ichisaka, T., Aoi, T., Kanagawa, O., Nakagawa, M., Okita K., and Yamanaka, S. (2009). Suppression of induced pluripotent stem cell generation by the p53-p21 pathway. Nature *460*, 1132-1135.

Hori, K., Cholewa-Waclaw, J., Nakada, Y., Glasgow, S.M., Masui, T., Henke, R.M., Wildner, H., Martarelli, B., Beres, T.M., Epstein, J.A., et al. (2008). A nonclassical bHLH Rbpj transcription factor complex is required for specification of GABAergic neurons independent of Notch signaling. Genes Dev. *22*, 166-178.

Hoshino, M., Nakamura, S., Mori, K., Kawauchi, T., Terao, M., Nishimura, Y.V., Fukuda, A., Fuse, T., Matsuo, N., Sone, M., et al. (2005). Ptf1a, a bHLH transcriptional gene, defines GABAergic neuronal fates in cerebellum. Neuron *47*, 201-213.

Huangfu, D., Osafune, K., Maehr, R., Guo, W., Eijkelenboom, A., Chen, S., Muhlestein, W., and Melton, D.A. (2008). Induction of pluripotent stem cells from primary human fibroblasts with only Oct4 and Sox2. Nat. Biotechnol. *26*, 1269-1275.

Ieda, M., Fu,J.D., Delgado-Olguin, P., Vedantham, P., Hayashi, Y., Bruneau, B.G., and Srivastava, D. (2010). Direct reprogramming of fibroblasts into functional cardiomyocytes by defined factors. Cell *142*, 375-386.

Ino, H. (2004). Immunohistochemical characterization of the orphan nuclear receptor RORα in the mouse nervous system. J. Histochem. Cytochem. *52*, 311-323.

Inoue, T., Ota, M., Ogawa, M., Mikoshiba, K., and Aruga, J. (2007). Zic1 and Zic3 regulate medial forebrain development through expansion of neuronal progenitors. J. Neurosci. *27*, 5461-5473.

Ito, M. (2002). Historical review of the significance of the cerebellum and the role of Purkinje cells in motor learning. Ann. N. Y. Acad. Sci. *978*, 273-288.

Ito, M. (2006). Cerbellar circuitry as a neuronal machine. Prog. Neurobiol. *78*, 272-303.

Jopling, C., Boue, S., and Belmonte, J.C.I. (2011). Dedifferentiation, transdifferentiation and reprogramming: three routes to regeneration. Nat. Rev. Mol. Cell Biol. *12*, 79-89.

Kapfhammer, J.P. (2004). Cellular and molecular control of dendritic growth and development of cerebellar Purkinje cells. Prog. Histochem. Cytochem. *39*, 131-182.

Kawauchi, D., and Saito, T. (2008). Transcriptional cascade from Math1 to Mbh1 and Mbh2 is required for cerebellar granule cell differentiation. Dev. Biol. *322*, 345-354.

Kele, J., Simplicio, N., Ferri, A.L., Mira, H., Guillemot, F., Arenas, E., and Ang, S.L. (2006). Neurogenin 2 is required for the development of ventral midbrain dopaminergic neurons. Development *133*, 495-505.

Kim, D., Kim, C.H., Moon, J.I., Chung, Y.G., Chang, M.Y., Han, B.S., Ko, S., Yang, E., Cha, K.Y., Lanza, R., et al. (2009). Generation of human induced pluripotent stem cells by direct delivery of reprogramming proteins. Cell Stem Cell *4*, 472-476.

Kinney, G.A., Overstreet, L.S., and Slater, N.T. (1997). Prolonged physiological entrapment of glutamate in the synaptic cleft of cerebellar unipolar brush cells. J. Neurophysiol. *78*, 1320-1333.

Knoepfler, P.S., Zhang, X.Y., Cheng, P.F., Gafken, P.R., McMahon, S.B., and Eisenman, R.N. (2006). Myc influences global chromatin structure. EMBO J. *25*, 2723-2734.

Lai, C.S., Gerrelli, D., Monaco, A.P., Fisher, S.E., and Copp, A.J. (2003). FOXP2 expression during brain development coincides with adult sites of pathology in a severe speech and language disorder. Brain *126*, 2455-2462.

Laine, J., and Axelrad, H. (2002). Extending the cerebellar Lugaro cell class. Neuroscience *115*, 363-374.

Larramendi L.M., and Lemkey-Johnston N. (1970). The distribution of recurrent Purkinje collateral synapses in the mouse cerebellar cortex: an electron microscopic study. J. Comp. Neurol. *138*, 451-459.

Lee, G.P., Meador, K.J., Loring, D.W., Allison, J.D., Brown, W.S., Paul, L.K., Pillai, J.J., and Lavin, T.B. (2004). Neural substrates of emotion as revealed by functional magnetic resonance imaging. Cogn. Behav. Neurol. *17*, 9-17.

Lee, K.J., and Jessell, T.M. (1999). The specification of dorsal cell fates in the vertebrate central nervous system. Annu. Rev. Neurosci. *22*, 261-294.

Lein, E.S., Hawrylycz, M.J., Ao, N., Ayres, M., Bensinger, A., Bernard, A., Boe, A.F., Boguski, M.S., Brockway, K.S., Byrnes, E.J., et al. (2007). Genome-wide atlas of gene expression in the adult mouse brain. Nature *445*, 168-176.

Leiner, H., Leiner, A., and Dow, R. (1986). Does the cerebellum contribute to mental skills? Behav. Neurosci. *100*, 443-454.

Leiner, H.C., Leiner, A.L., and Dow, R.S. (1987). Cerebro-cerebellar learning loops in apes and humans. Ital. J. Neurol. Sci. *8*, 425-436.

Leiner, H.C., Leiner, A.L., and Dow, R.S. (1989). Reappraising the cerebellum: what does the hindbrain contribute to the forebrain? Behav. Neurosci. *103*, 998-1008.

Leiner, H.C., Leiner, A.L., and Dow, R.S. (1991). The human cerebro-cerebellar system: its computing, cognitive, and language skills. Behav. Brain Res. *44*, 113-128.

Leiner, H.C., Leiner, A.L., and Dow, R.S. (1993). Cognitive and language functions of the human cerebellum. Trends Neurosci. *16*, 444-447.

Lie, C.H., Specht, K., Marshall, J.C., and Fink, G.R. (2006). Using fMRI to decompose the neural processes underlying the Wisconsin Card Sorting Test. Neuroimage *30*, 1038-1049.

Llinas, R., and Sugimori, M. (1980). Electrophysiological properties of in vitro Purkinje cell somata in mammalian cerebellar slices. J. Physiol. *305*, 171-195.

Mallet, J., Christen, R., and Changeux, J.P. (1979). Immunological studies on the Purkinje cells from rat and mouse cerebella. I. Evidence for antibodies characteristic of the Purkinje cells. Dev. Biol. *72*, 308-319.

Maricich, S.M., and Herrup, K. (1999). Pax-2 expression defines a subset of GABAergic interneurons and their precursors in the developing murine cerebellum. J. Neurobiol. *41*, 281-294.

Martin, G.R. (1981). Isolation of a pluripotent cell line from early mouse embryos cultured in medium conditioned by teratocarcinoma stem cells. Proc. Natl. Acad. Sci. USA *78*, 7634-7638.

Miale, I.L., and Sidman, R.L. (1961). An autoradiographic analysis of histogenesis in the mouse cerebellum. Expl. Neurol. *4*, 277-296.

Middleton, F.A., and Strick, P.L. (1997). Cerebellar output channels. Int. Rev. Neurobiol. 4161-4182.

Middleton, F.A., and Strick, P.L. (1998). Cerebellar output: motor and cognitive channels. Trends Cogn. Sci. *2*, 348-354.

Millen, K.J., and Gleeson, J.G. (2008). Cerebellar development and disease. Curr. Opin. Neurobiol. *18*, 12-19.

Miquelajauregui, A., Varela-Echavarria, A., Ceci, M.L., Garcia-Moreno, F., Ricano, I., Hoang, K., Frade-Perez, D., Portera-Cailliau, C., Tamariz, E., De Carlos, J.A., et al. (2010). LIM-homeobox gene Lhx5 is required for normal development of Cajal-Retzius cells. J. Neurosci. *30*, 10551-10562.

Miyata, T., Maeda, T., and Lee, J.E. (1999). NeuroD is required for differentiation of the granule cells in the cerebellum and hippocampus. Genes Dev. *13*, 1647-1652.

Miyata, T., Nakajima, K., Aruga, J., Takahashi, S., Ikenaka, K., Mikoshiba, K., and Ogawa, M. (1996). Distribution of a reeler gene-related antigen in the developing cerebellum: an immunohistochemical study with an allogeneic antibody CR-50 on normal and reeler mice. J. Comp. Neurol. *372*, 215-228.

Miyata, T., Ono, Y., Okamoto, M., Masaoka, M., Sakakibara, A., Kawaguchi, A., Hashimoto, M., and Ogawa, M. (2010). Migration, early axonogenesis, and Reelin-dependent layer-forming behavior of early/posterior-born Purkinje cells in the developing mouse lateral cerebellum. Neural Dev. *5*, 23.

Mizuguchi, R., Sugimori, M., Takebayashi, H., Kosako, H., Nagao, M., Yoshida, S., Nabeshima, Y., Shimamura, K., and Nakafuku, M. (2001). Combinatorial roles of Olig2 and Neurogenin2 in the coordinated induction of pan-neuronal and subtype-specific properties of motoneurons. Neuron *31*, 757-771.

Morikawa, Y., Zehir, A., Maska, E., Deng, C., Schneider, M.D., Mishina, Y., and Cserjesi, P. (2009). BMP signaling regulates sympathetic nervous system development through Smad4-dependent and -independent pathways. Development *136*, 3575-3584.

Morita, S., Kojima, T., and Kitamura, T. (2000). Plat-E: an efficient and stable system for transient packaging of retroviruses. Gene Ther. *7*, 1063-1066.

Mugnaini, E., Dino, M.R., and Jaarsma, D. (1997). The unipolar brush cells of the mammalian cerebellum and cochlear nucleus: cytology and microcircuitry. Prog. Brain Res. *114*, 131-150.

Muguruma, K., Nishiyama, A., Ono, Y., Miyawaki, H., Mizuhara, E., Hori, S., Kakizuka, A., Obata, K., Yanagawa, Y., Hirano, T., et al. (2010). Ontogeny-recapitulating generation and tissue integration of ES cell-derived Purkinje cells. Nat. Neurosci. *13*, 1171-1180.

Nagai, N., Kawao, N., Okada, K., Okumoto, K., Teramura, T., Ueshima, S., Umemura, K., and Matsuo, O. (2010). Systemic transplantation of embryonic stem cells accelerates brain lesion decrease and angiogenesis. Neuroreport *21*, 575-579.

Nakagawa, M., Koyanagi, M., Tanabe, K., Takahashi, K., Ichisaka, T., Aoi, T., Okita, K., Mochiduki, Y., Takizawa, N., and Yamanaka, S. (2008). Generation of induced pluripotent stem cells without Myc from mouse and human fibroblasts. Nat. Biotechnol. *26*, 101-106.

Natochin, M., Gasimov, K.G., and Artemyev, N.O. (2001). Inhibition of GDP/GTP exchange on Gα subunits by proteins containing G-protein regulatory motifs. Biochemistry *40*, 5322-5328.

Palkovits, M., Magyar, P., and Szentagothai, J. (1971). Quantitative histological analysis of the cerebellar cortex in the cat: II. Cell numbers and densities in the granular layer. Brain Res. *32*, 15-30.

Pan, N., Jahan I., and Lee, J.E. (2009). Defects in the cerebella of conditional Neurod1 null mice correlate with effective Tg(Atoh1-cre) recombination and granule cell requirements for Neurod1 for differentiation. Cell Tissue Res. *337*, 407-428.

Pascual, M., Abasolo, I., Mingorance-Le Meur, A., Martinez, A., Del Rio, J.A., Wright, C.V.E., Real, F.X., and Soriano, E. (2007). Cerebellar GABAergic progenitors adopt an external granule cell-like phenotype in the absence of Ptf1a transcription factor expression. Proc. Natl. Acad. Sci. USA *104*, 5193-5198.

Peng, G., and Westerfield, M. (2006). Lhx5 promotes forebrain development and activates transcription of secreted Wnt antagonists. Development *133*, 3191-3200.

Philopona, D., and Coenen, O.J.-M.D. (2004). Model of granular layer encoding of the cerebellum. Neurocomputing *58*, 575-580.

Pinson, J., Mason, J.O., Simpson, T.I., and Price, D.J. (2005). Regulation of the Pax6 : Pax6(5a) mRNA ratio in the developing mammalian brain. BMC Dev. Biol. *5*,13.

Plath, K., and Lowry, W.E. (2011). Progress in understanding reprogramming to the induced pluripotent state. Nat. Rev. Genet. *12*, 253-265.

Pons, S., Trejo, J.L., Martinez-Morales, J.R., and Marti, E. (2001). Vitronectin regulates Sonic hedgehog activity during cerebellum development through CREB phosphorylation. Development *128*, 1481-1492.

Qin, L., Wine-Lee, L., Ahn, K.J., and Crenshaw, E.B., III. (2006). Genetic analyses demonstrate that bone morphogenetic protein signaling is required for embryonic cerebellar development. J. Neurosci. *26*, 1896-1905.

Rakic, P. (1971). Neuron-glia relationship during granule cell migration in developing cerebellar cortex. A Golgi and electronmicroscopic study in Macacus Rhesus. J. Comp. Neurol. *141*, 283-312.

Raman, I.M., and Bean, B.P. (1999). Ionic currents underlying spontaneous action potentials in isolated cerebellar Purkinje neurons. J. Neurosci. *19*, 1663-1674.

Ramnani, N. (2006). The primate cortico-cerebellar system: anatomy and function. Nat. Rev. Neurosci. *7*, 511-522.

Ramon y Cajal, S. (1926). Sur les fibre moussues et quelques points douteux de la texture de l'ecorce cerebelleuse. Trab. Lab. Invest. Biol. Univ. Madrid *24*, 215-251.

Rio, C., Rieff, H.I., Qi, P., Khurana, T.S., and Corfas, G. (1997). Neuregulin and erbB receptors play a critical role in neuronal migration. Neuron *19*, 39-50.

Rios, I., Alvarez-Rodriguez, R., Marti, E., and Pons, S. (2004). Bmp2 antagonizes sonic hedgehog-mediated proliferation of cerebellar granule neurones through Smad5 signalling. Development *131*, 3159-3168.

Rossi, D.J., and Hamann, M. (1998). Spillover-mediated transmission at inhibitory synapses promoted by high affinity α6 subunit GABAA receptors and glomerular geometry. Neuron *20*, 783-795. (Erratum in: Neuron 21 (1998) 527).

Rowitch, D. H. & McMahon, A. P. (1992). Pax-2 expression in the murine neural plate precedes and encompasses the expression domains of Wnt-1 and En-1. Mech. Dev. *52*, 3-8.

Salero, E., and Hatten, M.E. (2007). Differentiation of ES cells into cerebellar neurons. Proc. Natl. Acad. Sci. USA *104*, 2997-3002.

Scardigli, R., Baumer, N., Gruss, P., Guillemot, F., and Le Roux, I. (2003). Direct and concentration-dependent regulation of the proneural gene Neurogenin2 by Pax6. *130*, 3269-3281.

Schell, G.R., and Strick, P.L. (1984). The origin of thalamic inputs to the arcuate premotor and supplementary motor areas J. Neurosci. *4*, 539-560.

Schilling, K., Oberdick, J., Rossi, F., and Baader, S.L. (2008). Besides Purkinje cells and granule neurons: an appraisal of the cell biology of the interneurons of the cerebellar cortex. Histochem. Cell Biol. *130*, 601-615.

Schmahmann, J.D. and Sherman, J.C. (1998). The cerebellar cognitive affective syndrome. Brain *121*, 561-579.

Schuller, U., Kho, A.T., Zhao, Q., Ma, Q., and Rowitcha, D.H. (2006). Cerebellar 'transcriptome' reveals cell-type and stage-specific expression during postnatal development and tumorigenesis. Mol. Cell. Neurosci. *33*, 247-259.

Schuurmans, C., Armant, O., Nieto, M., Stenman, J. M., Britz, O., Klenin, N., Brown, C., Langevin, L. M., Seibt, J., Tang, H., et al. (2004). Sequential phases of cortical specification involve Neurogenin-dependent and -independent pathways. EMBO J. *23*, 2892-2902.

Serinagaoglu, Y., Zhang, R., Zhang, Y., Zhang, L., Hartt, G., Young, A.P., and Oberdick, J. (2007). A promoter element with enhancer properties, and the orphan nuclear receptor RORα, are required for Purkinje cell-specific expression of a $G_{i/o}$ modulator. Mol. Cell. Neurosci. *34*, 324-342.

Shi, Y., Desponts, C., Do, J.T., Hahm, H.S., Scholer, H.R., and Ding, S. (2008). Induction of pluripotent stem cells from mouse embryonic fibroblasts by Oct4 and Klf4 with small-molecule compounds. Cell Stem Cell *3*, 568-574.

Sillitoe, R.V., Stephen, D., Lao, Z., and Joyner, A.L. (2008). Engrailed homeobox genes determine the organization of Purkinje cell sagittal stripe gene expression in the adult cerebellum. J. Neurosci. *28*, 12150-12162.

Simeone, A., Acampora, D., Gulisano, M., Stornaiuolo, A., and Boncinelli, E. (1992). Nested expression domains of four homeobox genes in developing rostral brain. Nature *358*, 687-690.

Sotelo, C. (2004). Cellular and genetic regulation of the development of the cerebellar system. Prog. Neurobiol. *72*, 295-339.

Stadtfeld, M., Nagaya, M., Utikal, J., Weir, G., and Hochedlinger, K. (2008). Induced pluripotent stem cells generated without viral integration. Science *322*, 945-949.

Stolt, C.C., Lommes, P., Sock, E., Chaboissier, M.C., Schedl, A., and Wegner, M. (2003). The Sox9 transcription factor determines glial fate choice in the developing spinal cord. Genes Dev. *17*, 1677-1689.

Stoodley, C.J. (2011). The cerebellum and cognition: Evidence from functional imaging studies. Cerebellum doi: 10.1007/s12311-011-0260-7.

Stoodley, C.J., and Schmahmann, J.D. (2010). Evidence for topographic organization in the cerebellum of motor control versus cognitive and affective processing. Cortex *46*, 831-844.

Su, H.L., Muguruma, K., Matsuo-Takasaki, M., Kengaku, M., Watanabe, K., and Sasai, Y. (2006). Generation of cerebellar neuron precursors from embryonic stem cells. Dev. Biol. *290*, 287-296.

Szabo, E., Rampalli, S., Risueno, R.M., Schnerch, A., Mitchell, R., Fiebig-Comyn, A., Levadoux-Martin, M., and Bhatia, M. (2010). Direct conversion of human fibroblasts to multilineage blood progenitors. Nature *25*, 521-526.

Tada, M., Takahama, Y., Abe, K., Nakatsuji, N., and Tada, T. (2001). Nuclear reprogramming of somatic cells by in vitro hybridization with ES cells. Curr. Biol. *11*, 1553-1558.

Takahashi, K., and Yamanaka, S. (2006). Induction of pluripotent stem cells from mouse embryonic and adult fibroblast cultures by defined factors. Cell *126*, 663-676.

Takeuchi, J.K., and Bruneau, B.G. (2009). Directed transdifferentiation of mouse mesoderm to heart tissue by defined factors. Nature *459*, 708-711.

Tam, W.Y., Leung, C.K.Y., Tong, K.K., and Kwan, K.M. (2011). Foxp4 is essential in maintenance of Purkinje cell dendritic arborization in the mouse cerebellum. Neuroscience *172*, 562-571.

Tao, O., Shimazaki, T., Okada, Y., Naka, H., Kohda, K., Yuzaki, M., Mizusawa, H., and Okano, H. (2010). Efficient generation of mature cerebellar Purkinje cells from mouse embryonic stem cells. J. Neurosci. Res. *88*, 234-247.

Thach, W.T. (1972). Cerebellar output: properties, synthesis and uses. Brain Res. *40*, 89-102.

Thach, W.T., and Jones, E.G. (1979). The cerebellar dentatothalamic connection: terminal field, lamellae, rods and somatotopy. Brain Res. *169*, 168-172.

Traiffort, E., Charytoniuk, D., Watroba, L., Faure, H., Sales, N., and Ruat, M. (1999). Discrete localizations of hedgehog signalling components in the developing and adult rat nervous system. Eur. J. Neurosci. *11*, 3199-3214.

Traiffort, E., Charytoniuk, D.A., Faure, H., and Ruat, M. (1998). Regional distribution of Sonic Hedgehog, patched, and smoothened mRNA in the adult rat brain. J. Neurochem. *70*, 1327-1330.

Trenkner, E. (1979). Postnatal cerebellar cells of staggerer mutant mice express immature components on their surface. Nature *277*, 566-567.

Trommsdorff, M., Gotthardt, M., Hiesberger, T., Shelton, J., Stockinger, W., Nimpf, J., Hammer, R.E., Richardson, J.A., and Herz, J. (1999). Reeler/Disabled-like disruption of neuronal migration in knockout mice lacking the VLDL receptor and ApoE receptor 2. Cell *97*, 689-701.

Tyrrell, T., and Willshaw, D. (1992). Cerebellar cortex: its simulation and the relevance of Marr's theory. Philos. Trans. R. Soc. Lond. B. Biol. Sci. *336*, 239-257.

Uittenbogaard, M., and Chiaramello, A. (2002). Constitutive overexpression of the basic helix-loop-helix Nex1/MATH-2 transcription factor promotes neuronal differentiation of PC12 cells and neurite regeneration. J. Neurosci. Res. *67*, 235-245.

Vierbuchen, T., Ostermeier, A., Pang, Z.P., Kokubu, Y., Sudhof, T.C., and Wernig, M. (2010). Direct conversion of fibroblasts to functional neurons by defined factors. Nature *463*, 1035-1041.

Vogel, M.W., Sinclair, M., Qiu, D., and Fan, H. (2000). Purkinje cell fate in staggerer mutants: agenesis versus cell death. J. Neurobiol. *42*, 323-337.

Vos, B.P., Maex, R., Volny-Luraghi, A., and De Schutter, E. (1999). Parallel fibers synchronize spontaneous activity in cerebellar Golgi cells. J. Neurosci. *19*, RC6.

Wallace, V.A. (1999). Purkinje-cell-derived Sonic hedgehog regulates granule neuron precursor cell proliferation in the developing mouse cerebellum. Curr. Biol. *9*, 445-448.

Wang, V.Y., Rose, M.F., and Zoghbi, H.Y. (2005). Math1 expression redefines the rhombic lip derivatives and reveals novel lineages within the brainstem and cerebellum. Neuron *48*, 31-43.

Wang, W.F., Wang, Y.G., Reginato, A.M., Glotzer, D.J., Fukai, N., Plotkina, S., Karsenty, G., and Olsen, B.R. (2004). Groucho homologue Grg5 interacts with the transcription factor Runx2-Cbfa1 and modulates its activity during postnatal growth in mice. Dev. Biol. *270*, 364-381.

Wang, W.F., Wang, Y.G., Reginato, A.M., Plotkina, S., Gridley, T., and Olsen, B.R. (2002). Growth defect in Grg5 null mice is associated with reduced Ihh signaling in growth plates. Dev. Dyn. *224*, 79-89.

Warren, L., Manos, P.D., Ahfeldt, T., Loh, Y.H., Li, H., Lau, F., Ebina, W., Mandal, P.K., Smith, Z.D., Meissner, A., et al. (2010). Highly efficient reprogramming to pluripotency and directed differentiation of human cells with synthetic modified mRNA. Cell Stem Cell *7*, 618-630.

Wassarman, K.M., Lewandoski, M., Campbell, K., Joyner, A.L., Rubenstein, J.L., Martinez, S., and Martin, G.R. (1997). Specification of the anterior hindbrain and establishment of a normal mid/hindbrain organizer is dependent on Gbx2 gene function. Development *124*, 2923-2934.

Wechsler-Reya, R.J. and Scott, M.P. (1999). Control of neuronal precursor proliferation in the cerebellum by Sonic Hedgehog. Neuron *22*, 103-114.

Wernig, M., Tucker, K.L., Gornik, V., Schneiders, A., Buschwald, R., Wiestler, O.D., Barde, Y., and Brustle O. (2002). Tau EGFP embryonic stem cells: an efficient tool for neuronal lineage selection and transplantation. J. Neurosci. Res. *69*, 918-924.

Willard, F.S., McCudden, C.R., and Siderovski, D.P. (2006). G-protein alpha subunit interaction and guanine nucleotide dissociation inhibitor activity of the dual GoLoco motif protein PCP-2 (Purkinje cell protein-2). Cell Signal. *18*, 1226-1234.

Wilmut, I., Schnieke, A.E., McWhir, J., Knid, A.J., and Campbell, K.H.S. (1997). Viable offspring derived from fetal and adult mammalian cells. Nature *385*, 810-813.

Woltjen, K., Michael, I.P., Mohseni, P., Desai, R., Mileikovsky, M., Hamalainen, R., Cowling, R., Wang, W., Liu, P., Gertsenstein, M., et al. (2009). piggyBac transposition reprograms fibroblasts to induced pluripotent stem cells. Nature *458*, 766-770.

Wurst, W., and Bally-Cuif, L. (2001). Neural plate patterning: upstream and downstream of the isthmic organizer. Nat. Rev. Neurosci. *2*, 99-108.

Xie, H., Ye, M., Feng, R., and Graf, T. (2004). Stepwise reprogramming of B cells into macrophages. Cell *117*, 663-676.

Yamanaka, S. (2009). Elite and stochastic models for induced pluripotent stem cell generation. Nature *460*, 49-52.

Yamanaka, S., and Blau, H.M. (2010). Nuclear reprogramming to a pluripotent state by three approaches. Nature *465*, 704-712.

Yamasaki, T., Kawaji, K., Ono, K., Bito, H., Hirano, T., Osumi, N., and Kengaku, M. (2001). Pax6 regulates granule cell polarization during parallel fiber formation in the developing cerebellum. Development *128*, 3133-3144.

Yang, J., van Oosten, A.L., Theunissen, T.W., Guo, G., Silva, J.C.R., and Smith, A. (2010). Stat3 activation is limiting for reprogramming to ground state pluripotency. Cell Stem Cell *7*, 319-328.

Yang, X.W., Wynder, C., Doughty, M.L., and Heintz, N. (1999). BAC-mediated gene-dosage analysis reveals a role for Zipro1 (Ru49/Zfp38) in progenitor cell proliferation in cerebellum and skin. Nat. Genet. *22*, 327-335.

Yoshida, Y., Takahashi, K., Okita, K., Ichisaka, T., and Yamanaka, S. (2009). Hypoxia enhances the generation of induced pluripotent stem cells. Cell Stem Cell *5*, 237-241.

Yuasa, S., Kitoh, J., Oda, S., and Kawamura, K. (1993). Obstructed migration of Purkinje cells in the developing cerebellum of the reeler mutant mouse. Anat. Embryol. *188*, 317-329.

Zhao, Y., Kwan, K.M., Mailloux, C.M., Lee, W.K., Grinberg, A., Wurst, W., Behringer, R.R., and Westphal, H. (2007). LIM-homeodomain proteins Lhx1 and Lhx5, and their cofactor Ldb1, control Purkinje cell differentiation in the developing cerebellum. Proc. Natl. Acad. Sci. USA *104*, 13182-13186.

Zhao, Y., Sheng, H.Z., Amini, R., Grinberg, A., Lee, E., Huang, S., Taira, M., and Westphal, H. (1999). Control of hippocampal morphogenesis and neuronal differentiation by the LIM homeobox gene Lhx5. Science *284*, 1155-1158.

Zhao, Y., Yin, X., Qin, H., Zhu, F., Liu, H., Yang, W., Zhang, Q., Xiang, C., Hou, P., Song, Z., et al. (2008). Two supporting factors greatly improve the efficiency of human iPSC generation. Cell Stem Cell *3*, 475-479.

Zhou, H., Wu, S., Joo, J.Y., Zhu, S., Han, D.W., Lin, T., Trauger, S., Bien, G., Yao, S., Zhu, Y., et al. (2009). Generation of induced pluripotent stem cells using recombinant proteins. Cell Stem Cell *4*, 381-384.

Zhu,S., Li, W., Zhou,H., Wei, W., Ambasudhan, R., Lin,T., Kim, J., Zhang, K., and Ding, S. (2010). Reprogramming of human primary somatic cells by OCT4 and chemical compounds. Cell Stem Cell *7*, 651-655.

Zong, H., Espinosa, J.S., Su, H.H., Muzumdar, M.D., and Luo, L. (2005). Mosaic analysis with double markers in mice. Cell *121*, 479-492.

Zordan, P., Croci, L., Hawkes, R., and Consalez, G.G. (2008). Comparative analysis of proneural gene expression in the embryonic cerebellum. Dev. Dyn. *237*, 1726-1735.